Mauritius Research Council

INNOVATION FOR TECHNOLOGY

EFFECTIVE USE OF COCONUT OIL, SHELL AND HUSK

Final Report

May 2018

Mauritius Research Council

Address:

Level 6, Ebene Heights
34, Cybercity
Ebene

Telephone: (230) 465 1235
Fax: (230) 465 1239
e-mail: mrc@intnet.mu
Website: www.mrc.org.mu

This report is based on work supported by the Mauritius Research Council under award number MRC/RUN-1511. Any opinions, findings, recommendations and conclusions expressed herein are the author's and do not necessarily reflect those of the Council.

PI Name and Address;
B.Yashwansingh R. Surnam
Associate Professor, Mechanical and Production Eng. Dept,
Faculty of Engineering, University of Mauritius, Reduit

Co-Investigator Name and Address;
Geeta Devi Somaroo
Senior Lecturer, Chemical and Environmental Engineering Dept
Faculty of Engineering, University of Mauritius, Reduit

MAURITIUS RESEARCH COUNCIL FINAL REPORT

PART I- PROJECT IDENTIFICATION INFORMATION
1. Unsolicited Research Grant and Innovation Scheme
2. Award Dates (MM/YYYY) From: November 2015 To: May 2018
3. Organisation and Address: University of Mauritius, Reduit
4. Award Number: MRC/RUN/1511
5. Project Title: Effective use of coconut oil, shell and husk

Mauritius Research Council

Table of Contents

LIST OF TABLES iii

LIST OF FIGURES iv

ACKNOWLEDGEMENT vi

DECLARATION vii

ABSTRACT viii

1. INTRODUCTION 1

1.1 Aims and Objectives 1

2. LITERATURE SURVEY 3

2.1 Characteristics of coconut oil 3

2.1.1 Viscosity 3

2.1.2 Viscosity index 3

2.2 Coconut oil for corrosion resistance 4

2.3 Coconut husk and shell in composite material 6

2.4 Coconut husk and shell as activated carbon 6

3. METHODOLOGY AND TECHNICAL INFORMATION 16

3.1 Determining properties of coconut fibres 16

3.1.1 Preparation of raw materials 16

3.1.2 Testing tensile strength and Young's modulus of coconut fibres 17

3.1.2.1 Results for Tensile Testing and Young's Modulus 19

3.1.3 Lignocellulosic content of coconut fibres (cellulose, hemicellulose & lignin) 20

3.1.3.1 Lignocellulosic content of coconut fibres 23

3.2 Coconut oil for temporary corrosion prevention 23

3.2.1 Increasing viscosity of coconut oil 23

3.2.2 Preparation of mild steel 24

3.2.3 Corrosion Monitoring 26

3.2.3.1 Image analysis by ImageJ Software 27

3.2.3.2 Results of corrosion tests 31

3.2.3.3 Mass loss method 32

3.3.1 Resin Injection and Vacuum Infusion apparatus 33

3.3.2 Critical fibre length 40

3.3.3 Manufacturing of composite from coconut fibre 41

3.3.4 Manufacturing of composite from coconut fibre and coconut shell powder 41

3.5 Coconut husk and shell briquettes 47

4. ANALYSIS OF RESULTS 55

4.1 Determining properties of coconut fibres 55

4.2 Coconut oil for temporary corrosion prevention 55

4.3 Manufacturing of composite board from coconut fibre and shell 56
4.4 Activated carbon production from coconut husk and shell 57
4.5 Coconut husk and shell briquettes 59
4.5.1 Characteristics 59
4.5.2: Briquettes Testing 60
5. CONCLUSIONS 62
REFERENCES 64
APPENDIX 68
Annex 1: Potential corrosion inhibitors for mild steel 69
Annex 2: Composites with coconut husk 80
Annex 3: Composites with coconut shell 83
Annex 4: Activated carbon from coconut husk and shell 86
Annex 5: Measured diameter of coconut fibres 92
Annex 6: Tensile strength of coconut fibres 98
Annex 7: Coconut Fibre Lignocellulosic contents 104
Annex 8: Corrosion inhibitor trials 106
Annex 9: Caramelisation of honey 109
Annex 10: Mild steel samples and ImageJ analysis 110
Annex 11: Problems encountered and solution in Resin injection and vacuum infused 116
Annex 12: Details on composite making for Agalega and Mauritius fibres 126
Annex 13: Tensile strength result for Agalega and Mauritius fibres composites 130
Annex 14: Tensile strength result for fibre-shell composites 134
Annex 15: Characterisation of raw materials for briquettes 136
Annex 16: Characterisation of briquettes 142
Annex 17: SEM test results 155

LIST OF TABLES

Table 2.1: Liquid and gas phase applications of activated carbon in industry 9
Table 2.2: Characteristics of coconut shell activated carbon prepared by heat action and acid activation 11
Table 3.1: Summary of tensile strength and young's modulus of coconut fibres 19
Table 3.2- Summary of coconut fibre lignocellulosic contents (%) 23
Table 3.3- Preparation of mild steel 24
Table 3.4: Mild steel samples measurements 26
Table 3.5- Samples for corrosion tests 26
Table 3.6: Percentage area corroded from image analysis of Outdoor Exposure 31
Table 3.7: Percentage area corroded from image analysis of Sheltered Exposure 32
Table 3.8: Mass loss for outdoor steel samples exposure 33
Table 3.9- Results obtained from the UTM 41
Table 3.10- UTM results for composites made of coconut shell powder and coconut fiber 42
Table 3.11: Optimum condition for activation of coconut shell by phosphoric acid. 43
Table 3.12: Coconut shell and husk activated carbon compositions 45
Table 3.13: parameters analysed and standard test methods used 45
Table 3.14; Non-carbonised briquette compositions 49
Table 3.15; Charcoal briquette compositions 49
Table 4.1: Summary of test report for wastewater analysis 58
Table 4.2: Amount of pollutants adsorbed on the activated carbon at equilibrium 58
Table 4.3: Characteristic of coconut husk and shell 59
Table 4.3: Gross Calorific Value of raw materials 59
Table 4.4: Density of Non-carbonised and Charcoal briquettes 60
Table 4.6: Gross Calorific Value of Non-carbonised & Charcoal briquettes 61
Table 4.7: Drop Shatter Test 61
Table 4.8; Result from flue gas analyser meter reading 62

LIST OF FIGURES

Figure 2.1: Determination of Viscosity Index (Noria Corporation) 4
Figure2.2: The relationship between the reaction time and the method used (left side) and the relationship between chemical yields and the method used (right side) in synthesising imidazoline derivative compounds (Wahyuningrum et al., 2008) 5
Figure 2.3: Flowchart for activated carbon production (Marsh and Rodriguez-Reinoso, 2006) 7
Figure 2.4: (a) SEM image of raw coconut husk (1000×). (b) SEM image of coconut husk-based activated carbon prepared under optimum conditions (1000×) (Tan et al., 2008) 10
Figure 2.5: Cylindrical, prismatic and cubic shaped briquettes (UNDP / CEDRO, 2016). 12
Figure 2.6: Schema of a piston pressing briquetting machine (UNDP / CEDRO, 2016) 13
Figure 2.7: Schema of a screw pressing briquetting machine (UNDP / CEDRO, 2016). 13
Figure 2.8: Schema of a hydraulic pressing briquetting machine (UNDP / CEDRO, 2016). 14
Figure 3.1: Dehusked and cleaned of coconut fibres 16
Figure 3.2: Alkaline treatment of coconut fibres 17
Figure 3.3: NIKON microscope image 17
Figure 3.4: Universal Testing Machine used to Test Coconut Fibre Tensile Strength 19
Figure 3.5: Equipment and apparatus used 20
Figure 3.6: Thermal treatment of EVA in coconut oil 24
Figure 3.7: Acid pickling process (New Zealand Institute of Chemistry, 2008) 25
Figure 3.8(a): Sample before cleaning 25
Figure 3.8(b): Sample after cleaning 25
Figure 3.9: Mild steel samples outdoor exposure on rack 27
Figure 3.10: Mild steel samples sheltered exposure 27
Figure 3.11: Back surface of outdoor exposure sample after 23 days of exposure 27
Figure 3.12: Photo opened in imageJ 28
Figure 3.13: Colour threshold adjustment 28
Figure 3.14: Image converted to 8-bit 29
Figure 3.15: Plot profile 29
Figure 3.16: Threshold limit 30
Figure 3.17: ImageJ results 30
Figure 3.18: Graph of percentage area corroded against number of days exposed in the atmosphere 31
Figure 3.19: Graph of percentage area corroded against number of days exposed in sheltered place 32
Figure 3.20: Resin Injection and Vacuum Infusion Set Up 33
Figure 3.21: Mould gasket 34
Figure 3.22: Silicone used for airtight pipe connections 34
Figure 2.23: Spindle no. 3 and viscometer 35
Figure 2.24: Vacuum infusion of resin 35
Figure 3.25: Vacuum infused resin 36
Figure 3.26: VMC cutting resin sample 36
Figure 3.27: Specimen dimensions as per ASTM D638 37
Figure 3.28: Tensile strength test of resin sample using UTM 37
Figure 3.29: Fractured specimens from tensile strength testing using UTM 37
Figure 3.30: Levelled table, bubble clinometer and circular bubble clinometer 38
Figure 3.31: Graph of viscosity measured against amount of styrene added 38

Figure 3.32: Vacuum pump and degassing chamber 39
Figure 3.33: Degassing resin in degassing chamber 39
Figure 3.34a: Resin sample without degassing Figure 3.34b: Degassed resin sample 40
Figure 3.35: Discontinuous and randomly oriented fibre-reinforced composite (Callister, 2009) 40
Figure 3.36: Pulveriser Figure 3.37: Sieve shaker 42
Figure 3.38: (a) Coconut husk (2.38 – 1.41 mm) and (b) Coconut shell (2.38 – 1.41 mm) 43
Figure 3.39: Stainless steel horizontal cylindrical reactor 44
Figure 3.40: (a) Coconut husk activated carbon and (b) Coconut shell activated carbon 44
Figure 3.41: Batch adsorption process 46
Figure 3.42: Wastewater samples after batch adsorption. 46
Figure 3.43: Reactor used for pyrolysis 48
Figure 3.44: (a) Coconut husk less than 1mm (b) Coconut shell less than 1mm 48
Figure 3.45: (a) Coconut husk charcoal less than 1mm (b) Coconut shell charcoal less than 1mm 48
Figure 3.47; (a) Non-carbonised briquette (b) Charcoal briquette 50
Figure 3.46; Briquetting machine 50
Figure 3.48: Schema of cylindrical holey type briquette 51
Figure 3.49: Schematic of oxygen bomb calorimeter (Helmenstine, 2018.) 52
Figure 3.50: Non-carbonised briquettes after drop shatter test 53
Figure 3.51: Charcoal briquettes after drop shatter test 53
Figure 3.53: Apparatus used in the analysis of emission from briquette combustion 54
Figure 3.52: Briquette samples ignition 54

ACKNOWLEDGEMENT

I would like to express my profound gratitude to the Mauritius Research Council for funding this project.

I wish to thank University of Mauritius for providing the necessary support in order to complete it.

My sincere gratitude also goes to Dr G. Somaroo for her constant support as co-investigator in the project.

I would finally wish to extend my thanks to the Research Assistants, Ms A. Chineah and Mr J.R. Toinette, and the technicians of the workshop and the metallurgical lab for their constant support in successfully completing the project.

DECLARATION

I certify to the best of my knowledge (1) the statement herein (excluding scientific hypotheses and scientific opinion) are true and complete, and (2) the text and graphics in this report as well as any accompanying publications or other documents, unless otherwise indicated, are the original work of the signatories or of individuals working under their supervision. I understand that willfully making a false statement or concealing a material fact in this report or any other communication submitted to MRC is a criminal offense.

Principal Investigator Signature: 	Date:16 July 2019

ABSTRACT

Coconut is being extensively grown in the Agalega Island (around 800 hectares) and in other islands of the Indian Ocean. Currently, the production of coconut oil in Agalega is 100 drums per year. With the expected increase in the production of coconut products in the future, it has become important to not only aim to develop coconut oil as a fuel but to use the whole coconut as a source of green material for sustainable development.

This study will look into novel uses of coconut oil and possible uses of coconut husk and coconut shell in Mauritius. Therefore, the aims of the project are:

1. To investigate the use of coconut oil as a temporary corrosion prevention method.
2. To explore the various avenues for the integration of coconut husk and shell in the manufacture of composite boards.
3. To analyse the possible production and use of high quality charcoal briquettes from coconut husk, as an alternative to petroleum stove.
4. To analyse the possible production and use of activated carbon from coconut shell and husk.

To fulfil the aims of the study, some relevant properties of coconut oil and fibers were determined. To develop the composites, an injection moulding equipment was developed.

Hence, for the local coconut coir fibers, the average diameter was determined to be 191 ⌈m. The average tensile strength was also found to be on average 33 MPa which is, in general, quite lower than those determined by other researchers worldwide (ranging above 100 MPa). The coconut fibre lignocellulosic contents obtained for the local fibers were presented and were found to be very similar to those obtained by other researchers.

Several mixtures of coconut oil were tested to determine the corrosion prevention properties of coconut oil for temporary outdoor exposures. Cooconut oil mixed with honey and ethylene vinyl acetate (EVA) as additive was found to significantly improve the corrosion prevention properties of coconut oil. EVA was used to increase the viscosity of the coconut oil so as to prevent it from running off the samples when exposed outdoors. Though EVA is not a green material, a convenient green material to replace it needs to be investigated. After 90 days of sheltered exposure, it was found that the mixture consisting of 4% EVA with 71% coconut oil and 25% honey has been found to provide better resistance for the short and long term period, with only 3.6% of the total surface area was corroded after 92 days of exposure. For unsheltered outdoor exposures, the samples coated with the same mixture was found to have corroded 40% less than that of the uncoated one, after 19 days of exposure.

As for the coconut fiber and polyester composites, it was found that their tensile strength was quite low (22-23 MPa) but this was also in accordance with the results obtained from other studies. Various reasons can explain these low values. However, much better results would be expected with a change of the manufacturing method. Compression moulding would be more appropriate and would give better results. However, it would also be interesting to determine other applications of composite, especially for thermal insulation.

1. INTRODUCTION

Coconut is being extensively grown in the Agalega Island (around 800 hectares) and in other islands of the Indian Ocean. Currently, the production of coconut oil in Agalega is 100 drums per year. However, there is a plan to increase the coconut cultivation to 1500 hectares (Veer-Ramjeawon & Chan, 2010). Based on a study performed by the Mauritius Research Council (MRC) and the Outer Islands Development Corportation (OIDC), coconut oil has been considered as a substitute for diesel for transportation and generation of electricity in the island.

Taking into consideration the production of coconut in Agalega and its potential for production in the other islands of the Republic, it is time to start thinking about a coconut industry. Also there is a need to effectively use all the parts of the coconut as efficiently as possible so that none of the parts would be wasted or thrown away.

The aim is not only to use extracted coconut oil as a fuel, but to use the whole coconut as a source of green material for a sustainable development. Coconut oil can have other applications, such as for corrosion prevention and lubrication. Coconut husk and shell, on the other hand, can be used to make composite boards. Moreover, coconut husk has a relatively high calorific value of around 18 MJ/kg which is similar to that of bagasse. Thus, it has a potential to be used as a biomass. Therefore, this project will look into novel uses of coconut oil and possible uses of coconut husk and coconut shell in Mauritius.

1.1 Aims and Objectives

The project involves a study on the effective use of coconut oil, husk and shell. Subsequently, coconut oil as a lubricant and for corrosion prevention will be investigated, and coconut husk and shell will be considered for the manufacture of composite boards, high quality charcoal briquettes and activated carbon.

Therefore, the aims of the project are:

1. To investigate the use of coconut oil as a temporary corrosion prevention method.
2. To explore the various avenues for the integration of coconut husk and shell in the manufacture of composite boards.
3. To analyse the possible production and use of high quality charcoal briquettes from coconut husk, as an alternative to petroleum stove.
4. To analyse the possible production and use of activated carbon from coconut shell and husk.

To fulfil the aims of the study, some relevant properties of coconut oil and fibers were determined. To develop the composites, an injection moulding equipment was developed.

Coconut husk, has been used for making of ropes, etc. Coconut shell has been rarely used for any purpose. Hence, this projects looks into the use of coconut husk and coconut shell for various applications. Such applications include:

- The use of coconut husk and shell in the manufacture of composite boards which can be used for panelling, etc.
- The use of the husk as a potential biomass for the production of coconut husk charcoal briquette.

This project also looks into the use of coconut oil for temporary corrosion prevention. It should be noted that the use of coconut oil, husk and shell for these applications are new or are currently being investigated.

Positive results may lead to the development of a coconut industry. This project is, consequently, of very high commercial value because the results may not only be of potential use by the Mauritians in general but investors may also be interested in the project. It should be noted that the raw material is a cheap, renewable and easily available product commonly grown in the Indian Ocean islands.

2. LITERATURE SURVEY

The literature survey comprises the main findings regarding the use of coconut oil as lubricant, for corrosion prevention and use of corrosion inhibitors as additives. Existing research on coconut husk and shell as composite boards, and in the production of activated carbon and charcoal briquettes have also been reviewed.

The Agricultural Research and Extension Unit (Food and Agricultural Research Council) reported that there are three types of coconut in Mauritius, namely, Ceylan (local), Malayan Dwarf and Pemba. In this regards, the characteristics of the respective coconut varieties are expected to differ from one another.

2.1 Characteristics of coconut oil

2.1.1 Viscosity

Fluid viscosity is its resistance to flow, which is directly related to film formation that protects the metal surfaces from several attacks (Cavalcanti da Silva, 2011). Viscosity is measured using a capillary tube viscometer. The apparatus works by placing the oil sample into a glass capillary U-tube and the sample is drawn through the tube using suction until it reaches the start position indicated on the tube's side. The suction is then released, allowing the sample to flow back through the tube under gravity. The narrow capillary section of the tube controls the oil's flow rate. The procedure is described in ASTM D445 and ISO 3104. A viscosity range between 8 to 15 cSt at 100°C is preferred for biolubricants (Cavalcanti da Silva, 2011). Rani et al. (2015) recorded viscosities of 24.8 cSt and 5.5 cSt at 40^{o}C and 100^{o}C, respectively using a Redwood Viscometer as per ASTM D2270 method.

2.1.2 Viscosity index

Viscosity index (VI) is an arbitrary dimensionless number used to indicate the temperature dependence of an oil's kinematic viscosity (Cavalcanti da Silva, 2011). The viscosity index value is determined through calculation (ASTM D2270 method), which takes in account the product viscosities at 40 and 100°C as per Figure 2.1. A smaller change in kinematic viscosity with temperature will have a higher VI than an oil with a greater viscosity change across the same temperature range (Noria Corporation,n.d). Oils with viscosity index values higher than 130 find a wide diversity of applications (Cavalcanti da Silva, 2011). Coconut oil has a viscosity index of 169 (Rani et al., 2015).

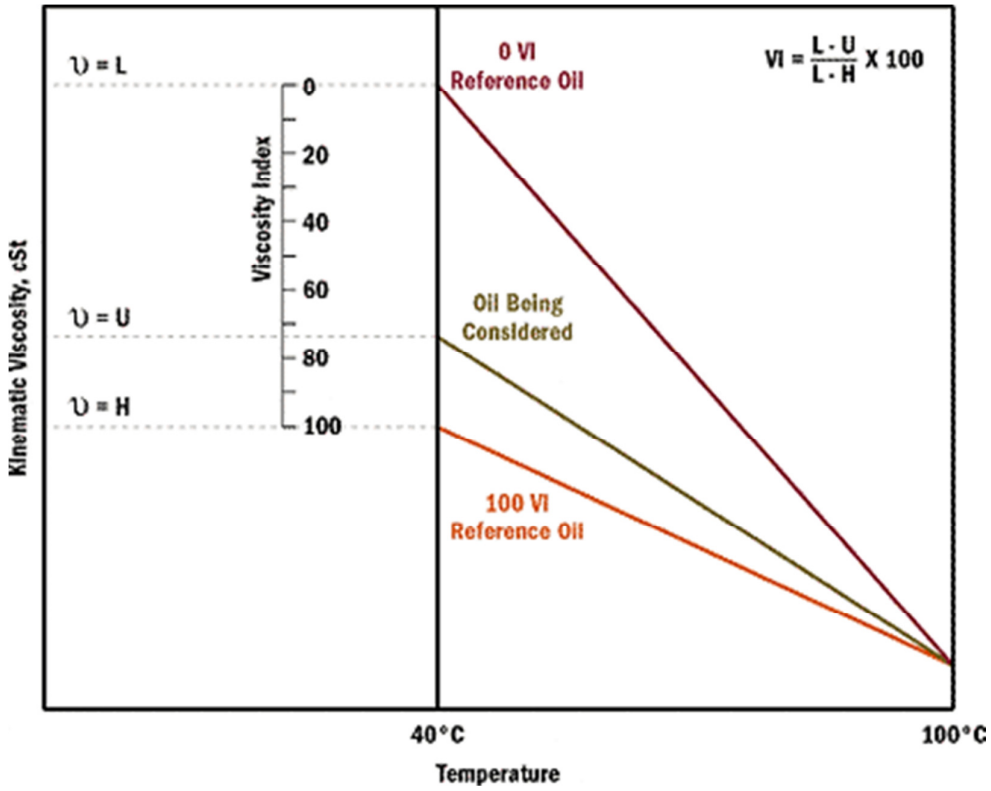


Figure 2.1: Determination of Viscosity Index (Noria Corporation)

2.2 Coconut oil for corrosion resistance

Ahmad et al. (2005) prepared coconut oil based conducting blend coatings of polyaniline and poly(esteramide urethane) by loading different ratios (2, 4 and 8 wt%) of polyaniline in poly(esteramide urethane). Then their physico-chemical, thermal, morphological, conductivity and anti-corrosive coating characteristics were investigated. The effect of a two-year environmental aging process on the coated samples was analysed by thermal methods as well as by corrosion studies. Results showed that the corrosion protective performance of the blend coatings was far superior to that of plain poly(esteramide urethane). These coatings showed enhanced corrosion protection in acid as well as alkaline environments up to 360 and 192 hr respectively. Conductivity of the blends was found to be in the range 2.5×10^{-5}–5.7×10^{-4} S/cm^{-1}. An increase in the thermal stability of the blend coatings and a decrease in their conductivity were noticed in the aged samples which were attributed to the crosslinking effect. The corrosion protective performance of the coatings remained almost unaffected even after two years of aging

Rivera-Grau et al. (2012) studied the corrosion inhibition performance of a coconut-oil modified imidazoline for carbon steel exposed to both carbon dioxide and hydrogen sulfide in 3% sodium chloride solution at 50°C. All the different techniques have shown that very small amounts of this vegetable-based inhibitor, 20 ppm, can be very efficient in decreasing the degradation rate of carbon steel in such aggressive conditions, forming a very stable, protective film.
Inhibition efficiencies [E(%)] were determined according to the following equation:

$$E(\%) = \frac{R_{p,i} - R_{p,b}}{R_{p,i}} \times 100$$

where *Rp,b* is the linear polarization resistance without inhibitor and *Rp,i* is the linear polarization resistance with inhibitor.

Wahyuningrum et al. (2008) studied the synthesis of imidazoline derivative compounds. Three types of compounds were produced: (*Z*)-2-(2-(heptadec-8-enyl)-4,5-dihydroimidazol-1-yl)ethanamine (compound 1a and 1b), (*Z*)-2-(2-(heptadec-8-enyl)-4,5-dihydroimidazol-1-yl)ethanol (compound 2a and 2b) and 2-(2-heptadecyl-4,5-dihydroimidazol-1-yl)ethanamine (compound 3a and 3b). The microwave assisted organic synthesis (MAOS) is more effective than the conventional method in synthesizing these compounds evidenced by the higher chemical yields and the shorter reaction times as shown in Figure 2.2. Compound 2b ((*Z*)-2-(2-(heptadec-8-enyl)-4,5-dihydroimidazol-1-yl)ethanol) has highest corrosion inhibition activity towards carbon steel (39.59%) at 8 ppm concentration in 1% NaCl solution. The increase in concentration of compounds 1b, 2b and 3b in 1% NaCl solution tends to improve the corrosion inhibition activity. Based on the analysis of the degree of surface coverage, θ, and the value of Gibbs adsorption energy, ΔG^0_{ads}, compounds 1b, 2b and 3b have the potential to interact with carbon steel through semi-physiosorption or semi-chemisorption because of their ΔG^0_{ads} values are in between – 20 kJ/mol and – 40 kJ/mol. The latter had been calculated using:

$$Kads=\frac{1}{55}\exp\left(\frac{-\Delta G^0_{ads}}{RT}\right)$$

Where,

R = ideal gas constant = 8.314 J/mol.K and T is temperature in K.

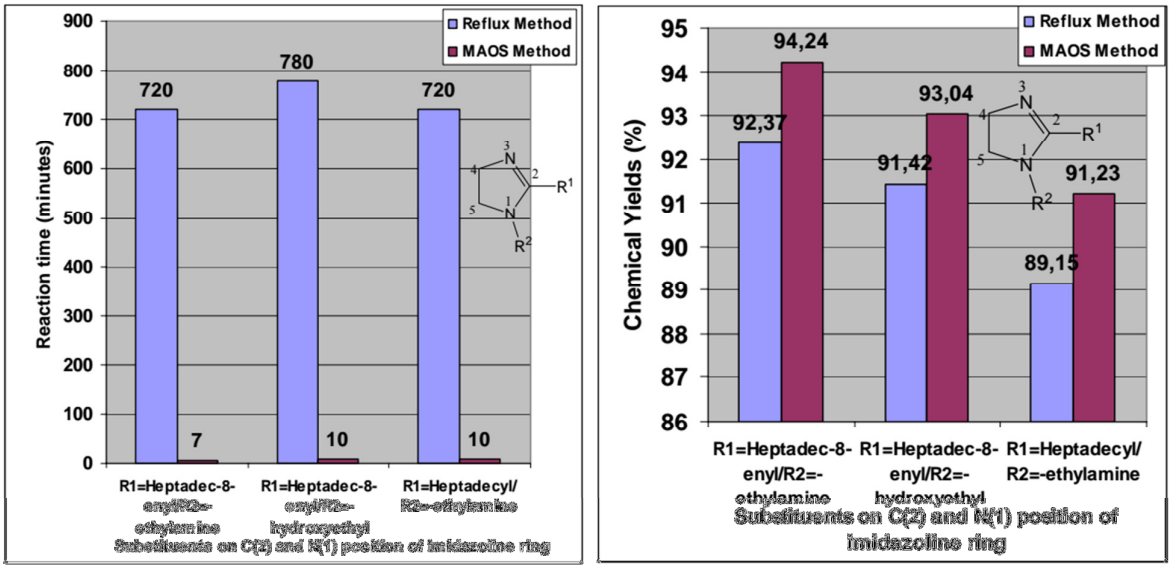


Figure2.2: The relationship between the reaction time and the method used (left side) and the relationship between chemical yields and the method used (right side) in synthesising imidazoline derivative compounds (Wahyuningrum et al., 2008)

El-Etre and Abdallah (2000) found that natural honey exhibited a very good inhibition performance towards steel corrosion in chloride containing water. However, none of this claimed effect was observed for the duplex stainless steel alloys in the acidic chloride solution investigated (Potgieter et al., 2012).

A list of findings pertaining to addition of potential corrosion inhibitors in coconut oil are found in Annex 1.

2.3 Coconut husk and shell in composite material

Gelfuso et al. (2013) made polymers with coconut fibre composites by injection processing (105.7 MPa pressure at 175^{o}C) and mechanically characterised by tensile (ASTM D638 method) and dynamic testing (ASTM E756 method). The fibre content ranged from 0 to 30wt%. The results of Young's modulus obtained from both methods decreased with fibre load and were nearly identical up to 15wt% of fibre, about 1.1GPa, but the increase in fibre concentrations distinctly interferes with each method in the values obtained.

The Dynamic Method used in this study to measure the elastic modulus for coconut fibre-polypropylene composites was revealed as a non-destructive method and a very reliable test. The vegetal fibre-polymer matrix composite usually presents lower mechanical strength than polymeric composite based on inorganic fibres, such as glass, carbon or aramid, but it presents much lower cost due to the natural source of these materials. These composites can be applied in non-structural elements, such as fence panels and linings (Gelfuso et al., 2013).

A detailed list of research in the use of coconut husk and shell in composites are presented in Annex 2 and Annex 3, respectively.

2.4 Coconut husk and shell as activated carbon

2.4.1 Activated Carbon

Activated carbon is a carbonaceous materials, with a high degree of porosity and an extended inter-particulate surface area (Bansal & Goyal, 2005). It is a tasteless black solid that resembles powder or granular charcoal and is generally amorphous, microcrystalline and non-graphite form of carbon (Yahya, 2015). Activated carbon has a high adsorptive surface area between 500 to 1500 m^2/g and the pore volume ranges between 0.7 to 1.8 cm^3/g (Çeçen & Aktaş, 2011).

2.4.2 Manufacture of Activated carbon

Pre-treatment of precursors

Activated carbons are mostly produced in granular and powdered forms depending on the final application. Prior to the activation process the raw material need to be pretreated. The precursor must first be reduced to the required particles size by crushing and sieving. Sometimes a water or acid washing step is applied in order to remove any dirt or to reduce any mineral matter. If coking coal is used as raw material, a peroxidation treatment is required so as to prevent the formation of a liquid phase during carbonization. Moreover some low volatile precursors (medium-high rank coals) need to be pulverized, briquetted and again crushed to an appropriate particle size, because the meso and macropore networks of these materials are not well developed if carbonized directly (Bandosz, 2006).

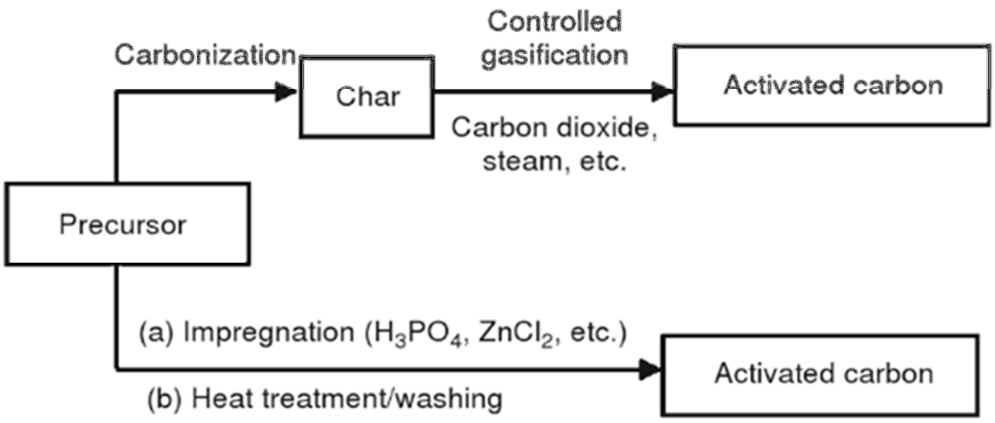


Figure 2.3: Flowchart for activated carbon production (Marsh and Rodriguez-Reinoso, 2006)

Activation Method

Generally there are two methods for the preparation of activated carbon, namely;

- Physical (thermal) activation
- Chemical activation.

1) Physical activation

The production of activated carbon by the physical activation process consists of two consecutive steps. Firstly the carbonization (or pyrolysis) of the precursor at moderate temperatures (280 – 500 ^{o}C) under inert atmosphere and secondly the activation of the char produced, where the char is partially gasified with oxidizing gases (usually steam or carbon dioxide or both) at higher temperature (usually 800 – 1000 ^{o}C). The aim of carbonizing the precursor is to produce a char rich in carbon, whereby non-carbon atoms are eliminated from its aromatic structure. Whereas the activation process as for objective to enlarge and open incipient porous structure developed during carbonization (Bandosz, 2006; Feng, 2015; Marsh and Rodriguez-Reinoso, 2006; Rufford et al., 2013).

During the physical activation process, the oxidants react with carbon atoms from the incipient porous structure according to the following equations;

$$C + H_2O \longrightarrow CO + H_2$$

$$C + CO_2 \longrightarrow 2CO$$

It should be noted that oxygen as an oxidizing agent is scarcely applied, because of its highly exothermic reaction, which makes the process difficult to control. On contrary for carbon dioxide and steam, the reactions are endothermic which provide a better control on temperature uniformity and activation rate (Rufford et al., 2013; Feng, 2015).

2) Chemical activation

The chemical activation of a precursor is done in a single carbonization stage, where the precursor is impregnated with an activating agent (typically H_3PO_4, $ZnCl_2$ and alkaline hydroxides) and then heated up in an inert gas atmosphere (the temperature would depend on the chemical agent used). After the carbonization, the activated carbon must be washed to eliminate the remaining chemical agent (Bandosz, 2006; Feng, 2015).

The most widely used chemical agents are $ZnCl_2$, H_3PO_4, KOH and NaOH, where $ZnCl_2$ and H_3PO_4 are preferred for the activation of lignocellulosic materials and alkyl hydroxides for activating of high-rank coals, chars and petroleum coke (Feng, 2015). The activation mechanism of these agents differ all from each other's, where $ZnCl_2$ promotes the extraction of water molecules from the lignocellulosic structure of the precursor, and H_3PO_4 combines chemically with the lignocellulosic structures. The mechanism for alkali metal hydroxides is more complex, which involves the disintegration of structure, followed by intercalation as well as some gasification by oxygen of the hydroxide. The advantage of these types of activation is that, there is a high carbonization yield, since there is no selective removal of carbon atoms as for physical activation (Marsh and Rodriguez-Reinoso, 2006).

i) Phosphoric acid activation

Phosphoric acid is generally used as activating agent for lignocellulosic material like wood and agricultural by-products, as well as for carbonaceous materials with high volatile content. Surface areas of about 1500 m^2/g are yielded for these types of precursors. Typical conditions for activation by H_3PO_4 are; an activation temperature of 350 – 550 ^oC, an activation time of 1 - 2h and an impregnation ratio of 1.5 g H_3PO_4/g precursor.

ii) Zinc Chloride activation

Raw materials with high oxygen content like low-rank carbons and lignocellulosic materials are often activated by zinc chloride, due to the high reactivity of $ZnCl_2$ and the OH group of the lignocellulosic materials. An activation temperature of around 300 – 600 ^oC are often used for activation by $ZnCl_2$. An impregnation ratio of 1.5 – 3.0 g $ZnCl_2$/g precursor and an activation time of 1 – 2 h are used depending on the precursor.

iii) Activation with alkali metal hydroxides

The activation process by metal hydroxides is completely different to that of H_3PO_4 and $ZnCl_2$. Precursors with high-rank carbons and chars are the most appropriate, because the reagent reacts directly with the carbon structure generated after the carbonization of the raw material. Activation by NaOH or KOH is normally done in an inert condition, because in air the precursor would be burned up and reacts with the metallic alkyl formed. Nevertheless the activation with metal hydroxides has a high influence on the surface area and pore structure of the activated carbon. Suitable temperatures for the activation by metal hydroxides are around 700 – 900 ^oC, with an impregnation ratio of 1 – 4 g reagent/g precursor and an activation temperature of 1 – 1.5 h are used to obtain activated carbons with surface areas of up to 3000 m^2/g.

Activating agent recovery

Environmental impacts are one of the main concerns when using chemical activation. Some chemical agents could be recovered and reused during chemical activation, which could reduce the production cost and expense concerning treatment and disposal of waste.

In order to recover activating agents, they must act as a catalyst during the process. The recovery of phosphoric acid varies with the production conditions. For instance, with a high activation temperature, there is a low H_3PO_4 recovery. $ZnCl_2$ is a reagent that can be recovered in high percentages at moderate activation conditions. But metal alkyl hydroxides cannot be recovered, because they are decomposed to metal carbonates or metal oxides during the activation process (Rufford et al., 2013).

Physical treatment versus chemical treatment

Chemical activation has shown more advantages over physical activation. Chemical activation needs lower temperatures, has higher surface area, produces higher yield, only involves one step, creates well developed micro porosities, and reduction of mineral matter content as compared to the physical activation. Nevertheless, there are some disadvantages in chemical activation such as, the need of washing for the removal the impurities that come from the activating agents and also the corrosiveness properties of the agents (Yahya et al., 2015).

2.4.3 Types of activated carbon

Activated carbon is mostly used in the form of powdered activated carbon (PAC) and granular activated carbon (GAC). According to the ASTM D5158, PAC particles have a size of less than 0.177 mm or 80 mesh (Marsh and Rodriguez-Reinoso, 2006; Çeçen & Aktaş, 2011), and also the American Water Works Association Standard, states 95 – 100% of PAC will pass through a sieve of 0.297 mm. Normally PAC has an average particle size of 15–25 µm and is usually produced from sawdust, while GAC has a particle size ranging from 0.2 – 5 mm and is generally in the form of crushed granules of shell or coal. GAC may also be produced by granulation of pulverized powders and binders like coal tar pitch. For liquid phase applications, GAC is designated by mesh sizes such as 8/20, 20/40, or 8/30 and 4/6, 4/8, or 4/10 for vapor phase applications. The optimum particle size for liquid phase adsorption is in the range of 12/42 mesh (Çeçen & Aktaş, 2011).

2.4.4 Use of Activated Carbon

Nowadays, activated carbon has a wide application, particularly in the environmental field, for environmental pollution control. Moreover in industry, it is mostly used in various liquid and gas phase adsorptions. Activated carbon is also used for the removal of pesticide residues, in medical and veterinary applications and in nuclear and vacuum technologies. Some of the industrial liquid and gas phase adsorptions applications are list in the Table 2.1 (Çeçen & Aktaş, 2011).

Table 2.1: Liquid and gas phase applications of activated carbon in industry

Liquid phase applications	Gas phase applications
Preparation of alcoholic beverages	Recovery of organic solvents
Decolorization of oils and fats	Recovery of sulfur and removal of sulfur-containing toxic components from exhaust gases
Product purification in sugar refining	Biogas purification
Purification of chemicals	Use in gas masks
Enzyme purification	
Decaffeination of coffee	
Gold recovery	
Refining of liquid fuels	
Purification in electroplating operations	
Purification in textile, cosmetics and pharmaceutical applications	

2.4.5 Review of studies on coconut husk and shell.

Tan et al. (2008) prepared activated carbon from coconut husk using physiochemical activation method, which consists of potassium hydroxide (KOH) treatment and carbon dioxide (CO_2) gasification. The investigation involved variables, such as activation temperature (698 to 951^oC), activation time (0.3 to 3.68 h) and chemical impregnation (KOH:char) ratio (0.01 to 4.89) on the adsorption capacity of methylblue dye and carbon yield (3.23 to 23.42 %). The optimum conditions found for preparing activated carbon were an activation temperature of 816^oC, an activation time of 1 h and KOH:char ratio of 3.9.

Figure 2.4 shows the scanning electron microscopy of raw coconut husk (Figure 2.4 (a)) and activated carbon (Figure 2.4 (b)). In figure 2.4 (a), very little pores are available on the surface of the coconut husk. However, after KOH treatment and CO_2 gasification under the optimum preparation conditions large pores in a honeycomb shape were developed on the surface of the activated carbon (Figure 2.4 (b)) (Tan et al., 2008).

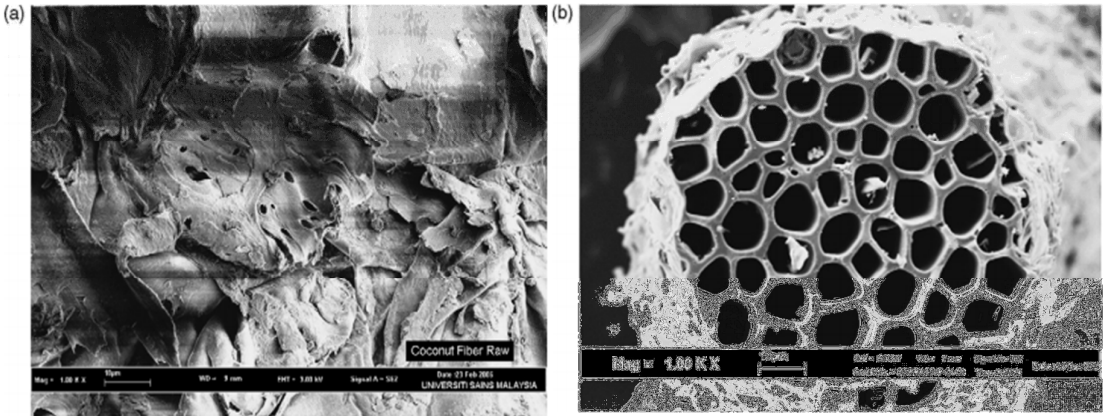


Figure 2.4: (a) SEM image of raw coconut husk (1000×). (b) SEM image of coconut husk-based activated carbon prepared under optimum conditions (1000×) (Tan et al., 2008)

Yusufu et al. (2012) considered the following characteristics of activated carbon from coconut shell:

- Iodine number (Okuo et al., 2008 as cited in Yusufu et al., 2012)
- Activated carbon sample free aliquot solution was prepared by centrifuging 0.5g of activated carbon in 75.0ml of 0.086M iodine solution using 5 ml of freshly prepared starch indicator
- 0.1 M sodium thiosulphate solution was then titrated against 60.0 ml of activated carbon sample free aliquot solution
- Iodine value (IV) is calculated using the formula:

$$IV\ (mg/g) = Y- X \div Y \times V \div W \times M\ (126.9)$$

Where, Y = volume of thiosulphate for blank, X = Titer value, V =volume iodine solution used, W= Weight of sample. M = molarity of iodine solution.

- Carbon hardness, using ASTM (2002) method.
- This involves measuring 2 g of carbon sample in a standard sieve no 40. The sieve was shaken for 1h using mechanical shaker (Millano Italia-type) at 160 strokes per minutes with four steel balls (6.0

mm diameter each) inside the sieve. The amount of activated carbon retained in the sieve after 1h was expressed in percent.

- Bulk density was determined according to the method of Okaka & Potter (1977). 5 g of activated carbon was weighed in a graduated glass cylinder and tap until a constant volume is noted. The density was calculated in g/cm^3.
- Moisture content was determined by the air-oven method as reported by AOAC (1994).
- Ash content was determined according to AOAC (1994).

The results obtained by Yusufu et al. (2012) are tabulated in Table 2.2.

Table 2.2: Characteristics of coconut shell activated carbon prepared by heat action and acid activation

Characteristic	**Heat activation**	**Acid activation**
Acid	-	Concentrated phosphoric acid (H_3PO_4)
Carbon:Acid	-	1:4
Activation Temperature	850^{o}C for 2 ½ h	600^{o}C, 2h
Activation yield	36.30-41.10%	40.40-46.21%
Iodine value	840.18mg/g	848.69mg/g
Hardness	96.5%	81.0%
Ash	2.4%	2.8%
Bulk density	0.66g/cm^3	0.68g/cm^3
Moisture	5.1%	6.4%
Surface area	895m^2/g	912m^2/g
Porosity,V_{meso}	0.040cm^3/g	0.035cm^3/g

Annex 4 provides more research in the preparation of activated carbon from coconut husk and shell.

2.5 Briquette production from coconut husk and shell

According to ISO 17225 standard, solid biofuels, fuel specifications and classes, a briquette is defined as "a densified biofuel made with or without additives, having a cubic, prismatic or cylindrical shape, with a diameter greater than 25 mm, produced from woody biomass compression or crushed herb."

In general, cylindrical sawdust briquettes have a diameter of 50 – 80 mm and a length of 150 mm, compressed at a high temperature, with a moisture content ranging between 10 to 20%. Rectangular or prismatic shapes, are also used, depending on the manufacturer and they may have holes in order to enhance their combustion. Briquettes may be composed of dried, crushed and densified wood or

charcoal, molded under high pressure.

2.5.1 Briquetting manufacturing process

Briquettes are basically manufactured by compressing and compacting vegetation or industrial materials. Typically a briquette production process consists of the following stages:

(i) Size reduction

(ii) Screening

(iii) Mixing

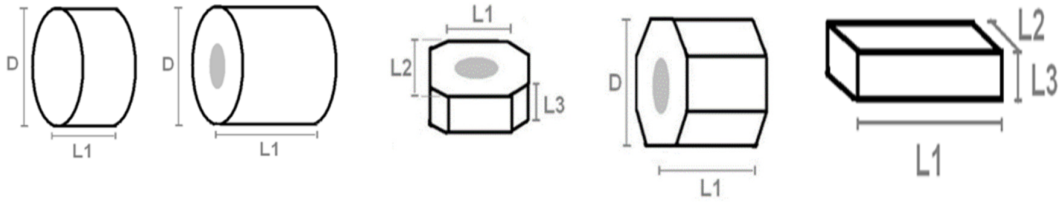
(iv) Briquetting

(v) Drying

The raw materials are pulverised and sieved to a size of about 3 mm or smaller, then dried if required. The raw materials are then homogenized through mixing. Different types of additives may be added, such as binding agents (starch), desulfuring agents ($Ca(OH)_2$), fillers ($CaCO_3$) or sodium nitrate (to enhance combustion), depending on the nature of raw materials and end-product requirements. The mixture is then compressed in a briquetting machine and shaped accordingly. If necessary, briquettes are dried, so as to achieve the ideal moisture content (~ 5%) for efficient combustion (NIIR, 2015; FAO, 1987).

When materials with high lignocellulosic content are used, the high temperature attained during the compressing stage causes the softening of the lignin, which acts as a binder as it cools down, thus any other compacting additives are required (Aguilà, 2013). However if the briquette obtained lacks of consistency and breaks apart, regulations like ISO 17225, allow the use of specific additives to improve and maintain briquettes' compaction. Additives such as starch (rice flour, cassava flour and mashed sweet potato), molasses or Arabic gum may be used. An adequate moisture content of 5 to 15% of the biomass weight is necessary to initiate the densification process (FAO, 1987).

Briquettes may have various geometries, whether cylindrical, prismatic or cubic, depending on the briquetting machine outlets, but the most typical ones are cylindrical or prismatic.



(i) Cylindrical *(ii) Prismatic* *(iii) Cubic*

Figure 2.5: Cylindrical, prismatic and cubic shaped briquettes (UNDP / CEDRO, 2016).

2.5.2 Briquetting technologies

The most widely used briquetting technologies are as following (Aguilà, 2013):

i) Piston Briquetting (Impact densification)

A piston driven by a flywheel is used to push the crushed biomass throughout a cylinder mould.

Generally the densities achieved are 1,000 to 1,200 kg/m^3 (UNDP / CEDRO, 2016).

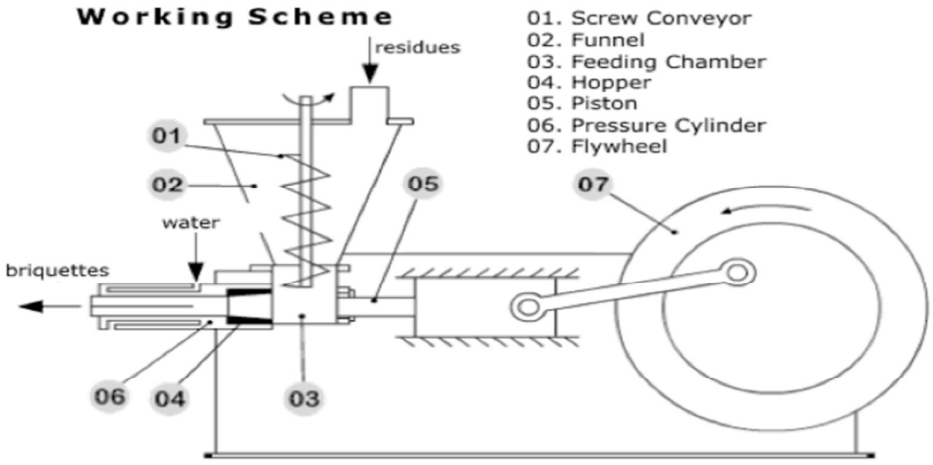


Figure 2.6: Schema of a piston pressing briquetting machine (UNDP / CEDRO, 2016).

The main components of briquetting piston machine are:

• **Biomass hopper**: the storage container that dispensed the crushed biomass for compaction. The amount of biomass to be dispensed into the compacting cylinder is controlled by automated valves.

• **Pressing cylinder, piston and matrix**: the chamber where briquettes are densified by the pressing action of a piston. A matrix with the desired shape is fixed, at the end of the compacting cylinder.

• **Flywheel**: the rotating component that drives the piston. It is used to store kinetic energy for a stable and continuous operation.

In terms of maintenance, periodically inspection is required to ensure that there is no remaining biomass in the cylinder, which may affect the proper compacting process. The rotating mechanisms will also require periodic checking up and lubrication of moving elements.

ii) Screw Briquetting (Extrusion densification):

In this technology, the raw material is pressed by a special screw within a chamber that becomes progressively narrower. This system also enables the formation of inner holes in briquettes and it can achieve higher briquette densities, ranging between 1,300 – 1,400 kg/m^3 (UNDP / CEDRO, 2016).

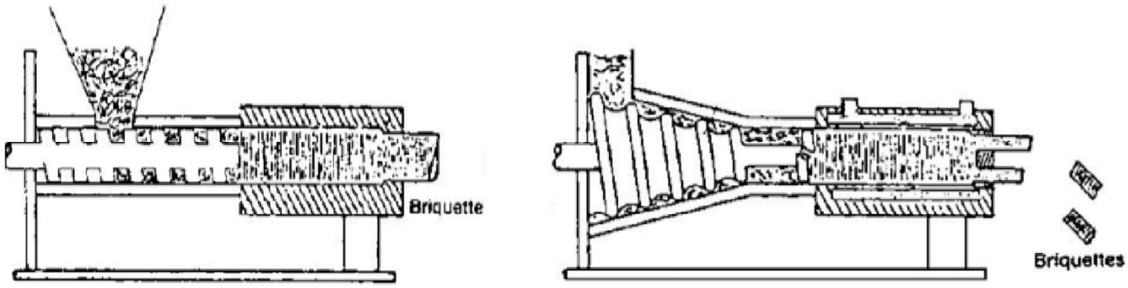


Figure 2.7: Schema of a screw pressing briquetting machine (UNDP / CEDRO, 2016).

The major elements of the screw briquetting units are:

• **Hopper**: which stores the crushed biomass prior to densification process.

• **Extrusion screw**: the component that is responsible for moving and compressing of biomass.

• **Extrusion matrix**: it is the place where the densification of briquette is produced and shaped accordingly.

• **Briquette cutter**: the briquettes are cut in a fixed length.

• **Control panel:** contains the electrical circuits and protects the mechanism that powers the moving components, as well as the electronics that control the whole system.

Concerning the maintenance of the screw briquetting machines, it is important to ensure that there are no traces of resin on the screw and matrix, and to check the sharpness and cleanliness of the cutter's edge, in order to have a neat briquette cutting. The moving elements will also require regular lubrication and checking up their rotating mechanisms.

iii) Hydraulic or pneumatic briquetting

In hydraulic briquetting, the pressure is applied by the action of a cylinder operated by a hydraulic or pneumatic system. This process is usually used when the raw material is of poor quality, such as a high moisture content (< 30%) or when not requiring detailed definition of the briquette form (clearly cut and shaped). The briquettes have densities ranging between 700 to 1000 kg/m^3 (UNDP / CEDRO, 2016).

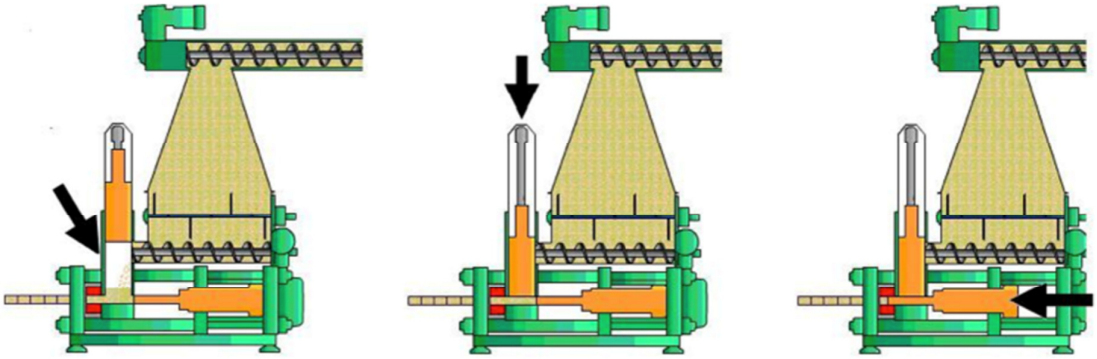


Figure 2.8: Schema of a hydraulic pressing briquetting machine (UNDP / CEDRO, 2016).

The hydraulic briquetting systems are very similar to the other types of briquetting units discussed above (hopper, control panel, matrix) with the exception that a hydraulic or pneumatic system is used to move the piston.

The hydraulic briquetting is an energy efficient equipment with low maintenance costs, basically required some checking up of eventual material adhesions in the cylinders or matrix. It also accepts a thicker and more heterogeneous biomass, or biomass with a higher moisture content. But a less dense briquette and an unstable shape is obtained compared to other densifier technologies (UNDP / CEDRO, 2016).

2.5.3 Charcoal briquettes

Charcoal is a blackish solid carbon residue obtained by the removal of water and other volatile constituents from vegetation substances through the process of carbonization (or pyrolysis), where the carbonaceous raw materials are burnt in the absence of oxygen.

During carbonisation or pyrolysis, the woody materials are heated in a closed vessel (kiln or retort) at temperature around 450 to 510 ^{o}C, in limited or absence of oxygen otherwise the materials would be

ignited and burned away to ashes. Without oxygen, the wood substance is decomposed into various substances, mainly charcoal and other by-products (liquid and gaseous products) which may be collected from the vapours driven off if a retort is used (Bekele et al., 2013; sugumaram & seshadri, 2010).

When wood is heated in a retort it passes through definite stages, prior to charcoal conversion. In a study done by FAO, the formation of charcoal was investigated under laboratory conditions and the following stages were predicted;

20 – 110°C; The wood absorbs heat and gives off its moisture (water vapour/steam) as it dries. The temperature remains at or slightly above 100°C until the wood is bone dry.

110 – 270°C; The decomposition of wood begins, giving off some carbon monoxide, carbon dioxide, acetic acid and methanol.

270 – 290°C; The wood starts to decompose exothermically. Heat is evolved and breakdown continues spontaneously and mixed gases continue to be given off along with some tar.

290 – 400°C; Decomposition of the wood continues, the vapours given off which consist of combustible gases (hydrogen and methane), condensable vapours (water, acetic acid, methanol, acetone, etc.), together with carbon monoxide and carbon dioxide, plus further tars which start to predominate as the temperature increases.

400 – 500°C; The transformation of the wood to charcoal is almost completed at 400°C. But the charcoal still contains significant amounts of tar (~30% by weight trapped in the structure). Hence further heating is required to drive off more tar and increase the fixed carbon content to about 75% (typically for a good quality commercial charcoal). Therefore the charcoal is subjected to further heat until its temperature meets 500°C, for completing the carbonisation stage.

Charcoal briquettes are made of three main constituents; charcoal fines, binder and filler or burn-rate controller. The latter decreases the production cost and slow down the burning rate of the fuel, which is supposed to be beneficial for some kinds of cooking.

The manufacturing process of charcoal briquettes is as follows:

The charcoal must be first milled and screened to reduce it to a uniform size and remove gross impurities. The pulverised charcoal is then mixed with binder, filler or any other additives if used. If starch is used as binder it must first be cooked with hot water before mixing. A proper mixing is necessary to reduce binder consumption. The mixture is next passed to the briquetting machine. The wet pressed briquettes are then dried to complete the binding action. The briquettes generally contain about 10% of binder and 30% of water before drying down to around 5% moisture content (FAO, 1987).

3. METHODOLOGY AND TECHNICAL INFORMATION

The varieties of coconut cultivated in Agalega are the same as that in Mauritius, and these are namely; Ceylan (local), Malayan Dwarf and Pemba. The Ceylan (local) is of big variety and its flowering begins around the 5th year and arrives in full production during its 7th year. Whereas the Dwarf varieties such as the Malayan Dwarf and Pemba begin to produce around the 3rd year. (ARC, n.d). Since the properties of the coconut vary from region to region, it is important to first determine the properties of the coconut available locally. The use of coconut oil for corrosion prevention and lubrication were investigated. Sample slabs made from coconut husk and shell were tested and their possible uses in Mauritius were evaluated. The calorific value of coconut husk and shell were determined in order to investigate their potential use as briquettes. In addition, the coconut husk and shell in the form of activated carbon was assessed for the treatment of textile wastewater.

3.1 Determining properties of coconut fibres

The tensile properties of coconut fibres were determined according to ASTM C1557-03, the standard test method for tensile strength and Young's modulus of fibres. And the lignocellulosic content (cellulose, hemicellulose and lignin contents) of the fibres were determined through the Van Soest fibre analysis method.

3.1.1 Preparation of raw materials

Prior to the determination of the properties of coconut fibres, the raw materials was prepared. The steps involved in preparation of coconut fibres were:

- Dehusking and cleaning of coconut.
- Alkaline treatment of fibres.
- Drying and storing fibres for testing.

i) Dehusking and cleaning of coconut

Dehusking and cleaning process of coconut was carried out manually. A machete was used to open and detach the husk from the shell. Hammering method was used to partially separate the fibres. The latter were combed to remove the pith attached to the fibres. However, it was observed that the fibres were breaking while combing, therefore the hammered husks were soaked in water overnight before combing. The cleaned coconut fibres were then allowed to air dry for two to three days and stored in a dry and cool storage area. Figure 3.1 shows the dehusked coconut and cleaned coconut fibres.

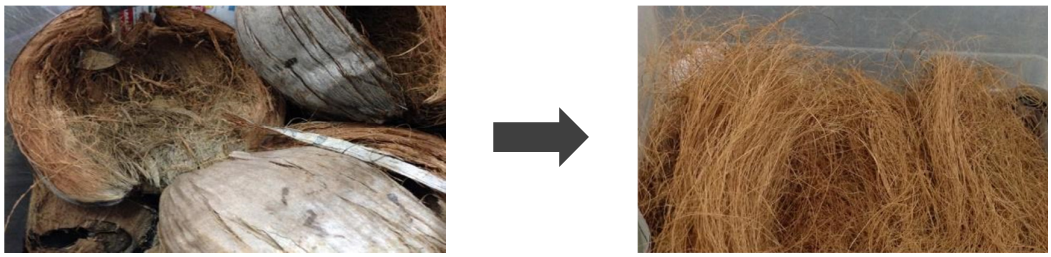


Figure 3.1: Dehusked and cleaned of coconut fibres

ii) Alkaline treatment of coconut fibres

The cleaned coconut fibres were treated with 6% w/w sodium hydroxide (NaOH). The procedure

followed were:

- 500 mL of distilled water was added in a beaker
- 54g of NaOH pellets was measured on a weighing balance
- the NaOH was added in the beaker and stirred till the pellets dissolved
- Additional water (346 mL) was added to make 900 mL of solution
- The fibres to be treated were then added into the beaker and continuously stirred for two hours using a magnetic stirrer (see Figure 3.2)
- The fibres were then rinsed with water and air dried for 72 hours
- The treated coconut fibres were stored in a dry and cool place

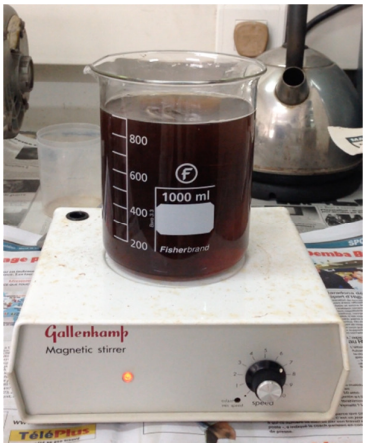


Figure 3.2: Alkaline treatment of coconut fibres

3.1.2 Testing tensile strength and Young's modulus of coconut fibres

Alkaline treated and untreated coconut fibres were used to test for their tensile strength and Young's modulus using the ASTM C1557-03 method. Ninety fibres from the treated and untreated bunch each were randomly selected. The diameter of the fibres was first measured using a calibrated NIKON microscope with magnification 50x and a microscope image capture and measurement (MICAM) software prior to tensile strength testing. The microscope and image obtained are as shown in Figure 3.3. Diameter was measured at five different positions and an average was calculated as in Annex 5.

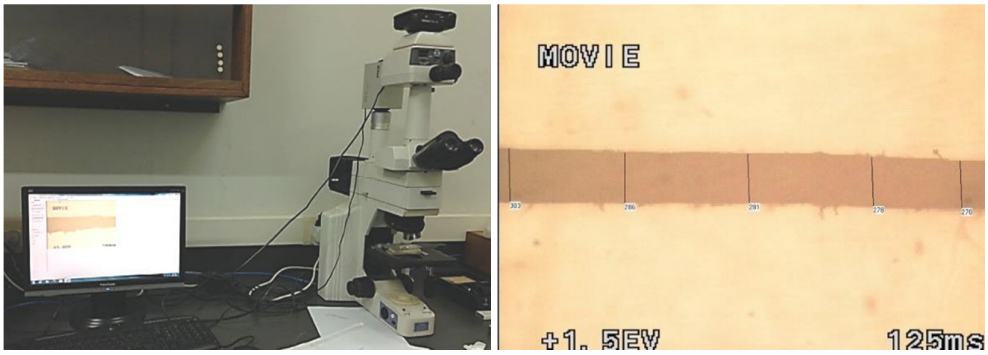


Figure 3.3: NIKON microscope image

ASTM C1557 method was chosen to screen fibres (alkaline treated and untreated coconut fibres) for making of composite materials. Preliminary precautions to be taken prior to tests involved:

- Risk of slow crack growth effects is to be minimised through rapid testing rates to obtain maximum strength of a fibre.

- The gripping area need not exert insufficient pressure which might cause slippage nor too much pressure which would cause fracture. The fibres are not to be twisted and contact with the fibre within the gate length is to be avoided.

The test was carried out with the Testometric M500-50AT Universal Testing Machine (UTM) as shown in Figure 3.4, which was last calibrated in June 2016, as follows:

- The gage length was set at 25.4×10^{-3} m
- Fibre length used had to be 1.5 times longer than the gage length ($\geq 38.1 \times 10^{-3}$ m)
- A constant cross-head displacement rate of 25 mm/min (4.2×10^{-3} m/s) was selected as maximum strength at fracture was obtained within 30s as specified in the standard
- Specimen was mounted using pneumatic grips of the machine, and it was ensured that it was axially aligned
- A load cell of 20N was used
- The load cell was zeroed before initiating the test
- Gage length elongation was determined indirectly by the difference in displacement from gage length
- The force to failure was determined and cross sectional area of the fibre at fracture was measured using the NIKON microscope and MICAM software.
- Tensile strength, T (Pa) was calculated as in the equation below; that is the force to failure, F (N) over fibre cross-sectional area at fracture plane, A (m^2).

$$T = \frac{F}{A}$$

- Strain, E was calculated as the elongation of the gate length, l (m) over the gage length, Δl_0 (m).

$$E = \frac{\Delta l}{l_0}$$

- Hence, the Young's modulus was obtained as the ratio of the tensile stress over strain.

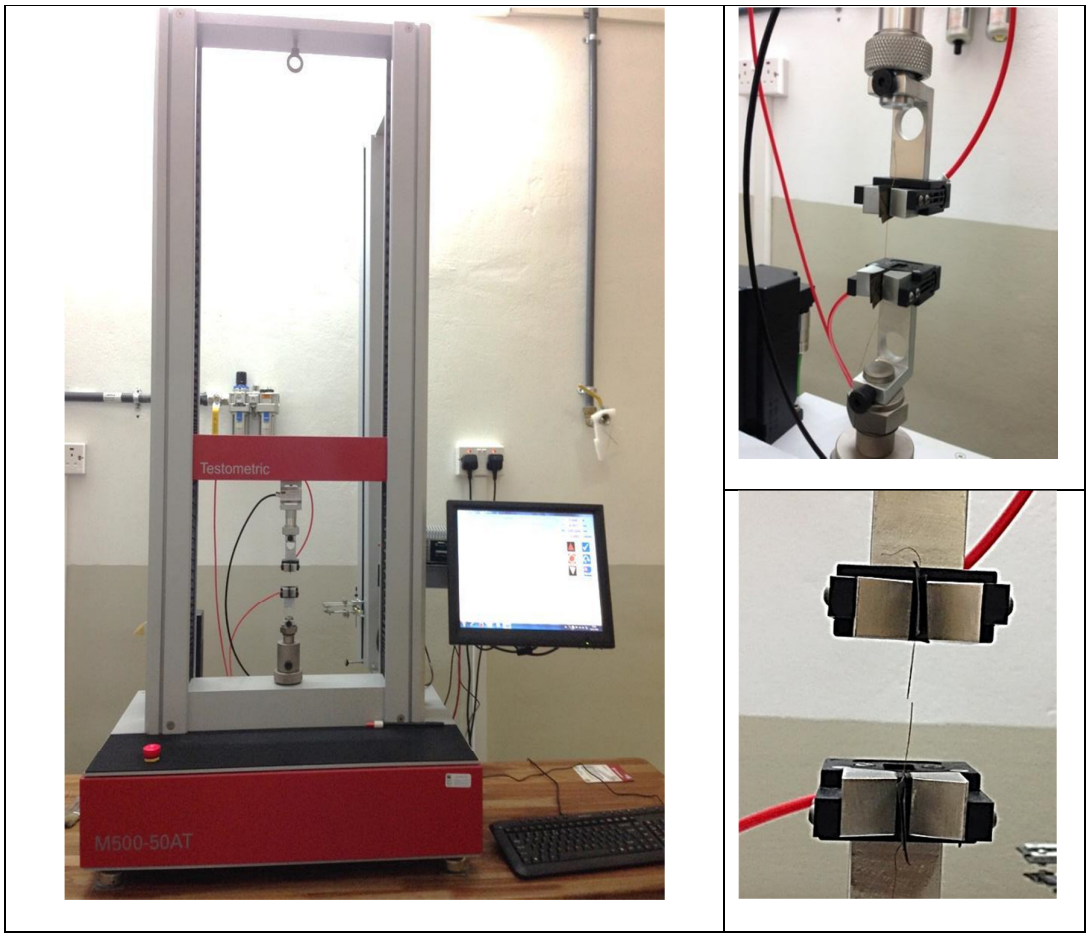


Figure 3.4: Universal Testing Machine used to Test Coconut Fibre Tensile Strength

According to ASTM C1557, an initial test speed of 8 x 10^{-6} m/s (0.480 mm/min) may be used. Hence, the tensile properties of coconut fibres were first being testing at a test rate of 0.480 mm/min with a load cell of 100 N. However, the time taken for the sample to break was around 15 to 20 minutes for untreated and treated fibres, respectively. Therefore, trials were carried out with test speed ranging from 0.480 to 25 mm/min to identify the required one to obtain fibre fracture within 30 s as per ASTM C1557. The load cell was changed to 20 N for better accuracy since for the 100 N load cell had a deviation of 28.5 % for a force of 14.3 N whereas the 20N load cell had a deviation of 7.8% for a 3.69 N force. The final parameters used were a 20 N load cell and a test rate at 25 mm/min.

3.1.2.1 Results for Tensile Testing and Young's Modulus

The tensile strength and Young's modulus results obtained are presented in Annex 6. A summary of the results obtained are shown in Table 3.1.

Table 3.1: Summary of tensile strength and young's modulus of coconut fibres

	Untreated coconut fibres	**Treated coconut fibres**
Average Diameter (µm)	236	191
Average Tensile strength (MPa)	30.049	33.058
Average Young's modulus (MPa)	1.343	0.964

3.1.3 Lignocellulosic content of coconut fibres (cellulose, hemicellulose & lignin)

To determine the lignocellulosic content of coconut fibres, the procedure and equipment described below were used.

Apparatus; -

Refluxing apparatus (Round-bottom flask connected to reflux condenser)
Heating Mantle
Vacuum filtration
Oven
Analytical balance (to nearest 0.1mg)
Furnace
Desiccator



Figure 3.5: Equipment and apparatus used

The ISO 16472 referring to Analysis of Neutral Detergent Fibre (NDF) in Feed, was used as procedure for the determination of the NDF content. Neutral detergent solution (NDS) is used to dissolve the easily digestible proteins, lipids, starches, sugars and pectins in feeds, leaving an insoluble fibrous residue that is mainly plant cell wall components (cellulose, hemicellulose and lignin) and some indigestible nitrogenous matters.

The ADF and ADL contents were determined according to the ISO 13906:2008, Animal feeding stuffs - Determination of acid detergent fibre (ADF) and acid detergent lignin (ADL) contents. The first stage of this method is the determination of the ADF, where acid detergent solution (ADS) is used to remove acid-labile carbohydrates, protein that is not complexed into Maillard products (heat damaged), and fats. The remaining fibrous residue is primarily cellulose and lignin or insoluble protein complexes (animal products and heat-damaged feeds). In the second stage, the remaining residue is solubilized by 72 % mass fraction (12,00 mol/l) sulfuric acid, leaving the lignin (ADL) which is determined gravimetrically.

The percentages of cellulose, hemicelluloses and lignin were then calculated using the equations below:

$$\textit{Cellulose (\%)} = \textit{ADF} - \textit{ADL}$$

$$\textit{Hemi-cellulose (\%)} = \textit{NDF} - \textit{ADF}$$

$$\textit{Lignin (\%)} = \textit{ADL}$$

i) Neutral Detergent Fibre (NDF) Procedure

Preparation of neutral detergent solution

- Put 18.61g EDTA Disodium Ethylene Diamine Tetraacetate Dihydrate, ($C_{10}H_{14}N_2Na_2O_8.2H_2O$) and 6.81g Sodium Tetraborate (Sodium Borate decahydrate), ($Na_2B_4O_7$.$10H_2O$) in a beaker and add some distilled water and heat until dissolved.
- Add 30g Sodium Lauryl sulphate, ($C_{12}H_{25}OSO_3Na$), 10mL Triethylene glycol, ($C_6H_{14}O_4$) and 4.56g anhydrous Disodium Hydrogen phosphate, (Na_2HPO_4). Add water and heat until dissolved.
- Mix and dilute to 1000 ml check pH in the range 6.9 – 7.1.

Conventional apparatus method;

1) Weigh approximately 1g ± 0,001 g of air-dry sample (particle size < 1mm) and place it into a round-bottom flask connected with a condensing unit.
2) Followed by 100mL preheated neutral detergent solution being added into the flask.
3) Heat the mixture for 1h at its boiling temperature.
4) The solution was then cooled down to room temperature and filtered.
5) Wash the residue 3 times with hot distilled water, followed by 3 times with acetone and then vacuum dried.
6) Further dry the sample at 105°C for a minimum of 8 h and leave to cool in the desiccator and weigh to the nearest 0,000 1 g.
7) Calculate NDF content on an "as-received" basis in percent, by using the following equation;

$$\%\ NDF = \frac{Mass\ of\ dry\ residue\ after\ NDS\ treatment}{Initial\ mass\ of\ sample} \times 100$$

ii) Acid Detergent Fibre (ADF) Procedure

Preparation of acid detergent solution (1N H_2SO_4 with CTAB)

- Into a 1000 ml volumetric flask containing 400 ml of water, weigh and add 49.04g (or 28 ml) of conc. sulphuric acid. Make up to volume with distilled water at 20 ^oC.
- Add 20g cetyl trimethylammonium bromide to the acid and dissolved.

Conventional apparatus method;

1) Weigh approximately 1 000 mg ± 2 mg of dried or as-received material (particle size < 1mm) and record as m1.
2) Place the sample into a round-bottom flask connected with a condensing unit, followed by 100mL preheated acid detergent solution.
3) Heat the mixture for 1h at its boiling temperature.
4) The solution was then cooled down to room temperature and filtered.
5) Wash the residue 3 times with hot distilled water, followed by 3 times with acetone and then

vacuum dried.

6) Further dry the sample not less than 5 h (preferably overnight) at 103 °C ± 2 °C in an air-ventilated oven and cool to room temperature in a desiccator and weigh. Record the mass as m2.

7) Calculate ADF content on an "as-received" basis in percent, by using the following equation;

$$\%\ ADF = \frac{Mass\ of\ dry\ residue\ after\ ADS\ treatment\ (m2)}{Initial\ mass\ of\ sample\ (m1)} \times 100$$

iii) Acid Detergent Lignin (ADL) Procedure

Preparation of 72% Sulphuric acid

Calculate the grams of acid and water required to prepare 1000 ml of solution by using the following formula;

Acid required (g) = $\frac{\mathbf{100 \times 98.08 \times 12}}{\boldsymbol{H2SO4\ assay}\ (\%)}$

Water required (g) = $(1000\ \times 1.634) - \text{Acid used (g)}$

(Note: 1.634 is the density of 72% Sulphuric acid)

Weight water into 1000 ml volumetric flask and add the calculated amount of H_2SO_4 slowly with occasional swirling. The flask must be cooled in water in order to add the required weight of acid. Cool to 20 ^oC and check if the volume is right. If volume is too large, take out 5 ml water and add 4.55ml H_2SO_4. If volume is too small, take out 1.5 ml and add 2.5 ml water. Repeat if necessary. Meniscus must be within 0.5 cm of the calibration mark at 20 ^oC.

Conventional apparatus method;

1) Place the residue from the ADF analysis in a 50 ml beaker and covered it with 72% H_2SO_4 (~25ml), cooled to 20 – 23 °C and stir with a glass rod to break up all lumps. Let soaked for 3h and stirred 3 times at an hourly intervals.

2) After 3 h, filter as completely as possible with vacuum, and wash with hot water until acid-free to litmus paper.

3) Dry the sample at 130 °C ± 2 °C for 2 h or 103 °C ± 2 °C for at least 5 h, cool to room temperature in a desiccator and weigh. Record the mass as m3.

4) Ignite the sample at 525 °C ± 15 °C for at least 3 h or until carbon-free. Cool to room temperature in a desiccator and weigh. Record the mass as m4.

5) Calculate ADL content on an "as-received" basis in percent, by using the following equation;

$$\%\ ADL = \frac{Mass\ of\ dry\ residue\ after\ 72\%\ H2SO4\ treatment\ (m3) - Mass\ of\ residue\ after\ ashing\ (m4)}{Initial\ mass\ of\ sample\ (m1)} \times 100$$

3.1.3.1 Lignocellulosic content of coconut fibres

The coconut fibre lignocellulosic contents obtained are presented in Annex 7. A summary of the results obtained are shown in Table 3.2.

Table 3.2- Summary of coconut fibre lignocellulosic contents (%)

	Formula	Shell	Husk	Treated fibre	Untreated fibre
Cellulose	*(ADF - ADL)*	40.48	33.34	48.14	49.92
Hemi-cellulose	*(NDF - ADF)*	12.59	5.00	9.26	6.63
Lignin	*(ADL)*	36.20	37.06	27.74	29.66

3.2 Coconut oil for temporary corrosion prevention

Oils may be used for corrosion prevention. However, the use of coconut oil for corrosion prevention has been rarely studied. Coconut oil may provide a more sustainable solution for temporary corrosion prevention, as compared to Volatile Corrosion Inhibitors. Though VCIs are commonly used nowadays, they are not environment friendly.

The corrosion prevention capabilities of coconut oil may, however, be increased when mixed with other natural products. Please refer to Annex 1 for more information. Hence, in this project, the effect of honey on the corrosion prevention properties of coconut oil will be investigated.

Outdoor and sheltered exposures of mild steel with a coating of coconut oil and honey, as additive, were performed. The percentage corrosion of the samples, were determined through the mass loss method (according to BS 7545), and through image analysis (imageJ software). These trials were done to find the optimum composition of coconut oil to honey ratio in the coating.

The optimum percentage of coconut oil and honey were 75% and 25% respectively. It has been noted that the coconut oil and honey mixture had a tendency to melt, flow and run off the samples with the increasing outdoor temperature and there was a significant decrease in thickness of the coatings applied. Thus a potential solution is to increase the viscosity of the coconut oil to prevent it from flowing. Details on the trials are found in Annex 8.

3.2.1 Increasing viscosity of coconut oil

Viscosity is increased through use of viscosity modifiers, such as polymeric additives like ethylene vinyl acetate (EVA) and styrene-butadiene-styrene (SBS) copolymers. Quinchia et al. (2009) used 0.5 to 5% by weight of the additives in high oleic sunflower oil within a temperature range of 25^{o}C to 120^{o}C.

For this experiment the mixture was prepared by stirring the required composition of oil and polymer at a rotational speed of 300 rpm for 5-10 h, at a temperature of 100-150 °C. This thermal treatment was required to completely solubilise the additive in oil. 2 to 4 % by weight EVA was blend with the optimum coconut oil and honey mixture. The blend was prepared by stirring the required amount of EVA and 75g coconut oil, at a rotational speed of 300 rpm for 5h at 125 ^{o}C. Afterward, the mixture was cooled to room temperature and 25g of honey was added and stirred.

Note: The honey should not be added during the thermal treatment, otherwise caramelisation would occur. Please refer to Annex 9 for more details.



Figure 3.6: Thermal treatment of EVA in coconut oil

3.2.2 Preparation of mild steel

Mild steel samples used for this project had a black coating on its surface and with some corrosion. In order to remove the corrosion present and the black layer on the metal, the latter was cleaned as in Table 3.3.

Table 3.3- Preparation of mild steel

Purpose	**Procedure**
Reagent preparation	10% w/w NaOH was prepared. 50g NaOH was added to 450mL of water
Emulsifying: For removal of all polar substances such as fats and oils (they are converted to glycerol and soap). The sample becomes hydrophilic	Mild steel specimen was dipped in the 10% NaOH for 5 minutes
To remove alkali and loose deposits on the metal	The sample was then rinsed with high water flow
Reagent preparation	10% v/v hydrochloric acid (HCl) was prepared. 160mL of HCl was added to 340mL of water
Acid pickling process is as illustrated in Figure 3.7	The sample was dipped in the 10% v/v HCl for 4 hours
To remove chemical and loose deposits on the metal	The specimen was then rinsed with water
Passivation: To make it less susceptible to corrosion	Passivation was done with 10% NaOH for 5 minutes
Drying and storage	It was then dried in a specimen dryer and stored in a desiccator.

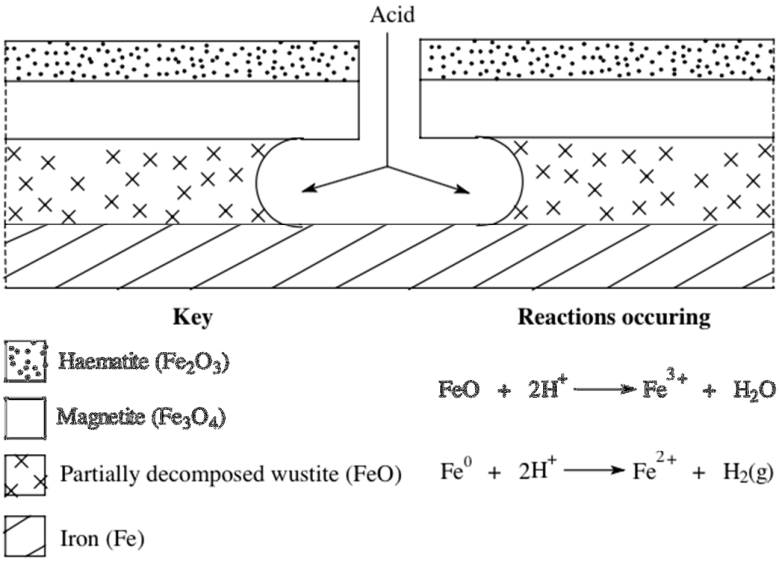


Figure 3.7: Acid pickling process (New Zealand Institute of Chemistry, 2008)

Figures 3.8(a) and 3.8(b) show a mild steel sample before and after the cleaning process.



Figure 3.8(a): Sample before cleaning



Figure 3.8(b): Sample after cleaning

According to ASTM G1, standard practice for preparing, cleaning, and evaluation of corrosion test specimens, the mild steel specimens were punched using the stencilling technique (3/16 inch) and weighed using an electronic balance (Sartorius balance, type BP 210 S) to four decimal places. The dimensions of the four specimens were measured using a vernier calliper. The weights and dimensions of the cleaned samples are as shown in Table 3.4.

Table 3.4: Mild steel samples measurements

Mild steel samples	Mass, g	Length, mm	Width, mm	Thickness, mm
Outdoor exposure				
OR1	168.813	150.00	98.10	1.60
OR2	168.583	150.00	98.20	1.68
OR3	166.883	149.42	98.08	1.62
O2	167.832	150.20	98.10	1.64
O3	168.693	149.82	98.10	1.62
O4	169.006	149.52	98.22	1.66
Sheltered exposure				
SR1	170.454	150.46	98.62	1.52
SR2	169.919	149.74	98.60	1.44
SR3	171.244	150.50	99.22	1.50
S2	169.823	149.74	99.80	1.46
S3	170.015	150.50	98.46	1.50
S4	169.688	150.40	98.56	1.44

3.2.3 Corrosion Monitoring

Corrosion was tested in two different environments, namely; outdoor exposure and sheltered exposure. The mild steel samples were coated on both sides (front and back) using a flat brush. The specimens' named and marked as shown below, based on the coating applied:

Table 3.5- Samples for corrosion tests

Samples	Coating composition (by wt %)
OR1, SR1,	Control (no coating)
OR2, SR2	100% coconut oil
OR3, SR3	75% coconut oil and 25% honey
O2, S2	2% EVA with 75% coconut oil and 25% honey
O3, S3	3% EVA with 75% coconut oil and 25% honey
O4, S4	4% EVA with 75% coconut oil and 25% honey

O refers to specimens exposed outdoors

S refers to specimens exposed under sheltered conditions

The coated samples were then placed on an exposure rack as shown in Figure 3.9. Nylon supports, bolts and nuts were used to attach the specimens firmly on the rack. For the sheltered ones, the samples were attached to the shelter support with a nylon line. See in Figure 3.10.

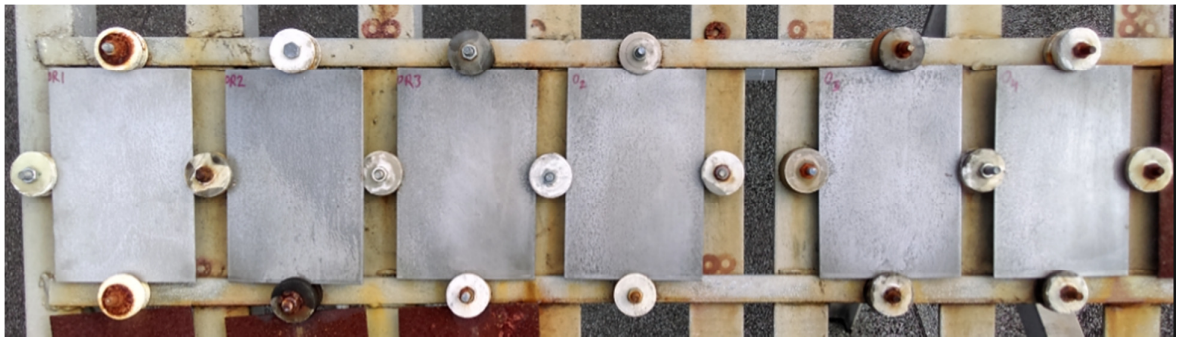


Figure 3.9: Mild steel samples outdoor exposure on rack



Figure 3.10: Mild steel samples sheltered exposure

The mild steel samples were exposed for a period of;

- 3 weeks, for outdoor exposure
- 3 months, for sheltered exposure

The exposed mild steel specimens were monitored every 24 hours for outdoor exposure and accelerated salt-spray apparatus, and every week for sheltered exposure. To avoid loss of coating on the samples, photographs were taken instead of scanning with a flatbed scanner. Annex 10 contains the pictures used to evaluate the degree of rusting.

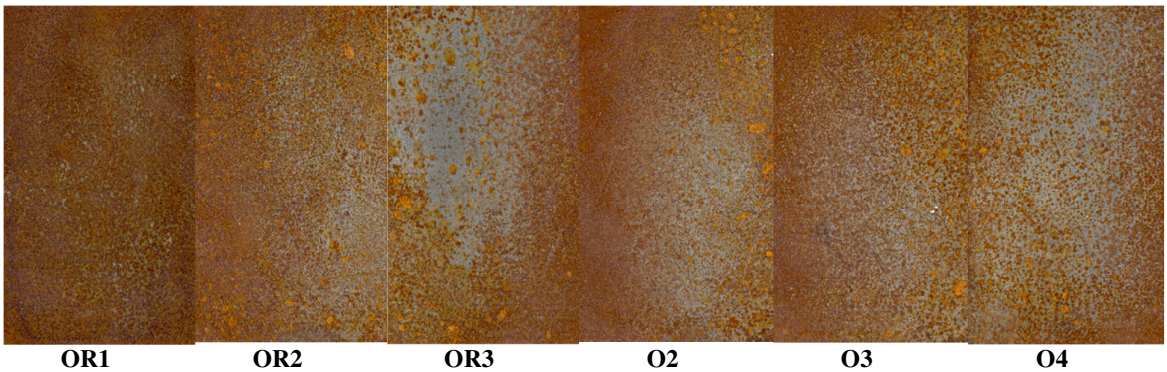


Figure 3.11: Back surface of outdoor exposure sample after 23 days of exposure

3.2.3.1 Image analysis by ImageJ Software

ImageJ software was used to analyse the area corroded. The picture taken was opened in the software (as shown in figure 3.12) and colour threshold was selected from the image tab. The saturation and brightness were adjusted such as to cover all the corroded zones (as shown in figure 3.13). The image was then converted to 8-bit (refer to figure 3.14) and the threshold limit of the corroded area was found through the plot profile option, which was 85 (as shown in Figure 3.15). The lower and upper thresholds

were thus set to 85 (figure 3.16). Finally, the percentage area of corrosion on the metal specimen was obtained as shown in Figure 3.17 and a graph of corroded area versus time of exposure were then plotted for each of the specimens in their respective environments. The detailed results obtained from imageJ are tabulated in Annex 10.

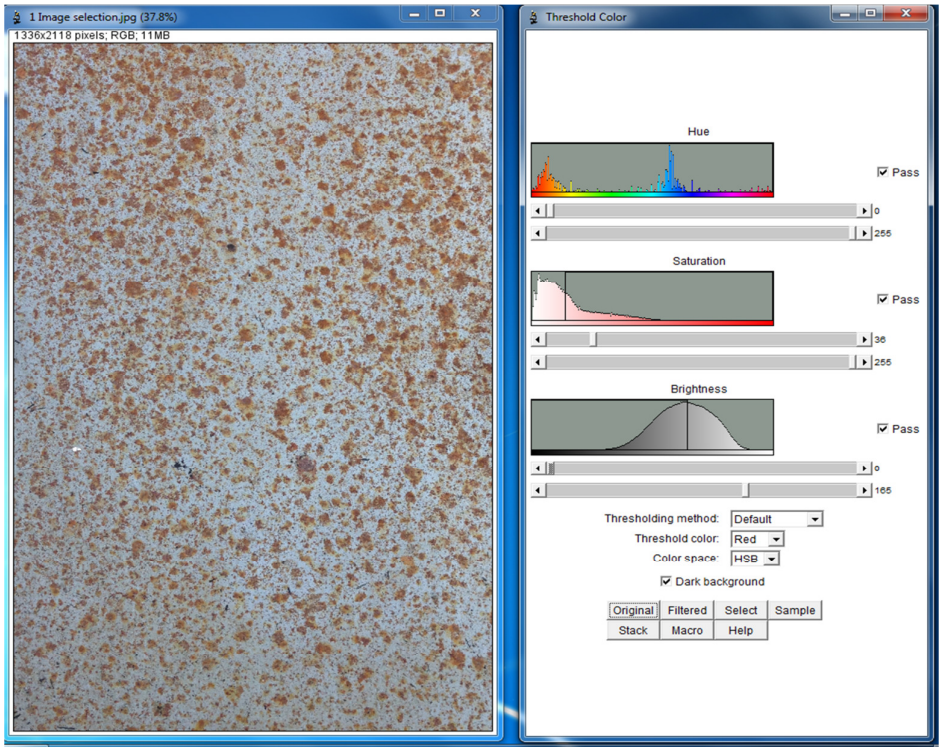


Figure 3.12: Photo opened in imageJ

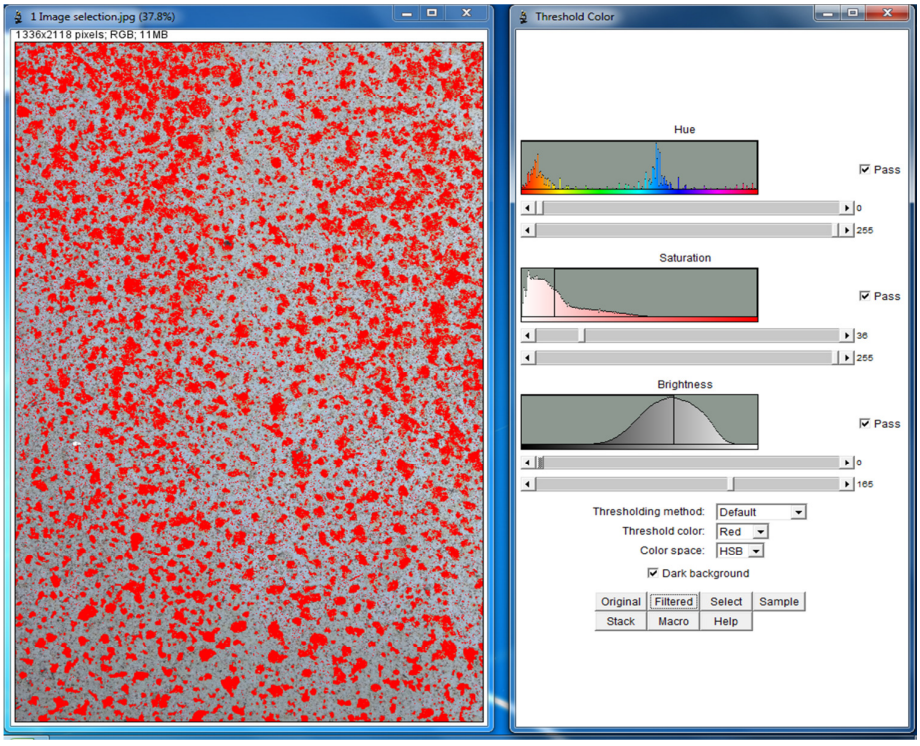


Figure 3.13: Colour threshold adjustment

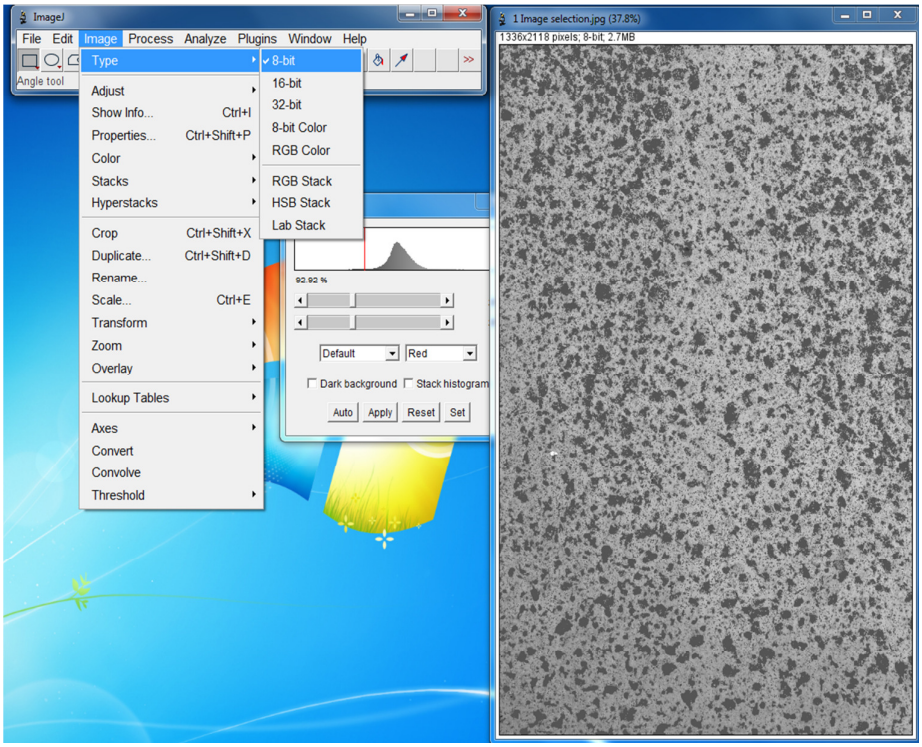


Figure 3.14: Image converted to 8-bit

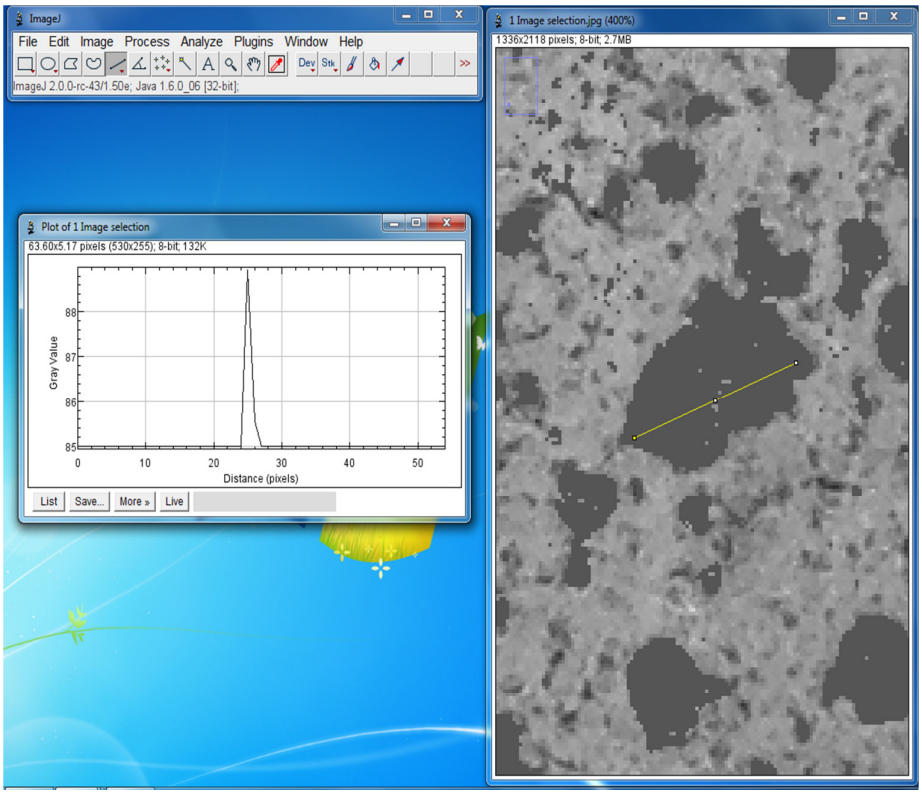


Figure 3.15: Plot profile

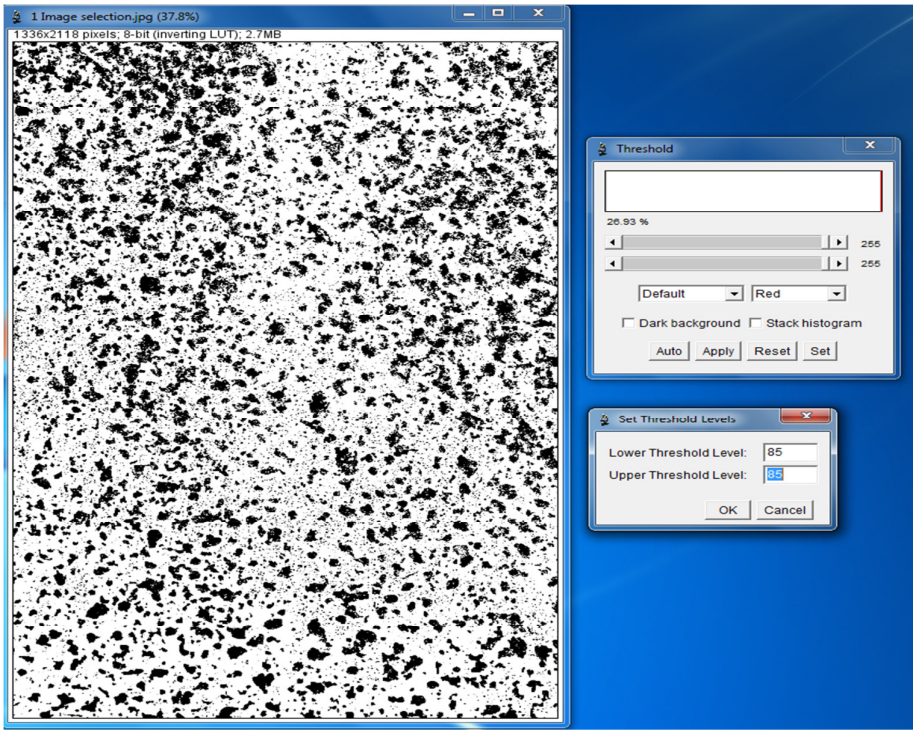


Figure 3.16: Threshold limit

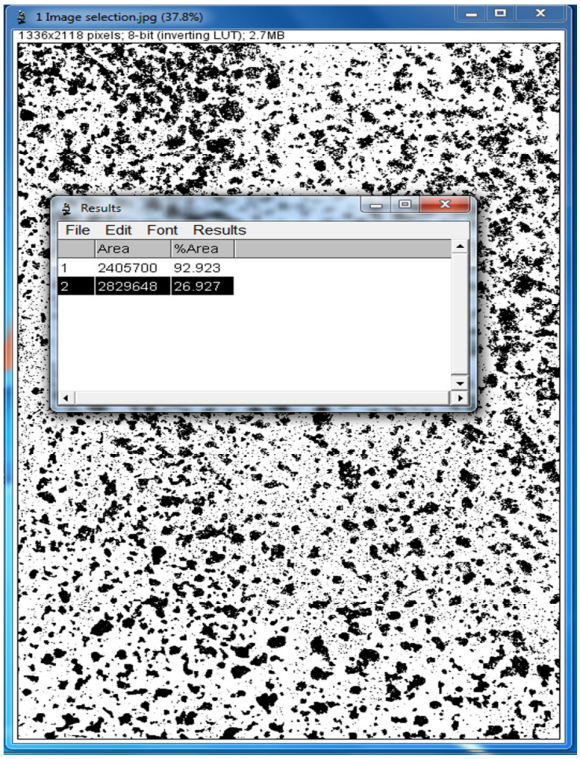


Figure 3.17: ImageJ results

3.2.3.2 Results of corrosion tests

The results of the corrosion tests are shown in Tables 3.6 and 3.7 and in Figures 3.18 and 3.19.

Table 3.6: Percentage area corroded from image analysis of Outdoor Exposure

Outdoor Exposure						
Time of exposure (day)	**Percentage area corroded (%)**					
	OR1	**OR2**	**OR3**	**O2**	**O3**	**O4**
0	0.000	0.000	0.000	0.000	0.000	0.000
1	0.481	0.316	0.202	0.092	0.017	0.000
2	17.221	7.812	0.759	3.198	0.297	0.028
5	50.560	37.060	31.128	24.254	15.368	2.227
6	53.021	48.914	40.710	38.018	35.881	21.397
7	59.201	50.611	45.919	43.820	39.653	30.007
8	73.714	66.999	48.520	46.002	44.080	37.295
9	78.608	68.340	57.132	53.053	47.921	42.730
13	81.854	73.892	66.756	60.171	57.013	51.055
19	98.911	87.614	79.013	70.004	67.689	62.025

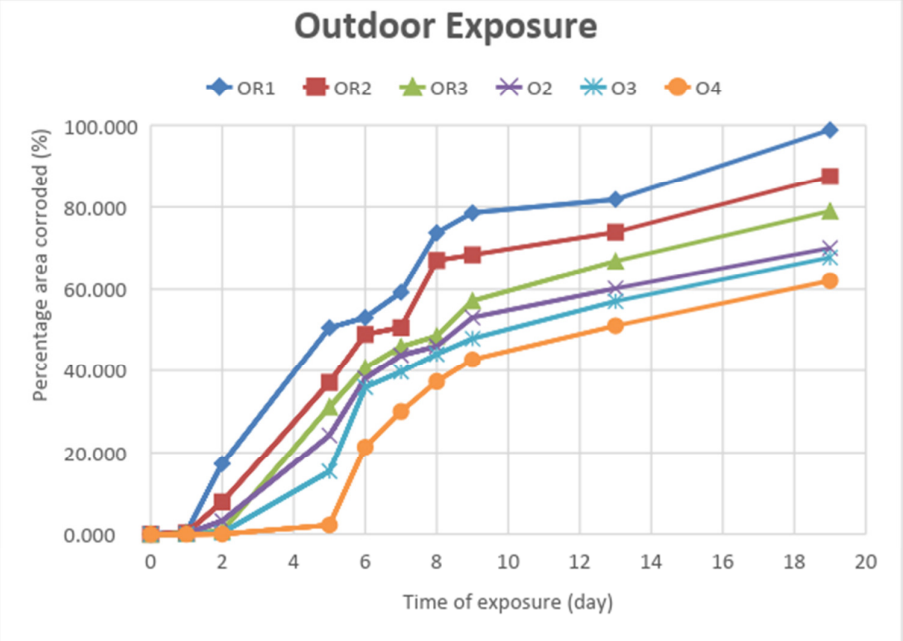


Figure 3.18: Graph of percentage area corroded against number of days exposed in the atmosphere

Table 3.7: Percentage area corroded from image analysis of Sheltered Exposure

Sheltered Exposure						
Time of exposure (day)	Percentage area corroded (%)					
	SR1	SR2	SR3	S2	S3	S4
0	0.000	0.000	0.000	0.000	0.000	0.000
7	0.342	0.330	0.301	0.257	0.219	0.193
15	1.594	1.187	0.711	0.863	0.481	0.205
22	3.013	1.848	1.577	0.998	0.516	0.255
31	4.343	3.381	2.562	2.008	1.267	0.640
37	5.622	4.015	3.200	2.894	1.889	1.050
45	9.886	5.566	4.713	3.909	2.817	1.521
53	12.562	6.798	5.293	5.621	3.407	1.755
66	14.799	8.239	5.684	6.634	3.744	2.449
92	19.110	9.110	7.621	8.002	4.801	3.584

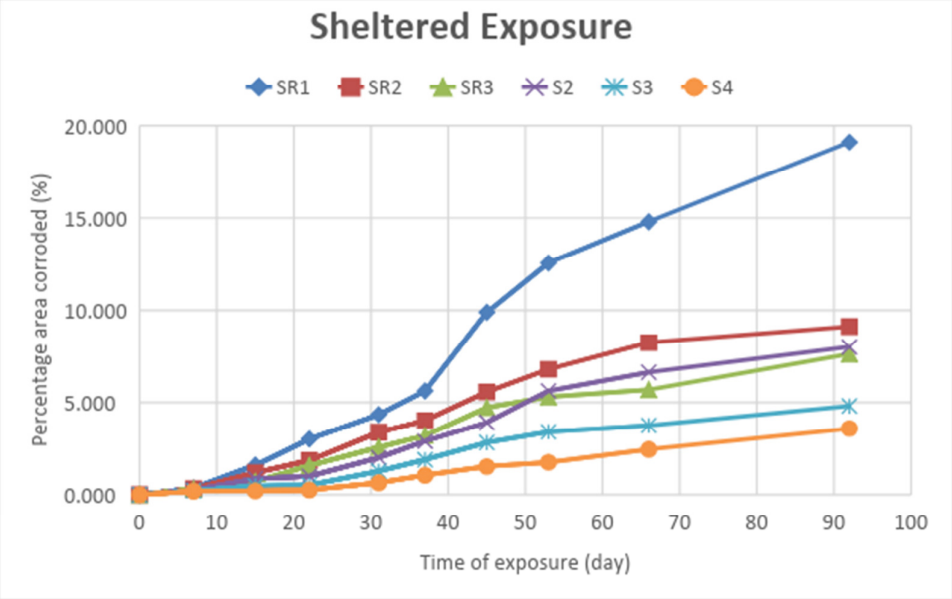


Figure 3.19: Graph of percentage area corroded against number of days exposed in sheltered place

3.2.3.3 Mass loss method

The corroded mild steel samples were cleaned according to ASTM G1. 500 mL of distilled water was measure and poured into a 1,000 mL volumetric flask. 500 mL of concentrated hydrochloric acid was then added slowly followed by 3.5 g of hexamethylenetetramine. The mixture was mixed and additional water was added up to the level. The mild steel sample was then immersed in this mixture for ten minutes. Mechanical cleaning consisted of a soft non-metallic brush to clean the specimen. The latter was rinsed with water and dried using a specimen dryer. The cleaned and dried samples were measured using an electronic balance. The mass loss was determined as the difference between mass of mild steel before exposure and the mass of mild steel after cleaning.

To account for loss of metal while cleaning, a reference mild steel specimen was first prepared as in section 3.2.3 and cleaned as explained above in this section. The corrected mass loss obtained was 0.048

g, which was added to the calculated mass loss. The results are shown in Table 3.8. It should be noted that the sheltered specimens were not considered for this test as they were not significantly corroded for mass loss analysis.

Table 3.8: Mass loss for outdoor steel samples exposure

Mild steel samples	Mass before Exposure, g	Mass after Cleaning, g	Mass Loss, g	Corrected mass loss, g	Corrected mass loss, %
OR1	168.813	167.443	1.370	1.418	0.840
OR2	168.583	167.515	1.068	1.116	0.662
OR3	166.883	165.937	0.946	0.994	0.596
O2	167.832	166.814	1.018	1.066	0.635
O3	168.693	167.762	0.931	0.979	0.580
O4	169.006	168.170	0.836	0.884	0.523

3.3 Manufacturing of composite board from coconut fibre and shell

3.3.1 Resin Injection and Vacuum Infusion apparatus

Figure 3.20 illustrates the set up used for making resin samples.

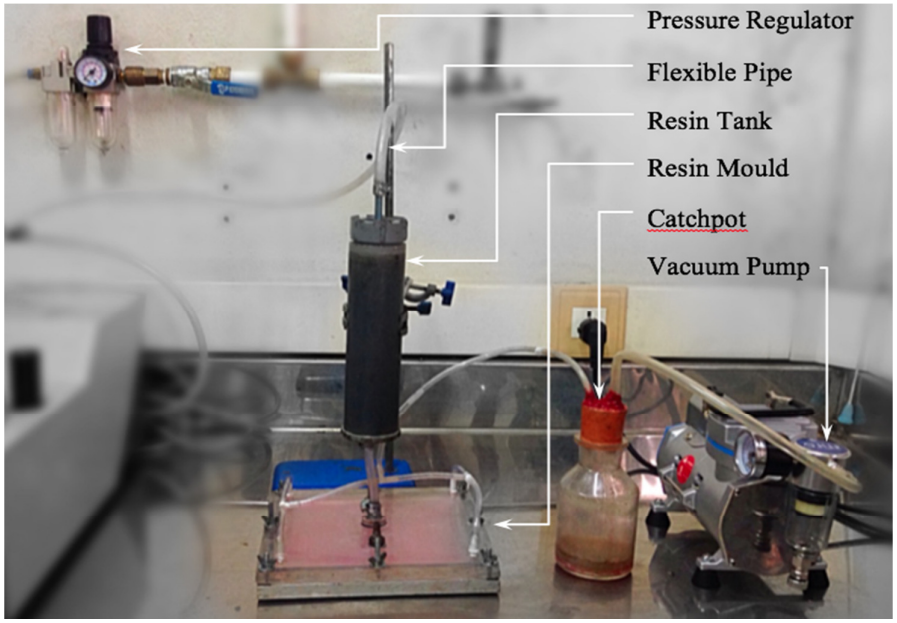


Figure 3.20: Resin Injection and Vacuum Infusion Set Up

The steps carried out were as follows:

- Foam tape shown in figure 3.21 was used as gasket. It was stuck at mould boundaries to minimise intake of air between the mould and cover when the vacuum pump is switched on.

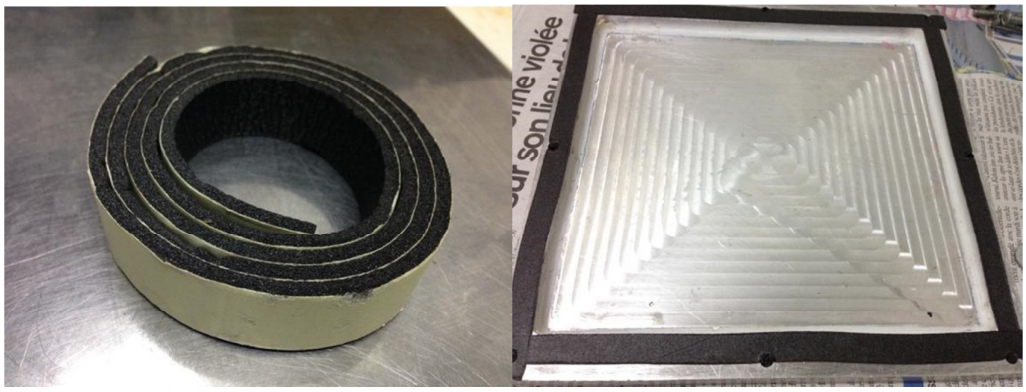


Figure 3.21: Mould gasket

- Mould and mould cover were cleaned with thinner prior to application of releasing agent (Polyvinyl Alcohol, PVA).
- Releasing agent was applied with a flat brush and allowed to dry. A specimen dryer used to increase its drying time. Additional coats were applied, if necessary.
- The required amount of coconut fibres were placed evenly and randomly oriented in the mould.
- The mould was tightly closed with acrylic cover using bolts and nuts.
- Flexible tube connections were sealed with silicone (as shown in figure 3.22) and seal tape to reduce potential gain in pressure.

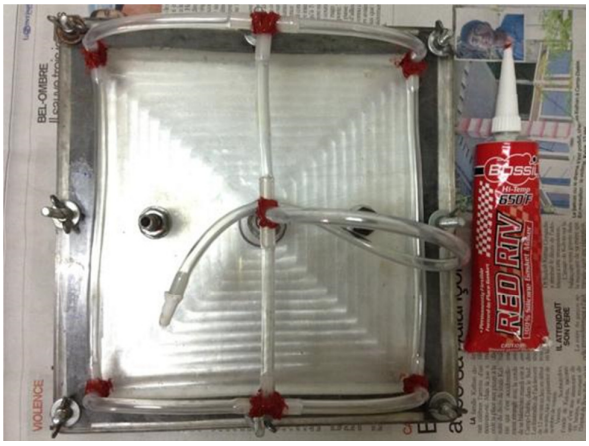


Figure 3.22: Silicone used for airtight pipe connections

- A catchpot was added between mould and vacuum pump to avoid resin contact with the pump.
- Resin tank outlet was closed with a G-clamp
- Vacuum pump was then switched on and allowed to reach its optimum pressure (~90 kPa)
- Vacuum pump was then switched off, and any change in pressure was checked
- Resin was then poured into resin tank. Resin was prepared as follows:

    i) Required amount of resin (around 320 g) was measured in a container

    ii) 1% catalyst (MEKP) by mass of resin was measured

iii) Required amount of styrene was measured using a syringe and added to resin to reduce viscosity of the mixture

iv) Resin viscosity was measured using a Brookefield viscometer with spindle number 3 at a dial speed of 100 r.p.m as shown in Figure 2.23.

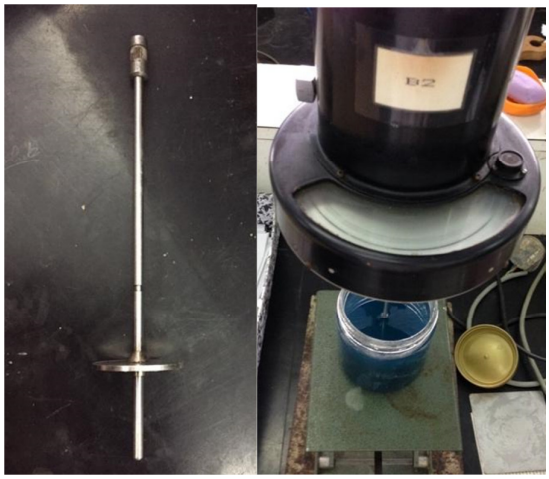


Figure 2.23: Spindle no. 3 and viscometer

v) Prior to vacuum infusion, catalyst was mixed with the resin mixture.

Note: care was taken to evenly mix resin, styrene and catalyst.

- G-clamp was opened to allow resin to flow into mould as shown in Figure 2.24.

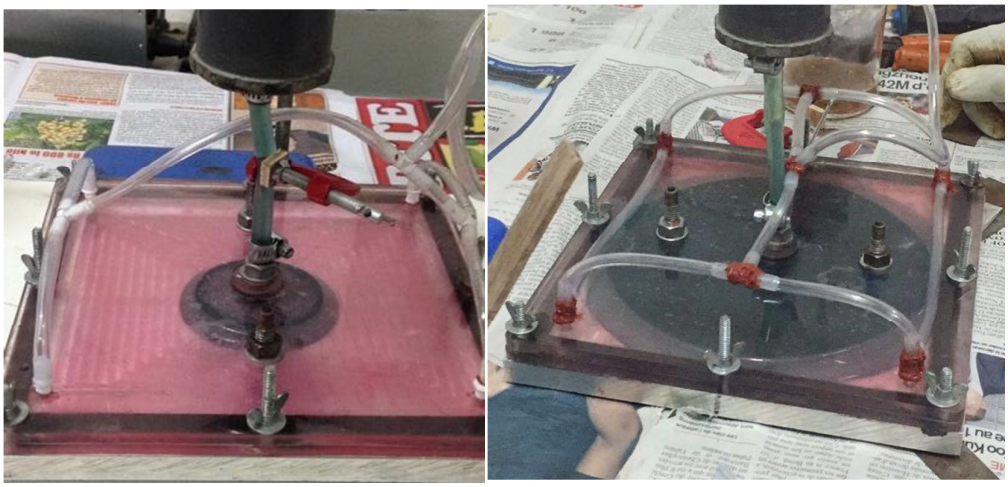


Figure 2.24: Vacuum infusion of resin

- When mould was fully impregnated with resin, the resin tank outlet was closed with G-clamp
- For mould injection pressure, G-clamp is opened, resin tank is closed and compressed air is inserted at its inlet.
- Pressure controlled by using the pressure regulator. When the bubbles of air in the resin is sufficiently compressed, the pressure valve as well as the G-clamp ares closed.
- Resin tank was then disconnected and cleaned with thinner.

- Mould was left for curing at room temperature for three to four hours (refer to figure 3.25).



Figure 3.25: Vacuum infused resin

- After curing, flexible tubes and connectors were unblocked, if in contact with resin.
- Resin sample was demoulded and was cut using a Vertical Machine Center (VMC) as in Figure 3.26. The specimen was cut according to ASTM D 638-10, standard test method for tensile properties of plastics. The dumbbell shaped sample (figure 3.23) have overall length, L_0=165mm, distance between grips, D=115mm, length of narrow section, L=57mm, gage length, G=50mm, radius of fillet, R=76mm, width of narrow section, W=10mm, width at center, W_c=W+0.00mm,-0.10mm, overall width, W_0=19mm, thickness, T=7mm. Seven dumbbell shaped specimens were obtained from each resin sample.



Figure 3.26: VMC cutting resin sample

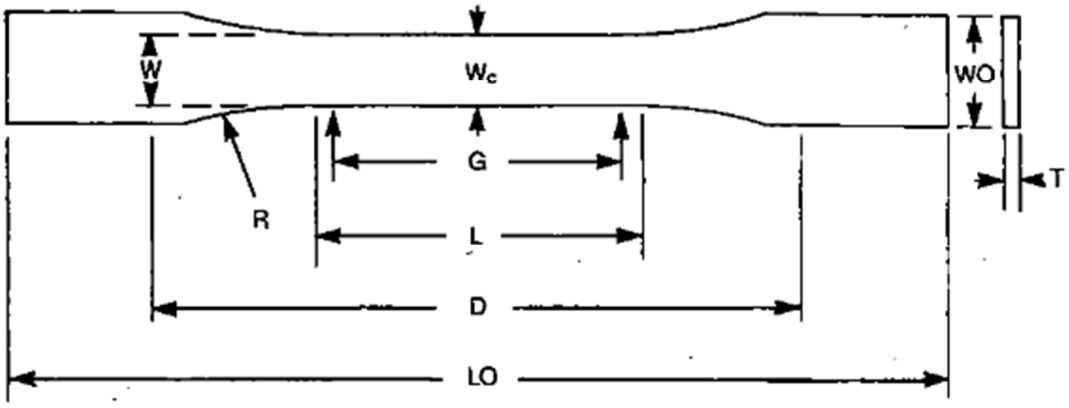


Figure 3.27: Specimen dimensions as per ASTM D638

- Tensile strength of the samples were determined using the Universal Testing Machine (UTM) as shown in Figure 3.27. A load cell of 50 kN and a test speed of 5 mm/min were used. However, since the resin samples contained air bubbles, most of the dumbell shaped specimens broke at both the upper and lower gripping areas as shown in Figure 3.28. The desired fracture is to be within the gage length of the specimen.



Figure 3.28: Tensile strength test of resin sample using UTM

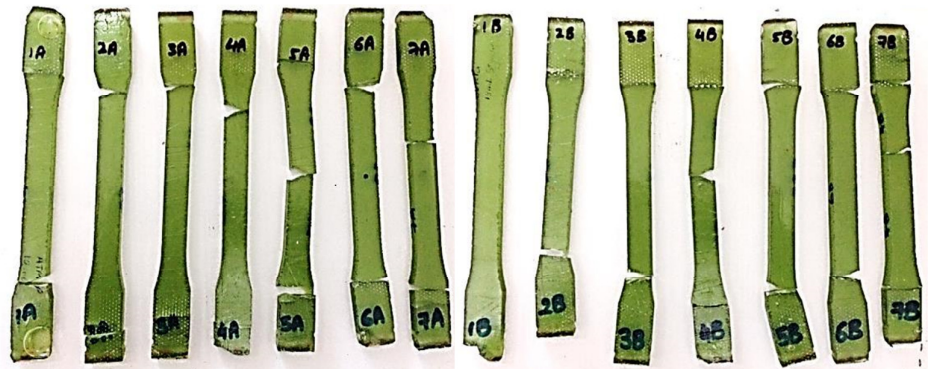


Figure 3.29: Fractured specimens from tensile strength testing using UTM

The problems encountered and related solutions found while making resin samples are detailed in Annex 11. The main issues were:

- To ensure even flow and distribution of resin in mould, a surface table was manufactured and levelled by adjusting the screws beneath it. Bubble clinometers, as shown in figure 3.30, were used to level the table.



Figure 3.30: Levelled table, bubble clinometer and circular bubble clinometer

- The eliminate air bubbles in resin samples, the viscosity had to be reduced to avoid the bubbles from being trapped in resin. The resin used had an initial viscosity greater than 5,000 cP. Hence styrene, a monomer, was used to decrease viscosity. According to Campbell (2010), typical flow is to be between 100 and 1,000 cP. Therefore, a new resin was used instead of the old one as its storage time was exceeded. The viscosity of the resins used against amount of styrene added are shown in Figure 3.31.

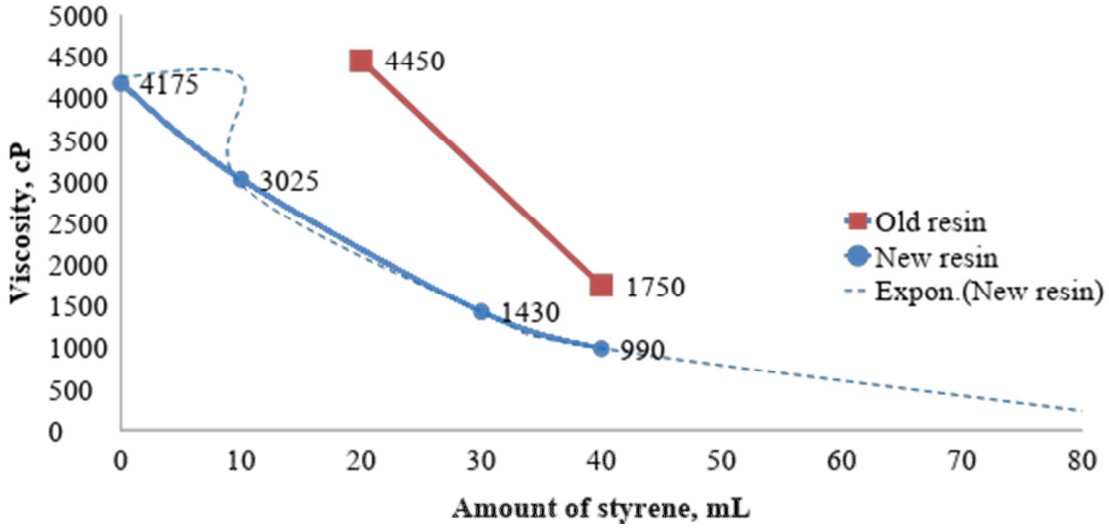


Figure 3.31: Graph of viscosity measured against amount of styrene added

- However, with addition of styrene, air bubbles were still present in the resin samples. Therefore, a degassing chamber and a new vacuum pump (see see figure 3.32) were purchased and a new mould cover was manufactured. Further trials were carried out with another fresh resin having viscosity of 450 cP.

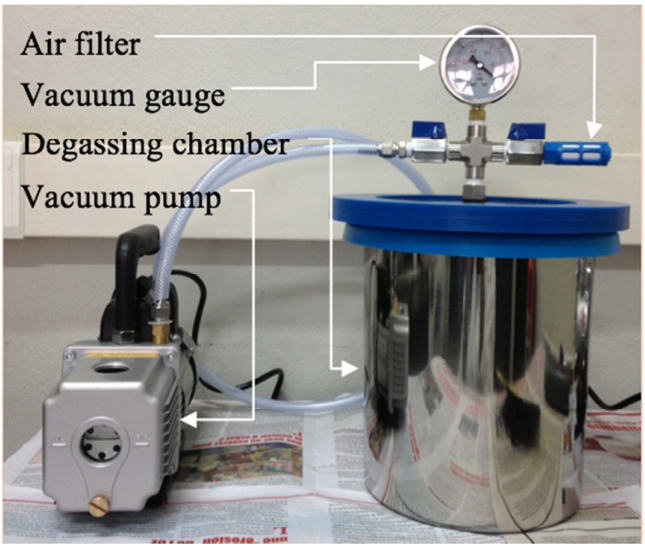


Figure 3.32: Vacuum pump and degassing chamber

Figure 3.33 shows how the degassing chamber expands bubbles of air in the resin. The resin was degassed for five minutes and when the pump was switched off, the valve was closed. Gas and air present in the resin formed bubbles from the bottom of the container and as moved to the top as they expanded. The resin was kept under vacuum for another two minutes and air was allowed inside by opening the air inlet valve. As air entered into the chamber, the bubbles remaining in the resin were compressed.

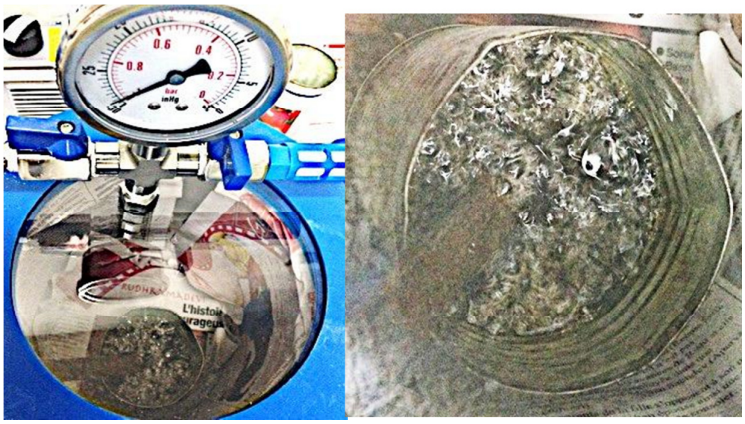


Figure 3.33: Degassing resin in degassing chamber

Figure 3.34a shows a resin sample made without degassing resin. The surface of the sample was rough due to the mould cover, which had scratches from cleaning of resin which stuck on it. Air bubbles are observed around the centre of the sample. The new mould cover made was used to reduce resistance of bubbles on the surface of the resin with the cover. Hence, figure 3.34b shows the degassed resin sample obtained with the new cover. Significantly fewer air bubbles are seen and the sample is visually clearer in figure 3.29b because gas and air content has been reduced through the degassing process.

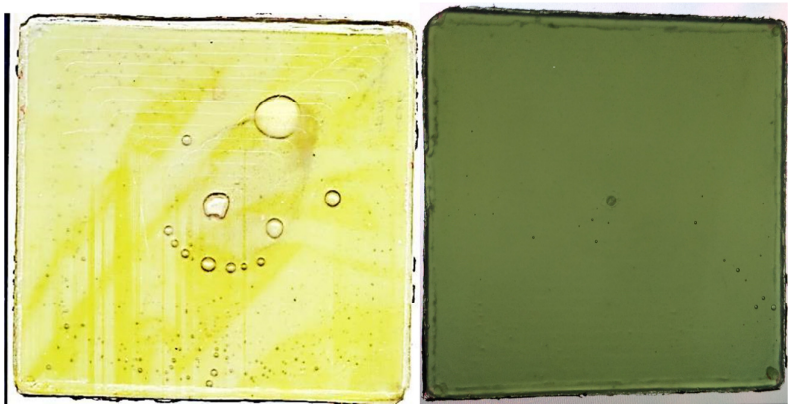


Figure 3.34a: Resin sample without degassing Figure 3.34b: Degassed resin sample

3.3.2 Critical fibre length

A critical fibre length of 1.62 mm was obtained using the below equation (Callister, 2009). Callister (2009) stated that fibre length is to be 15 times longer than the critical fibre length, hence untreated coconut fibres were trimmed to a length of around 25 mm prior to alkaline treatment.

$$l_c = \frac{\sigma_f \text{ x } d}{2 \text{ x } T_c}$$

Where;

l_c : critical fibre length, mm

σ_f : tensile strength, MPa

d : fibre diameter, mm

T_c : fibre-matrix bond strength (or shear yield strength of the matrix, whichever is smaller), MPa

The fibres were randomly oriented as shown in figure 3.35, which provides isotropic mechanical characteristic to the composite, implying that if a force is applied in any direction, the strength will be uniform.

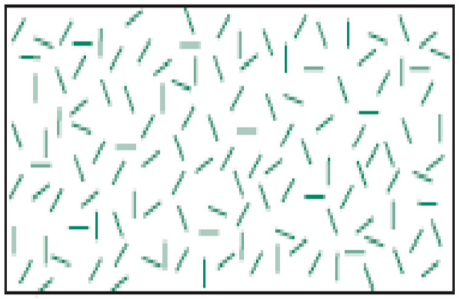


Figure 3.35: Discontinuous and randomly oriented fibre-reinforced composite (Callister, 2009)

3.3.3 Manufacturing of composite from coconut fibre

Composites were produced from treated coconut fibres from Mauritius and Agalega. The fibre content was varied ranging from 1 – 5% by volume. The coconut fibre has a density of 1.2 g/cm^3 (Bujang et al., 2007; Pickering et al., 2016) and that of unsaturated polyester resin is 1.1 g/cm^3. (See more details on composite produced in Annex 12)

The same apparatus and steps as mentioned previously were used in the production of composite from fibre, but prior to injection of resin, the mould was filled randomly and discontinuously oriented with the required amount of fibre. The results obtained from the UTM are presented in Annex 13. A summary of the results is shown in Table 3.9 below. The tests were performed under the following conditions:

- Coconut fibre: alkaline treatment (6% w/w NaOH)
- Resin viscosity; 1880 cP (Spindle No. = 2, Spindle speed = 20 rpm, Dial reading = 94, dial factor = 20)
- Degassing time: 5 min before adding catalyst + 10 min after mixing in catalyst
- Injection pressure: 80 kPa

Table 3.9- Results obtained from the UTM

Sample		Tensile Strength at Break, MPa	Percentage Elongation at Break, %	Calculated Young's Modulus, MPa
Type of sample/origin of coconut fibre	**% vol of coconut fibres**	**Average over 7 samples**		
Reference	0%	58.803	12.347	1514.823
Agalega	2%	21.010	2.830	2300.284
	3%	21.242	2.807	2333.671
	4%	19.561	2.432	2628.777
	5%	18.027	2.225	2724.360
Mauritius	2%	23.553	3.115	2365.363
	3%	23.541	3.002	2430.846
	4%	25.313	3.679	2180.195
	5%	23.614	3.357	2271.766

3.3.4 Manufacturing of composite from coconut fibre and coconut shell powder

Coconut shell powder was used together with coconut fibres in the manufacturing of composites. Powdered coconut shell was sieved to a particle size of less than 100µm and was mixed to different weight percent (2, 3 and 4%) with the coconut fibres (3% by volume) and the matrix to make slab samples of different composition. The samples were then tested for their mechanical properties using the Universal Testing Machine. It should be noted that the fibers and shell from Mauritius were used in the composites.

Procedure

Clean, dry and fiber-free coconut shells were pulverized in a shredder. The powder obtained was sieved in accordance with BS1377:1990 standard. Where around 100 g of the coconut shell powder was placed

onto a set of sieves arranged in descending order of fineness and shaken in a sieve shaker for 15 min which is the recommended time for achieving complete classification of the particles. Only particles that were retained below 100µm was used in this experiment.



Figure 3.36: Pulveriser



Figure 3.37: Sieve shaker

The required amount of coconut shell powder was weighed and mixed with the resin. The mixture was then degasified for 5 min and the 1% catalyst was added and mixed homogenously. The latter was further degasified for another 10 min, prior to vacuum infusion with the fibre in the mould. The detailed results obtained from the UTM are presented in Annex 14. A summary of the results is shown in Table 3.10.

Table 3.10- UTM results for composites made of coconut shell powder and coconut fiber

Sample	Tensile Strength at Break, MPa	Percentage Elongation at Break, %	Calculated Young's Modulus, MPa
% vol of coconut shell poewder	Average over 7 samples		
Reference (0%)	58.803	12.347	1514.823
2%	24.731	3.560	2104.777
3%	22.826	3.026	2313.662
4%	22.819	3.416	2108.839

3.4 Activated carbon production from coconut husk and shell

Granulated coconut husk and shell activated carbons were chemically prepared by using phosphoric acid as the activating agent. Wastewater which was obtained from a textile industry was treated using granular activated carbons (GAC). The treated effluent was then analyzed in terms of cation, anion and heavy metals.

3.4.1 Production of activated carbon using phosphoric acid

The optimum conditions used for the production of activated carbon using phosphoric acid as activating

agent was as per Gratuito et al (2008). The optimum conditions were as follows:

Table 3.11: Optimum condition for activation of coconut shell by phosphoric acid.

Parameters	Optimum range	Optimum point
Particle size	mesh 8 – 14	mesh 8
Impregnation ratio	1.345 – 2	1.725
Activation time	14.9 – 23.9 min	19.5 min
Activation temperature	394 – 416 ^{o}C	416 ^{o}C

Coconut husk and shell were used as precursors in the preparation of activated carbon. Clean and dry coconut husk and shell were milled separately in a shredder and sieved to a particle size between mesh 8 – 14 (2.38 – 1.41 mm). Phosphoric acid solution was prepared to an impregnation ratio of 1.7. According to Moliba-sabio et al. (1995), the impregnation ratio is defined as the ratio of dry weight of H_3PO_4 to the weight of the coconut shell (Gratuito et al., 2008). The initial concentration of the H_3PO_4 solution provided was 85% w/w. For 10g of coconut sample, 17g of dry weight of H_3PO_4 was required (i.e. 20g of 85% w/w H_3PO_4 solution).

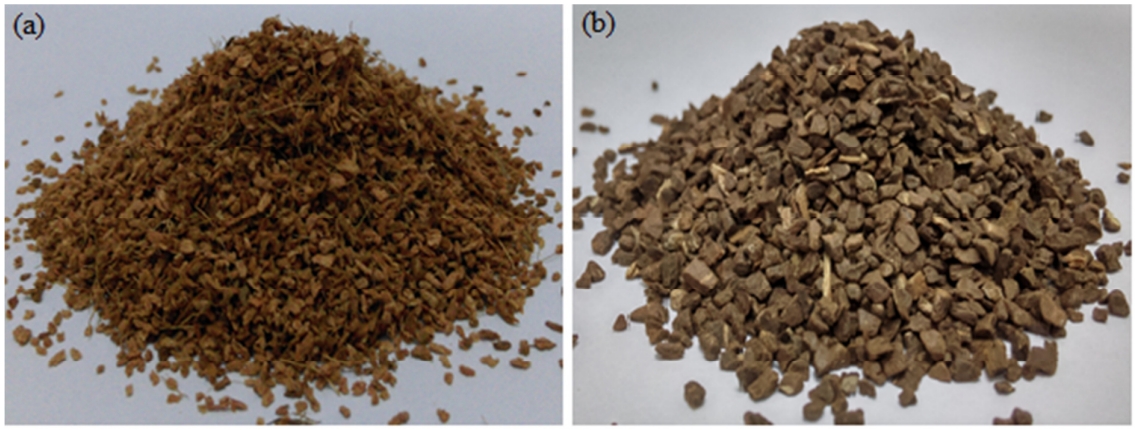


Figure 3.38: (a) Coconut husk (2.38 – 1.41 mm) and (b) Coconut shell (2.38 – 1.41 mm)

For a better impregnation process, the 20g of 85% w/w H_3PO_4 solution was further diluted with 5g of water for the shell and 100g of water for the husk. The liquid/solid mixtures were then stirred constantly at ambient temperature for 2 h and left to soak overnight to allow penetration of the H_3PO_4 into the coconut samples. After the stipulated soaking time, the impregnated samples were oven dried at 110°C for 24 h. For the carbonization step, the dried samples were placed in a stainless steel horizontal cylindrical reactor and purified nitrogen was used to evacuate air, so as to create an inert atmosphere through the reactor. The reactor was then placed in furnace and heated at 416 ^{o}C for 20 minutes.

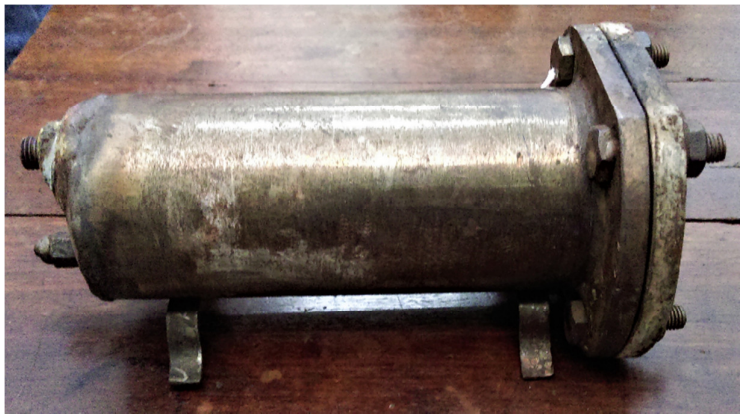


Figure 3.39: Stainless steel horizontal cylindrical reactor

After the activation process, the furnace was turned off and the carbonized materials were left to cool down. The carbonized samples were then washed with distilled water through a filter paper in order to remove the phosphoric acid from the activated carbons. The acidity of the filtrate was monitored until the pH is around 6 – 7. The activated carbons were then washed with 0.1 M NaOH solution and finally with distilled water. The samples were placed in an oven and dried at 105 ^{o}C.

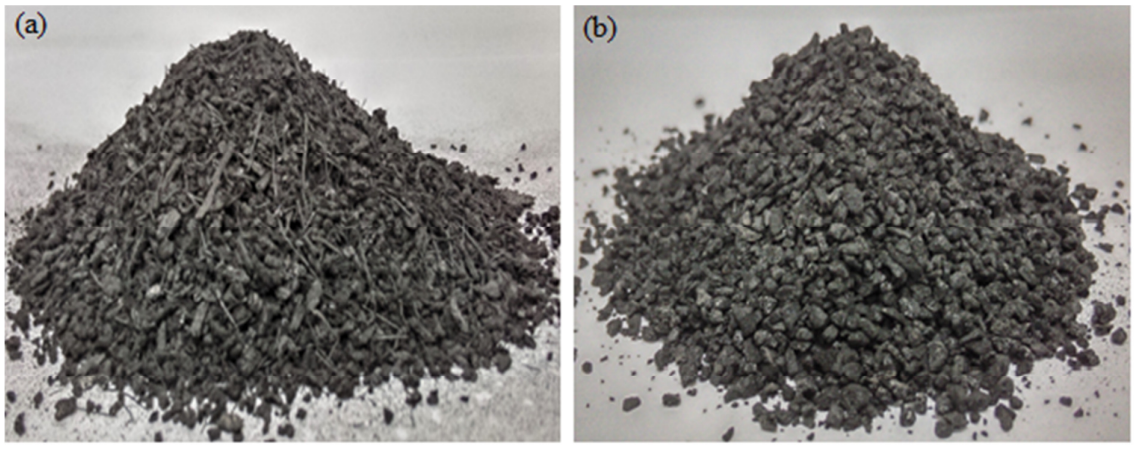


Figure 3.40: (a) Coconut husk activated carbon and (b) Coconut shell activated carbon

3.4.2 Batch adsorption study

In this experiment, granular activated carbons (GAC) were used to treat the wastewater of a local textile industry. The wastewater sample was collected at the inlet of the wastewater treatment plant of the textile industry. A batch adsorption process was used to treat the wastewater samples. The optimum particle size for liquid phase adsorption is in the range of 12/42 mesh (Çeçen & Aktaş, 2011). Each activated carbon was sieved in accordance with BS 1377:1990 standard, where 100g of activated carbon was placed onto a set of sieves arranged in descending order of fineness and shaken for 15 minutes which is the suggested time for complete classification of particles, the particles that were retained between mesh 12/42 were considered in this study. Various compositions of shell and husk activated carbons were used to determine the optimum pollutants removal as shown in Table 3.12.

Table 3.12: Coconut shell and husk activated carbon compositions

Trials	Coconut shell activated carbon (%)	Coconut husk activated carbon (%)
1	100	0
2	75	25
3	50	50
4	25	75
5	0	100

The parameters in Table 3.13 were analysed in the wastewater samples;

Table 3.13: parameters analysed and standard test methods used

Parameter	Test Method
Chemicals	
Chloride	Mercuric Nitrate Titration with Diphenylcarbazone Indicator Method – HMSO, London
Potassium	Flame Photometry
Sodium	Flame Photometer model 420 – APHA 23e 3500 – Na B
Heavy Metals	
Cadmium	Flame AAS – Direct Air- Acetylene, APHA 23e 3111B
Cobalt	Flame AAS – Direct Air- Acetylene, APHA 23e 3111B
Copper	Flame AAS – Direct Air- Acetylene, APHA 23e 3111B
Nickel	Flame AAS – Direct Air- Acetylene, APHA 23e 3111B
Total Chromium	Flame AAS – Direct Nitrous Oxide – Acetylene, APHA 23e 3111D
Zinc	Flame AAS – Direct Air- Acetylene, APHA 23e 3111B

The batch adsorption tests were performed in a set of 500 ml screw-cap flasks. The pH of the wastewater sample was adjusted to about 4.5 by using 0.05 M H_2SO_4, as it is known that the optimum adsorption of heavy metals occurs in acidic condition (Sekar et al., 2004). 1 g of activated carbon of different composition, followed by 500 ml of wastewater solution was placed in each flask and was agitated at a speed of 120 rpm in a shaker at room temperature for 48h, to ensure that equilibrium was reached (Kobya et al., 2005). After equilibrium, each wastewater sample was filtered individually to remove the adsorbents and the effluents were sent to Wastewater Management Authority for analysis.



Figure 3.41: Batch adsorption process

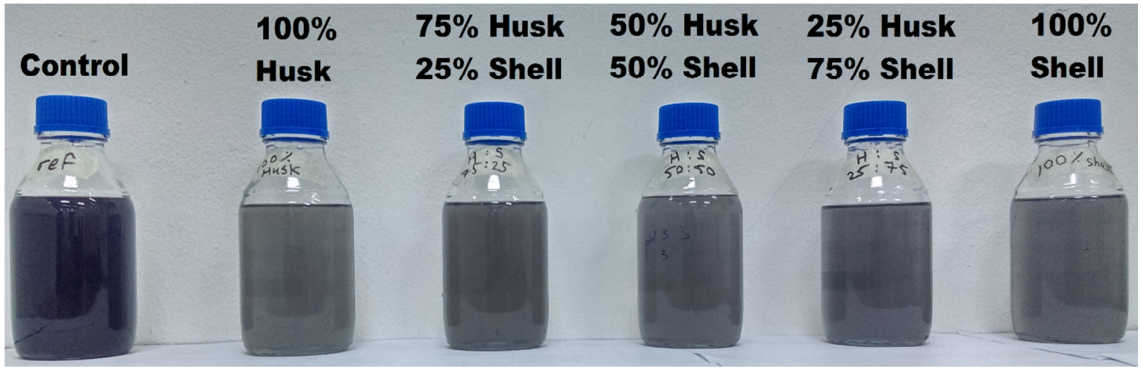


Figure 3.42: Wastewater samples after batch adsorption.

The amount of metal adsorbed on the activated carbon at equilibrium, q_e (mg/g) was calculated by using following equation;

$$q_e = \frac{(C_o - C_e)V}{W}$$

Where,

C_o is the initial metal ion concentration (mg/l)

C_e is the concentration of metal ions at equilibrium (mg/l)

V is the volume of the solution (l)

W is the mass of dry adsorbent used (g).

3.5 Coconut husk and shell briquettes

Prior to the production of briquettes from coconut shell and husk, it is important to characterize the raw materials in terms of their moisture content, ash content, volatile matter and calorific value. The standard test methods used in the characterization were as follows;

Proximate Analysis	Standard Test Method
Moisture content	**ASABE S358.2**; Moisture Measurement-Forages.
Ash content	**ASTM E1755 – 01**; Standard Test Method for Ash in Biomass
Volatile matter	**ASTM E872-82**; Standard Test Method for Volatile Matter in the Analysis of Particulate Wood Fuels
Calorific value	**ASTM D2015**; Standard Test Method for Gross Calorific Value of Coal and Coke by the Adiabatic Bomb Calorimeter

The procedures for the determination of these characteristics are found in Annex 15.

3.5.1 Manufacture of briquette

The stages involved in the manufacture of briquettes were as follows:-

- Preparation of raw materials
- Size reduction
- Screening
- Mixing
- Briquetting
- Drying

In this experiment, both non-carbonized briquettes and charcoal briquettes from coconut shell and husk were produced.

i) Raw materials preparation

The dehusking of dry coconut was carried out manually. A machete was used to open and detach the husk from the shell and the copra was removed from the shell. The husk was cut and shell broken into pieces so as to facilitate the shredding process.

Preparation of charcoal; the shell was crushed using a shredder to a size of about 4 mm and the husk was cut to about 3 – 5 cm, prior to carbonization. For the pyrolysis phase, a stainless steel horizontal cylindrical reactor was filled individually with the husk and shell. The reactor was then placed in a furnace and heated at 500 ^{o}C for about 2h. After the carbonization process, the furnace was turned off and the carbonized materials were left to cool down. The steps were repeated until sufficient materials was obtained for the briquetting process. The figure 3.43 shows the reactor used for pyrolysis, which is

design in a way to limited oxygen during carbonization.

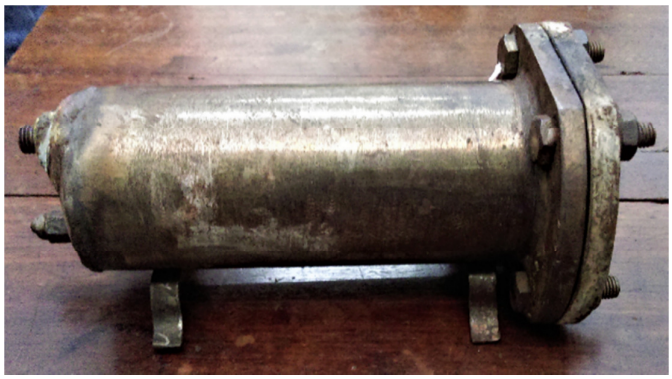


Figure 3.43: Reactor used for pyrolysis

ii) Size reduction & screening

For the production of non-carbonized briquette from coconut husk and shell, the material was reduced in size before it can be transformed into briquette. The shell and husk were milled separately in a pulveriser and sieved to a particle size of less than 1mm as shown in Figures 3.44 (a) (b). The same procedure was carried out for the charcoal samples.



Figure 3.44: (a) Coconut husk less than 1mm (b) Coconut shell less than 1mm

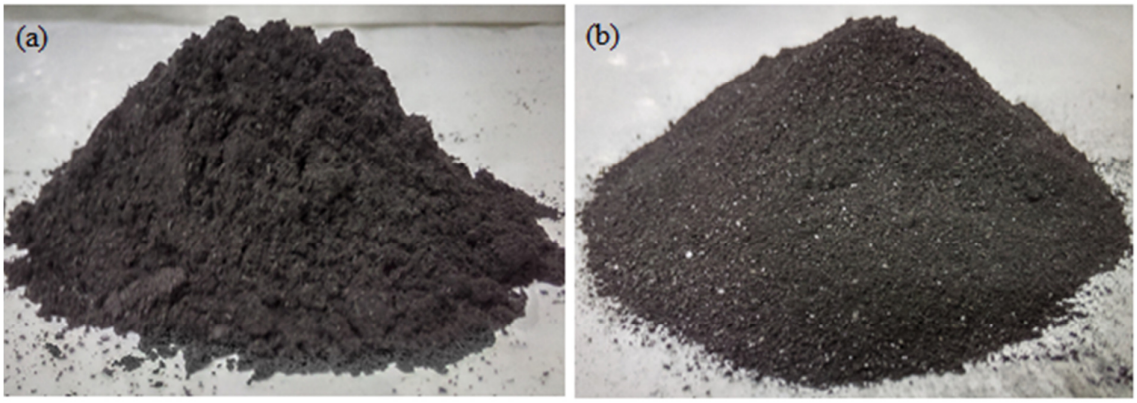


Figure 3.45: (a) Coconut husk charcoal less than 1mm (b) Coconut shell charcoal less than 1mm

iii) Mixing

The raw materials were weighed in the correct proportion before being mixed homogenously. Waste oil

with a calorific value of 39.547 MJ/kg was obtained from oil Refinery and was used for the following purposes:

- as a binder
- a smooth demoulding of briquettes.
- increasing the energy content of the briquettes
- increasing the combustibility of briquettes

Optimum Mix Determination

The aim of determining the optimum mix was to produce briquette having the highest calorific value, while taking into consideration the strength and consistency of briquettes. The percentages of coconut husk and shell were varied as shown in Tables 3.14 and 3.15. The maximum amount of oil that can be retained by each mixture of coconut husk and shell was then determined.

Table 3.14; Non-carbonised briquette compositions

Mixture	Non-carbonised composition (%)		Optimum oil used (%)
	Coconut Husk	Coconut Shell	
1	100	0	40
2	75	25	38
3	50	50	35
4	25	75	33
5	0	100	30

Table 3.15; Charcoal briquette compositions

Mixture	Charcoal composition (%)		Optimum oil used (%)
	Coconut Husk	Coconut Shell	
1	100	0	35
2	75	25	33
3	50	50	30
4	25	75	28
5	0	100	25

iv) Briquetting

The briquetting machine in figure 3.46 was used for the compaction of the homogenized mixture. A cylindrical mould of internal diameter 3cm was filled with a known mass of the sample and was positioned under a hydraulic jack of 4 ton. A constant pressure was applied on the sample and allowed to settle for about 5 minutes before demoulding.

Once all the briquettes were produced, they were allowed to dry in open air for at least 2 days prior to any testing.



Figure 3.47; (a) Non-carbonised briquette (b) Charcoal briquette

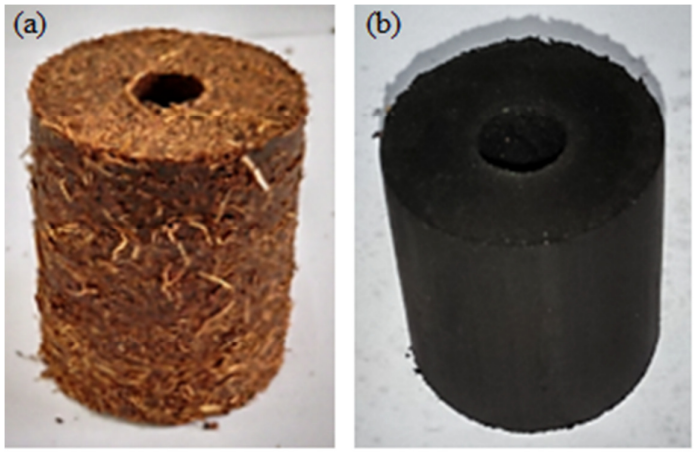


Figure 3.46; Briquetting machine

3.5.2 Tests

The following tests were performed on the briquette mixtures: density, gross calorific value, drop shatter test, combustion and flue gas analysis

Density of Briquettes

Each briquette mixture was measured and weighed after drying. The density was analysed stereometrically. The displacement method was not selected due to possible absorption of water by the briquette. The briquettes produced were in cylindrical holey type (see in figure 3.48), and were measured as follows;

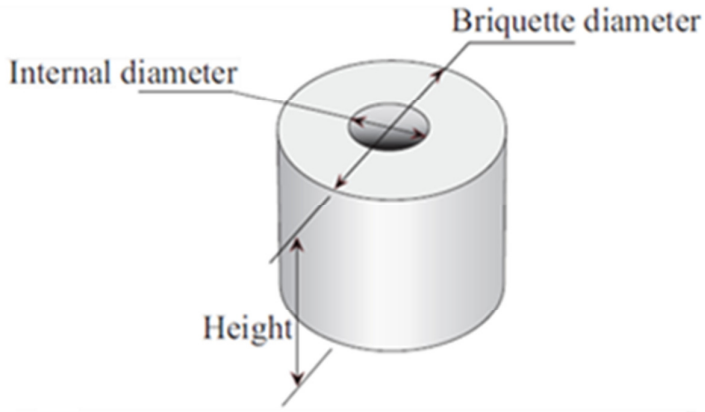


Figure 3.48: Schema of cylindrical holey type briquette

Step 1: Each briquette was weighed by using an electronic mass balance to the nearest 0.001g.

Step 2: A vernier caliper was used to measure the height and diameters of each cylindrical briquette. The height was measured in three positions around the briquette. For the external diameter, it was measured at the top, middle, and bottom positions and for the internal diameter, it is measured at both ends of the briquette.

Step3: The data obtained was tabulated and the volume of briquette was calculated. The density was determined from its mass and volume. See in Annex 16 (Part I).

Gross calorific value of briquettes

The calorific value is one of the most important parameter in the evaluation of materials to be used as fuels. The higher heating value of the briquettes were determined by the use of an oxygen bomb calorimeter and in accordance with the ASTM D2015 (Standard Test Method for Gross Calorific Value of Coal and Coke by the Adiabatic Bomb Calorimeter).

The oxygen bomb calorimeter is composed of these three main components:

- ***The bomb***; which retains the sample and oxygen for the combustion process.
- ***The steel bucket***; which holds a known amount of water, thermometer and bomb.
- ***The insulated outer jacket***; which completely insulates the apparatus thermally.

Basically the biomass sample is burned in the apparatus shown in figure 3.49, where the heat produced is transferred to a known mass of water. The steel bucket containing the water is completely insulated,

so it can be assumed that the entire energy of the sample is converted to the increase of the water internal energy. The calorific value of the sample is then calculated from its weight and the rise in temperature of the water. The calorific value obtained from the bomb calorimeter test represents the gross heat of combustion per unit mass of sample. The Gross calorific value of each briquette composition for non-carbonised and charcoal briquettes is found in Annex 16 (Part II).

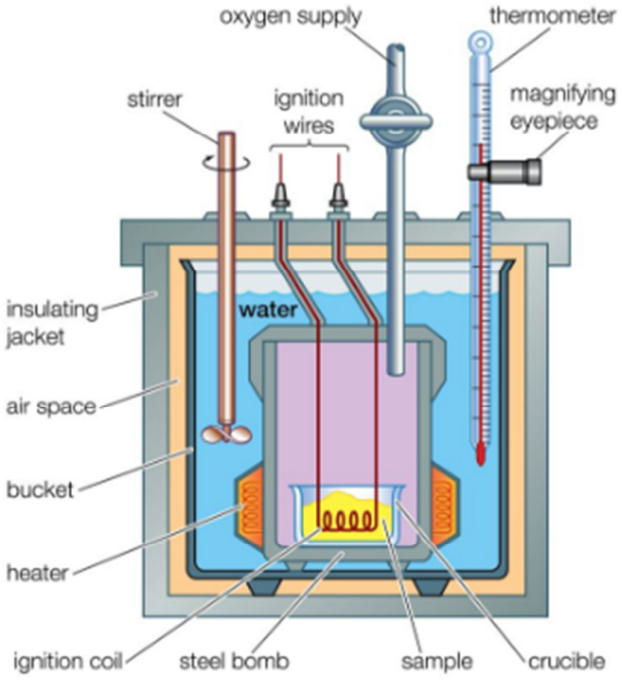


Figure 3.49: Schematic of oxygen bomb calorimeter (Helmenstine, 2018.)

Drop shatter test of briquettes

The ASTM D440 (standard test method of drop shatter test for coal) was used as reference to perform the drop shatter test of briquettes. This standard test method is used to determine the relative size stability and the friability of briquettes. It gives an indication of the ability of briquettes to withstand breakage when subjected to handling at production, storage and during transportation to customer.

The test was performed by placing each briquette of known mass in a resealable polythene bag and the bag was dropped twice from a distance of 6 ft (1.8m) onto a concrete floor. After the second drop, the briquette and its fractions was placed on the top of a set of sieves of the following sizes, 1, 0.75 and 0.5 in. and care was taken during sieving so as to prevent further breakage of the briquette. After sieving, the weight of the fragments remaining on each sieve and at bottom of sieves were measured. The test was done in triplicate for each category of briquettes. The percentage size stability is calculated as follows;

$$\text{Size stability}, \% = \frac{s}{S} \times 100$$

Where,

s is the sum of these products after testing and

S is the sum of these products before testing

On the other hand, the friability is expressed as,

$$Friability, \% = 100 - Size\ stability$$

(i.e. the sum of size stability and friability equal to 100%). The results for the drop shatter test of briquettes are found in Annex 16 Part III. Figure 3.50 and figure 3.51 show the state of the briquettes after drop shatter test for non-carbonised and charcoal briquette samples respectively.

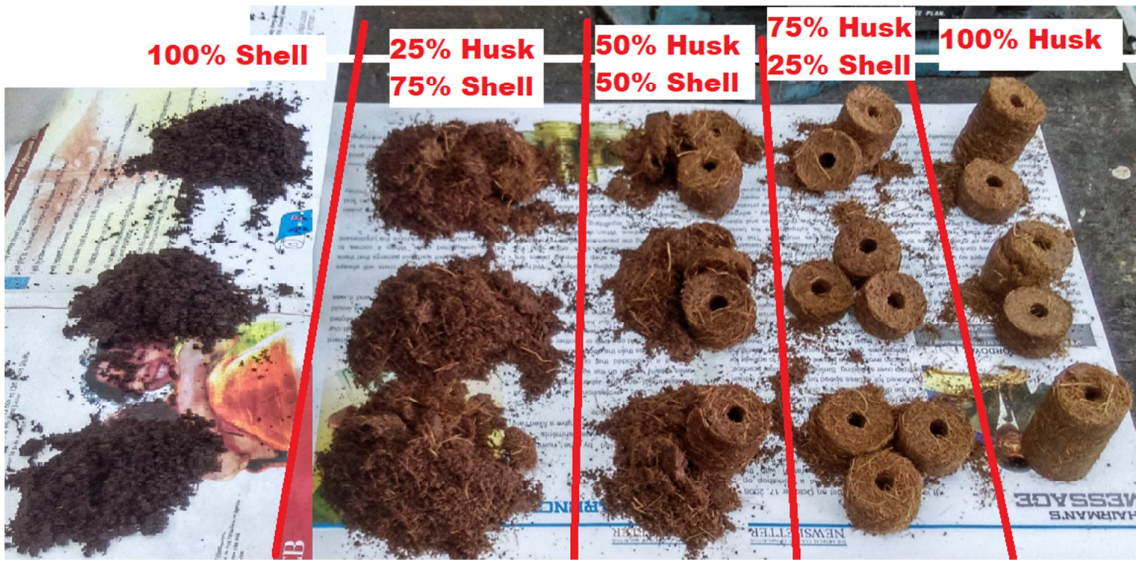


Figure 3.50: Non-carbonised briquettes after drop shatter test

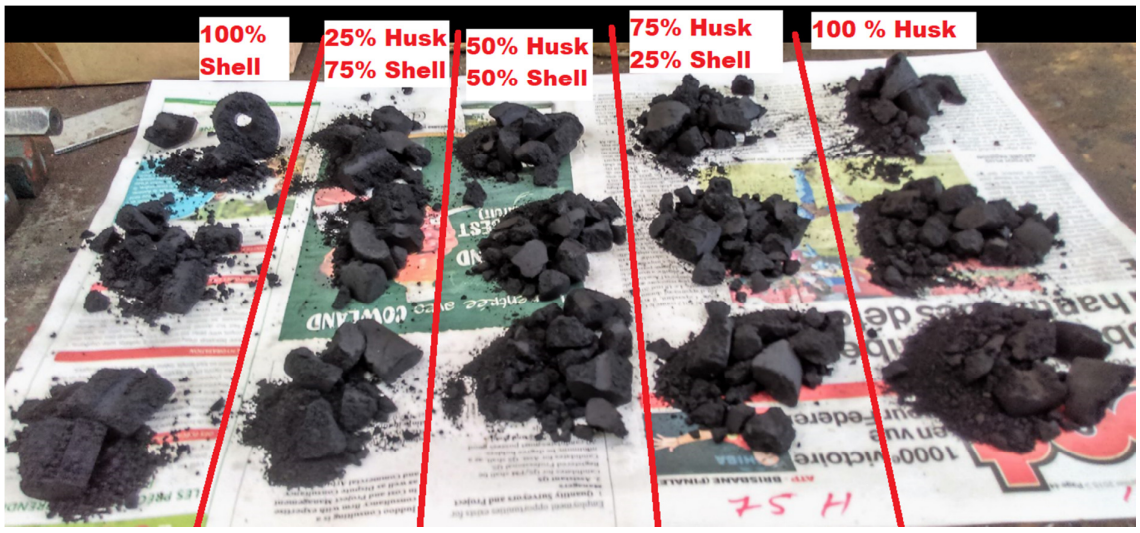


Figure 3.51: Charcoal briquettes after drop shatter test

Emission from combustion of briquettes

After performing the gross calorific value and the drop shatter tests, the non-carbonised briquette having a composition of 75% husk and 25% shell was the one with the optimum calorific value and strength. For charcoal briquette, briquette with a composition of 100% shell was the one which gave the optimal results in term of calorific value and strength. These briquettes were burned independently in the apparatus shown in Figure 3.53 and the flue gas emitted was then analysed by a flue gas analyser. The briquette was ignited before being placed in the apparatus and the blowers on the apparatus were switched on so as to supply oxygen for the combustion process. The probe of the flue gas analyser was

then placed in the aperture of the apparatus and the emission was read on the meter.

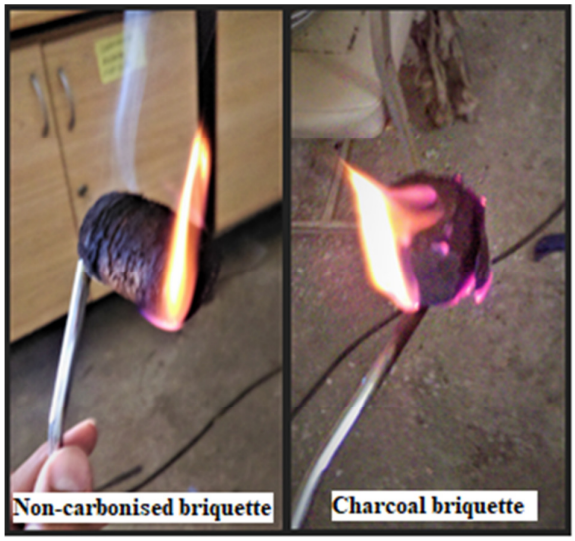


Figure 3.52: Briquette samples ignition



Figure 3.53: Apparatus used in the analysis of emission from briquette combustion

4. ANALYSIS OF RESULTS

4.1 Determining properties of coconut fibres

The diameter, tensile strength and Young's Modulus of the coconut fibers were tested before and after treatment with NaOH. A summary of the results are shown in Table 3.1. 6% NaOH has been used in the treatment of the fibers based on experiments already performed at the University of Mauritius and based on other studies which have had similar results (Karthikeyan *et al*., 2014). Treatment of the coconut fibre is essential to remove impurities such as lignin and pectin, which will negatively affect the adhesion of the fibers into the matrix during the composite fabrication.

The average diameter of the NaOH treated coconut fibre was found to be 191 ⌈m. This is in line with results obtained from other researchers in this field. In fact, the fiber diameter has been found to vary between 0.1 to 0.4 mm (Satyanarayana *et al.*, 1990; Aggarwal,1992; Agopyan *et al.*, 2005; Ramakrishna *et al.*, 2005; Toledo *et al.*, 2005; Reis, 2006).

Tensile strength above 100 MPa has been commonly recorded for coconut fibers (Satyanarayana et al., 1990; Aggarwal,1992; Agopyan et al., 2005; Ramakrishna et al., 2005; Toledo et al., 2005; Reis, 2006; Li et al., 2007). Lower values of the tensile strength have been rarely observed (Ramakrishna *et al*., 2005). For the local coconut fibers, the tensile strength is much lower (33 MPa) than those cultivated elsewhere. However, the results are still within the range that has been obtained by a few other researchers.

The coconut fibre lignocellulosic contents obtained for the local fibers were presented in Table 3.2. The results are very similar to those obtained by Agopyan *et al.* (2005) and Ramakrishna *et al.* (2005).

4.2 Coconut oil for temporary corrosion prevention

Several mixtures of coconut oil were tested to determine the corrosion prevention properties of coconut oil for temporary outdoor exposures. The results are shown in figures 3.17 and 3.18 and Tables 3.6 and 3.7. Honey, mixed with coconut oil, has been found to significantly improve the corrosion prevention properties of coconut oil. However, this mixture has a tendency to flow and run off the exposure racks. For this reason, EVA was used together with honey and coconut oil. EVA was used to increase the viscosity of the coconut oil so as to prevent it from running off the samples when exposed outdoors. Though EVA is not a green material, a convenient green material to replace it needs to be investigated. However, better results have been obtained when EVA was employed.

After 90 days of sheltered exposure, it was found that the mixture consisting of 4% EVA with 75% coconut oil and 25% honey has been found to provide better resistance for the short and long term period, with only 3.6% of the total surface area was corroded after 92 days of exposure. For unsheltered outdoor exposures, the samples coated with the same mixture was found to have corroded 40% less than that of the uncoated one, after 19 days of exposure. The main issue with the outdoor exposure was that the occasional rain could have adversely affected the performance of the coconut oil mixture. However, for the very short period of 7 days, the coconut oil had a very good effect on corrosion prevention. Further investigations would be essential to develop of unique mixture of coconut oil for temporary corrosion prevention. It should be noted that, worldwide, volatile corrosion inhibitors are commonly used for temporary corrosion prevention. These compounds are not

environmental friendly. However, it should also be noted that investigations on green solutions, such as the use of coconut oil, has been rarely performed. SEM results are shown in Annex 17.

4.3 Manufacturing of composite board from coconut fibre and shell

An injection moulding equipment was used fabricated to the University for the manufacturing of the composites with coconut fiber reinforcement in a polyester matrix.

The main observation, however, was that the polyester resin has a higher tensile strength than the composites. This is, however, in accordance with other research work performed with coconut coir fibers. It has been found that the water adsorbed into the lignocellulosic surface of the hydrophilic coir fiber apparently prevents an efficient adhesion to the hydrophobic polymer matrix, which also happens in other natural fiber composites. As a consequence the incorporation of coir fiber tends to decrease the mechanical strength of polyester composites for any volume fraction of fiber (Santafé Júnior H.P.G et al, 2010).

It should noted that the mechanical properties of short fiber-reinforced composites are expected to depend on (Karthikeyan A. et al., 2014):
(i) the intrinsic properties of matrix and fibers,
(ii) aspect ratio, content length distribution, and orientation of the fibers in the composites, and
(iii) fiber-matrix adhesion that is responsible for the efficiency of load transfer in the composites.
The adhesion of the fibers to the matrix may have a negative impact. In principle, there are ways to reverse this negative condition. For instance, a strong alkali treatment of coir fiber improves the adhesion to the polyester matrix and thus increases the composites strength by approximately 50% for a volume fraction of 30% of coir fiber (Santafé Júnior H.P.G et al, 2010). Other ways to improve the properties of the composites is through the use of a different manufacturing method, such as compression moulding. It should also be noted that the pressure used to feed the resin into the mould was quite low as compared to the work performed by other researchers. In fact, the pressure could not be increased above 0.8 bar and this was a major drawback in improving the properties of the composite.

It can be expected that with the use of higher pressure in the manufacture of the composite, use of other manufacturing methods such as compression moulding and, probably, a deeper investigation on the treatment of the fibers may lead to composites with better strength.
Though the tensile strength of the composites are low compared to that of the pure resin, it is comparable to those which have been obtained in other studies. In fact, tensile strength in the range 21-29 MPa has been reported (Santafe Junior *et al*, 2010). Lower tensile strength has been reported for epoxy based composites with coconut fiber reinforcements in the range 9-13 MPa (Karthikeyan *et al*., 2014). The fibre content that was tested ranged from 2% to 40%.

In the present study, the tensile strength of the composites have been found to decrease with increasing fibre content from 5% and above. The fiber content leading to the highest tensile strength was found to be 3% with the tensile strength on average being 21.2 MPa for coconut fibers from Agalega and 23.5 MPa for local coconut fibers. The Young's Modulus was found to increase considerably for the composites compared to the pure resin and this implied that they were more rigid.

However, they also became more brittle.

The shell powder was also added to the composite to investigate into its effect on its mechanical properties. A slight improvement in the tensile strength was observed (around 3%) when 2% coconut powder was added to the 3% coconut fibre into the polyester resin, with a slight decrease (around 8%) in the Young's Modulus. The composite has thus become stronger and tougher. Further investigation is therefore required to determine the effect of coconut powder on the properties of the composite.

Though the results for the tensile strength for the composites are not very interesting for engineering applications, it should be noted that higher strength may be expected with a change in the manufacturing system. Moreover, other tests may be performed to determine the performance of the composite for other uses such as thermal insulator, etc. SEM test results with respect to the fibres are shown in Annex 17.

4.4 Activated carbon production from coconut husk and shell

Granulated coconut husk and shell activated carbons were used to treat the wastewater that was generated from a textile industry. The batch adsorption experiments were carried out in the setup as shown in figure 3.41, where various husk to shell ratio of activated carbons were used to treat the wastewater samples until equilibrium were reached. After equilibrium, the treated effluents were analysed in terms of the presence of cations, anions and heavy metals. A summary of the results obtained is shown in Table 4.1.

Table 4.1: Summary of test report for wastewater analysis

Parameter	Unit	Control	Husk : Shell ratio				
			100:0	75:25	50:50	25:75	0:100
Chemical							
Chloride	mg/l	80	90	85	85	65	80
Potassium	mg/l	29	25	29	28	29	30
Sodium	mg/l	1280	1160	1100	1280	1070	1400
Heavy Metals							
Cadmium	mg/l	n.d	n.d	n.d	n.d	n.d	n.d
Cobalt	mg/l	n.d	n.d	n.d	< 0.05	n.d	n.d
Copper	mg/l	0.10	< 0.05	0.07	< 0.05	0.06	0.09
Nickel	mg/l	n.d	n.d	n.d	< 0.05	n.d	< 0.05
Total Chromium	mg/l	n.d	< 0.05	< 0.05	< 0.05	< 0.05	< 0.05
Zinc	mg/l	0.08	0.11	0.07	0.07	0.07	0.10

Among the parameters tested, it can be seen that the untreated wastewater (the control) only contains copper and zinc in terms of heavy metals and a high level of sodium. The present of the high level of sodium is due to the sodium salts used in processing units and is usually in the range of 975 to 2330 mg/l (Hussain et al. 2004).

Based on the results obtained, the amount of each pollutants adsorbed on the activated carbon at equilibrium was calculated and tabulated in Table 4.2. Since the untreated wastewater samples only indicated the presence of copper and zinc as heavy metals, consequently only the cations, anion, copper and zinc were considered for the calculation of q_e, mg/g (amount of substance adsorbed on the activated carbon at equilibrium).

Table 4.2: Amount of pollutants adsorbed on the activated carbon at equilibrium

Parameter	q_e (mg/g)				
	Husk : Shell ratio				
	100:0	75:25	50:50	25:75	0:100
Chloride	-5	-2.5	-2.5	7.5	0
Potassium	2	0	0.5	0	-0.5
Sodium	60	90	0	105	-60
Copper	> 0.025	0.015	> 0.025	0.02	0.005
Zinc	-0.015	0.005	0.005	0.005	-0.01

From Table 4.2, the mixture of 25% husk and 75% shell activated carbon adsorbed the highest amount of chloride (7.5 mg/g) and sodium (105mg/g). For copper more than 0.025 mg/g was adsorbed on both 100% husk and 50% husk/50% shell activated carbons. 0.005mg of zinc was adsorbed per g of activated carbon for the ratio of husk to shell of 75:25, 50:50 and 25:75. For the adsorption of pollutants, the 25% husk and 75% shell activated carbon could be recommended. Furthermore, as future works, additional tests such as Fourier transform infra-red spectrophotometer (FT-IR) and scanning electron microscope (SEM) could be carried out. Also, Aljeboree et al. (2017) investigated

other various physiochemical parameters such as, contact time, initial dye concentration, adsorbent dosage, particle size, pH of dye solution and temperature in a batch-adsorption technique.

4.5 Coconut husk and shell briquettes

4.5.1 Characteristics

The characteristics of coconut husk and shell were determined in terms of moisture content, ash content, fixed carbon, cellulose content, hemi-cellulose content and lignin content, respectively. The characteristics are summarised in Table 4.3.

Table 4.3: Characteristic of coconut husk and shell

Sample	Moisture Content, %	Ash Content, %	Volatile Matter, %	Fixed Carbon, %	Cellulose Content, %	Hemi-cellulose Content, %	Lignin Content, %
Coconut Husk	20.2	1.98	82.3	10.3	33.3	5.0	37.1
Coconut Shell	11.8	0.125	74.6	15.1	40.5	12.6	36.2

EsauMwinuka (2015) mentioned that biomass is a made up of three basic components; lignin, cellulose and hemicellulose. Lignin binds the biomass fibres to give them their natural strength while hemicellulose and cellulose polymers are the basic building blocks of the biomass fibres (EsauMwinuka, 2015). The lignin contents of coconut husk and shell were determined to be 37.1% and 36.2%, respectively. The moisture content and ash content of coconut husk was higher by 8.4% and by 1.855%, respectively, than that of coconut shell. Promdee et al. (2017) found that activated carbon particle (ACP) derived from coconut shell gave the highest fixed carbon content (55.42%), the low moisture content (23.55%) as compared to coal briquettes product (CBP) with a fixed carbon content of 47.35% and volatile matter content of 25.21%. In addition, ACP and CBP could be considered as a potential source of renewable solid fuel with a heating value of 33.45 and 27.45 MJ kg, respectively (Promdee et al., 2017).

Table 4.3: Gross Calorific Value of raw materials

Raw material	Average GCV (MJ/kg)
Non-carbonised husk	17.372
Non-carbonised shell	18.925
Charcoal husk	22.801
Charcoal shell	32.271
Waste oil	39.547

Table 4.3 gives the gross calorific value of the different raw materials that have been utilized for briquette formation. The average GCV of charcoal husk was found to be higher than that of non-carbonised husk by 23.8%. The average GCV of charcoal shell was determined to be 32.271 MJ/kg as compared to that of non-carbonised shell (18.925 MJ/kg). Waste oil was used as a binder for the

briquette formation and it average GCV was 39.547 MJ/kg.

4.5.2: Briquettes Testing

The briquettes produced were analysed in terms of their densities (Table 4.4), Gross Calorific Value (Table 4.5), Drop Shatter Test (Table 4.6) and emissions due to combustion (Table 4.7).

Table 4.4: Density of Non-carbonised and Charcoal briquettes

Non-carbonised composition (%)		Average Density (kg/m^3)
Coconut Husk	**Coconut Shell**	
100	0	888.0
75	25	929.4
50	50	977.0
25	75	1072.8
0	100	-
Charcoal composition (%)		**Average Density (kg/m^3)**
Coconut Husk	**Coconut Shell**	
100	0	1055.0
75	25	1147.2
50	50	1220.1
25	75	1275.8
0	100	1326.4

Densification improves the volumetric calorific value of a fuel, reduces the cost of transport and can help in improving the fuel situation especially in rural areas (Grover and Mishra, 1996). The densities of the biomass briquettes can be determined by measuring their masses and their volumes separately (EsauMwinuka, 2015). The non-carbonised mixture of 25% husk and 75% shell showed a highest average density of 1072.8 kg/m^3, followed by that of non-carbonised mixture of 50% husk and 50% shell and by that of non-carbonised mixture of 75% husk and 25% shell. It should be noted that the density for the 100% shell non-carbonised briquette could not be determined due to its fragility during handling. It was worth noting that the average densities for the charcoal briquettes for 100% coconut shell and the 25% husk and 75% shell were 1326.4 kg/m^3 and 1275.8 kg/m^3, respectively. Tembe et al. (2014) stated that high values of compressed density could be linked to moisture present in the starch, which in turn increased the mass per unit volume of the briquettes. The lowest average density was obtained for non-carbonised husk and 100% charcoal husk. Olorunnisola (2006) pointed out that the general decrease in compressed density with increase in coconut husk content may be due to the relatively low bulk density of coconut.

Table 4.5: Gross Calorific Value of Non-carbonised & Charcoal briquettes

Non-carbonised composition (%)		Average GCV (MJ/kg)
Coconut Husk	Coconut Shell	
100	0	21.872
75	25	22.327
50	50	22.648
25	75	22.179
0	100	21.890
Charcoal composition (%)		**Average GCV (MJ/kg)**
Coconut Husk	**Coconut Shell**	
100	0	28.979
75	25	29.691
50	50	30.941
25	75	31.832
0	100	32.743

Combinations with high coconut shell charcoal content resulted in high calorific value as coconut shell is a raw material which is considered to have high density and higher calorific value 32.271 MJ/kg. Arellano et al. (2015) pointed out that the blending of the raw material with high calorific value to a raw material with low calorific value greatly enhanced the calorific value of the briquette. Arellano et al. (2015) conducted a study on charcoal briquettes derived from combinations of coconut shell, corn cob and sugarcane bagasse and the results demonstrated that the charcoal combination with the highest calorific value was 50-25-25 of coconut shell, corn cob and sugarcane bagasse with 19951.40 J/g. In this study, the highest calorific was found to be that of 100% charcoal briquette (32.743 MJ/kg), followed by 25% husk and 75% shell charcoal briquette (31.832 MJ/kg).

Table 4.6: Drop Shatter Test

Non-carbonised composition (%)		Average size stability (%)	Average friability (%)
Coconut Husk	Coconut Shell		
100	0	99	1
75	25	96	4
50	50	77	23
25	75	36	64
0	100	20	80
Charcoal composition (%)		**Average size stability (%)**	**Average friability (%)**
Coconut Husk	**Coconut Shell**		
100	0	43	57
75	25	46	54
50	50	50	50
25	75	57	43
0	100	66	34

The results of the drop shatter test showed that the average size stability of the non-carbonised combinations of husk and shell was higher than that of the charcoal combinations of husk and shell. For instance, the average size stability of 100% non-carbonised husk was 99% with an average friability of 1% as compared to the average stability of 100% charcoal husk which was found to be

43% with an average friability of 57%. However, for the charcoal composition the best average size stability was obtained for 100% coconut shell (66%) followed by that of the mixture of 25% husk and 75% shell (57%).

Table 4.7: Result from flue gas analyser meter reading

Parameters	Non-carbonised briquettes	Charcoal briquettes
CO	861 ppm	454 ppm
NO	6 ppm	-
NO_x	6 ppm	-
Flue gas temperature	50.2 ^oC	46.0 ^oC

The Testo flue gas analyser showed the presence of carbon monoxide, nitrogen monoxide and nitrogen dioxide in the flue gas from the non-carbonized briquettes and only carbon monoxide for the charcoal briquettes. The presence of carbon monoxide and nitrogen monoxide may be due to the lack of oxygen required for complete combustion of the briquettes. However, these results also showed that there was no presence of oxides of sulfur that can lead to corrosion. Further studies will hence be required for the assessment of the emissions produced from the combustion of briquettes.

5. CONCLUSIONS

It should be noted that there are several factors which have led to a significant delay in the submission of the final report:

1. Problems cropped up with the manufacturing of the composites. In fact, the injection moulding equipment was fabricated at the University. However, it turned out to be extremely tedious to make the equipment work properly. The composites produced had much air bubbles and it was a real challenge to remove these bubbles. Eventually, several months were lost with the testing of prototype.
2. The main problem in Mauritius is that a standard supply of the resin is never obtained. In fact, several experiments have been performed, but the results could not be used or compared because of the differences in the viscosity of the resin which leads to different results.
3. It should also be noted that, for the investigation of coconut oil for temporary corrosion prevention, it was very difficult to come forward with an efficient mixture. Much work has been performed by trial and error and this led to a lot of time lost.

Several mixtures of coconut oil were tested to determine the corrosion prevention properties of coconut oil for temporary outdoor exposures. Honey, mixed with coconut oil, has been found to significantly improve the corrosion prevention properties of coconut oil. However, this mixture has a tendency to flow and run off the exposure racks. For this reason, EVA was used together with honey and coconut oil. EVA was used to increase the viscosity of the coconut oil so as to prevent it from running off the samples when exposed outdoors. Though EVA is not a green material, a convenient green material to replace it needs to be investigated. However, better results have been obtained when

EVA was employed.

After 90 days of sheltered exposure, it was found that the mixture consisting of 4% EVA with 75% coconut oil and 25% honey has been found to provide better resistance for the short and long term period, with only 3.6% of the total surface area was corroded after 92 days of exposure. For unsheltered outdoor exposures, the samples coated with the same mixture was found to have corroded 40% less than that of the coated one, after 19 days of exposure. The main issue with the outdoor exposure was that the occasional rain could have adversely affected the performance of the coconut oil mixture. However, for the very short period of 7 days, the coconut oil had a very good effect on corrosion prevention. Further investigations would be essential to develop of unique mixture of coconut oil for temporary corrosion prevention. It should be noted that, worldwide, volatile corrosion inhibitors are commonly used for temporary corrosion prevention. These compounds are not environmental friendly. However, it should also be noted that investigations on green solutions, such as the use of coconut oil, has been rarely performed.

However, for the local coconut coir fibers, the average diameter was determined to be 191 ⌈m. The average tensile strength was also found to be on average 33 MPa which is, in general, quite lower than those determined by other researchers worldwide (ranging above 100 MPa). The coconut fibre lignocellulosic contents obtained for the local fibers were presented and were found to be very similar to those obtained by other researchers.

As for the coconut fiber and polyester composites, it was found that their tensile strength was quite low (22-23 MPa) but this was also in accordance with the results obtained from other studies. Various reasons can explain these low values. However, much better results would be expected with a change of the manufacturing method. Compression moulding would be more appropriate and would give better results. However, it would also be interesting to determine other applications of composite, especially for thermal insulation.

The results of this study showed that the mixture of 25% husk and 75% shell activated carbon adsorbed the highest amount of chloride (7.5 mg/g) and sodium (105mg/g). Also, good quality briquettes with high energy content can also be produced from a mixture of 25% husk and 75% shell charcoal briquette with a difference of only 2.8 % higher for the 100% charcoal shell briquette. The density and average size stability of the 25% husk and 75% shell charcoal briquette and 100% charcoal shell briquette suggested that they could be transported over a long distance without any disintegration. Based on the conclusions, more research should be conducted on the combustion characteristics of coconut husk and shell briquettes so as to assess their potential as a fuel product.

REFERENCES

Aggarwal L. K., 1992, Studies on cement-bonded coir fibre boards. Cement and Concrete Composites, 14(1), pp. 63-69.

Agopyan, V., Savastano Jr, H., John, V. M., and Cincotto, M. A., 2005. "Developments on vegetable fibre-cement based materials in Sa?o Paulo, Brazil: An overview." Cement and Concrete Composites, 27(5), 527-536.

Agopyan, V., Savastano Jr, H., John, V. M., and Cincotto, M. A., 2005. "Developments on vegetable fibre-cement based materials in Sa?o Paulo, Brazil: An overview." Cement and Concrete Composites, 27(5), 527-536.

Aguilà, D., 2013. Estudi tècnic-econòmic sobre la biomassa d'origen forestal a Catalunya.

Ahmad, S., Ashraf, S.M. and Riaz, U., 2005. Corrosion studies of polyaniline/coconut oil poly (esteramide urethane) coatings. *Polymers for advanced technologies*, *16*(7), pp.541-548.

Aljeboree, A M., Abbas N. Alshirifi A N., Ayad F. Alkaim, A F., 2017. Kinetics and equilibrium study for the adsorption of textile dyes on coconut shell activated carbon. *Arabian Journal of Chemistry*, 10, pp. S3381–S3393.

AOAC, 1994. Official Methods of Analysis, Association og Oficial Analytical Chemists, 1111 North 19th suite 20,16th ed. Arlington, Virgina,USA 22209.

ARC n.d, la culture du Cocotier (Cocos Nucifera), Agricultural Research and Extension Unit (Food and Agricultural Research Council).

Arellano, G.M.T., Kato, Y.S., Bacani, F.T., 2015. Evaluation of Fuel Properties of Charcoal Briquettes Derived From Combinations of Coconut Shell, Corn Cob and Sugarcane Bagasse. DLSU Research Congress.

Bandosz, TJ. (ed.), 2006. *Activated Carbon Surfaces in Environmental Remediation.* Oxford, Elsevier.

Bansal R. C. and Goyal, M., 2005 "Activated Carbon Adsorption," CRC Press, Boca Raton, doi:10.1201/9781420028812.

Bekele, M. and Girmay, Z., 2014. Reading through the Charcoal Industry in Ethiopia: Production, Marketing, Consumption and Impact. Forum for Social Studies.

Bujang, I.Z., Awang, M.K., and Ismail, A.E., 2007. "Study On The Dynamic Characteristic Of Coconut Fibre Reinforced Composites", *Regional Conference on Engineering Mathematics, Mechanics, Manufacturing & Architecture (EM1 ARC).*

Callister W.D. Jr. and Rethwisch D.G., 2010. *Materials Science and Engineering: An Introduction,* 8th ed., John Wiley & Sons Inc.

Campbell, F.C., 2010. *Structural composite materials*. 1st ed. USA: ASM international.

Cavalcanti da Silva, J.A., 2011, *Biodegradable Lubricants and their Production via Chemical Catalysis*. INTECH Open Access Publisher.

Cecen, F. and Aktas, Ö., 2011. *Activated carbon for water and wastewater treatment: integration of adsorption and biological treatment*, Weinheim, Wiley VCH.

El-Etre, A.Y. and Abdallah M., 2000. Natural honey as corrosion inhibitor for metals and alloys. II. C-steel in high saline water. *Corrosion Science* Vol. 42, Pages 731-738.

EsauMwinuka, T., 2015. Effects of Process Parameters on the Density and Durability of Biomass Briquettes Made from Wet Method. International Journal of Engineering Research and Development, pp.32-38.

FAO, 1987. Food and Agriculture Organization (FAO), Industrial charcoal making technologies, FAO Forestry Department Available from, http://www.fao.org/docrep/x5555e/x5555e03.htm#TopOfPage, accessed 14 November 2017

Feng, X. (ed.), 2015. *Nanocarbons for Advanced Energy Storage*, Print ISBN: 978-3-527-33665-4.

Gelfuso, M.V., Silva, P.V.G.D. and Thomazini, D., 2011. Polypropylene matrix composites reinforced with coconut fibers. *Materials Research*, *14*(3), pp.360-365.

Gratuito M.K.B., Panyathanmaporn T., Chumnanklang R.A., Sirinuntawittaya N., and Dutta A., 2008. *Production of activated carbon from coconut shell: Optimization using response surface methodology*, Elsevier Science & Technology.

Grover. P.D. and Mishra, S.K., 1996. Biomass Briquetting:Technology And Practices. Food And Agriculture Organization Of The United Nations.

Helmenstine, A.M., 2018. "Calorimeter Definition in Chemistry." Ph.D., ThoughtCo, available from; thoughtco.com/definition-of-calorimeter-in-chemistry-604397.

Hussain, J., Hussain, I., and Arif, M., 2004, CHARACTERIZATION OF TEXTILE WASTEWATER, Journal of Industrial Pollution Control 20 (1) pp. 137 -144, India

Karthikeyan A., Balamurugan K., Kalpana A., 2014, The effect of sodium hydroxide treatment and fiber length on the tensile property of coir fiber-reinforced epoxy composites, Sci Eng Compos Mater, 21(3), pp.315–321.

Kobya, M., Demirbas, E. and Senturk, E., 2005. M. Ince, Bioresource Technology 96 1518-1521

Li, Z., Wang, L., and Wang, X., 2007. "Cement composites reinforced with surface modified coir fibers." Journal of Composite Materials, 41(12), 1445-1457.

Marsh, H. and Rodriguez Reinoso, F., 2006. *Activated Carbon*, Elsevier Science & Technology.
Pickering, K.L., Aruan Efendy, M.G. and Le, T.M., 2016. *A review of recent development in natural fibre composites and their mechanical performance*, Elsevier Science & Technology

Molina-Sabio,M., Rodríguez-Reinoso,F., Caturla, F. and Sellés, M.J., 1995. Porosity in granular carbons activated with phosphoric acid. Carbon, 33 (1995), p. 1105.

New Zealand Institute of Chemistry, 2008. Chemical cleaning of metals. Available from: nzic.org.nz/ChemProcesses/metals/8H.pdf, accessed on 23 June 2016.

NIIR, 2015. The complete book on biomass based products, niir board of consultants & engineers.

Noria Corporation. Oil Viscosity – How it's Measured and Reported. Available from: http://www.machinerylubrication.com/Read/411/oil-viscosity, accessed 1 May 2016

Okaka J.C and Potter N.N., 1977. Functional and storage properties of cow pea-wheat flour blends in

bread making. J Food Sci. 1977;42:828–833. doi: 10.1111/j.1365-2621.1977.tb12614.x.

Olorunnisola, A.O.2006. Strength and water absorption characteristics of cement-bonded particleboard produced from coconut husk. Journal of Civil Engineering Research and Practice 3(1):41-49.

Pickering, K.L., Aruan Efendy, M.G. and Le, T.M., 2016. *A review of recent development in natural fibre composites and their mechanical performance*, Elsevier Science & Technology

Potgieter, J.H., Olubambi, P.A. and Thanjekwayo, N.P., 2012. Investigation of the Potential of Some Plant Extracts to Inhibit the Corrosion of Duplex Stainless Steels in Acidic Media. *Journal of Metallurgical Engineering, 1(2),* pp 41-47.

Promdeea, K., Chanvidhwatanakita, J., Satitkunec, S., Boonmeec, C., Kawichaid, T., Jarernpraserte, S., Vitidsant, T., 2017. Characterization of carbon materials and differences from activated carbon particle (ACP) and coal briquettes product (CBP) derived from coconut shell via rotary kiln. Renewable and *Sustainable Energy Reviews 75*, pp. 1175–1186.

Quinchia, L. A., Delgado, M. A., Valencia C., Franco, J. M. and Gallegos C., 2009. "Viscosity Modification of High-Oleic Sunflower Oil with Polymeric Additives for the Design of New Biolubricant Formulations", *Environmental Science and Technology.*

Rani, S., Joy, M.L. and Nair, K.P., 2015. Evaluation of physiochemical and tribological properties of rice bran oil–biodegradable and potential base stoke for industrial lubricants. *Industrial Crops and Products*, *65*, pp.328-333.

Reis, J. M. L., 2006. "Fracture and flexural characterization of natural fiber-reinforced polymer concrete." Construction and Building Materials, 20(9), 673-678.

Rivera-Grau, L.M., Casales, M., Regla, I., Ortega-Toledo, D.M., Cuervo, D., Asencio, J., Gonzalez-Rodriguez, J.G. and Martine-Gomez, L., 2012. Corrosion Inhibition by a Coconut Oil Modified Imidazoline for Carbon Steel Under the Combined Effect of CO2 and H2S. *Int. J. Electrochem. Sci*, *7*, pp.12610-12620.

Rufford T E., Zhu, J. and Hulicova-Jurcakova D., 2013. *Green Carbon Materials: Advances and Applications*, Boca Raton, Taylor & Francis Group, LLC.

Santafé Júnior H.P.G, Lopes F.P., Costa L.L., Monteiro S.N., 2010, Tensile Behavior of lignocellulosic reinforced polyester composites: Part III coir fiber, Revista Matéria, v. 15, n. 2, pp. 202-207.

Satyanarayana, K. G., Sukumaran, K., Mukherjee, P. S., Pavithran, C., and Pillai, S. G. K., 1990. "Natural fibre-polymer composites." Cement and Concrete Composites, 12(2), 117-136.

Sekar, M., V. Sakthi and S. Rengaraj, 2004. Kinetics and equilibrium adsorption study of lead(II) onto activated carbon prepared from coconut shell. J. Colloid Interface Sci., 279: 307-313.

Sugumaram, P. & Seshadri S., 2010. Biomass charcoal briquettes 'Technology for alternative energy based income generation in rural areas.

Tan, I.A.W., Ahmad, A.L. and Hameed, B.H., 2008. Optimization of preparation conditions for activated carbons from coconut husk using response surface methodology. *Chemical Engineering Journal*, *137*(3), pp.462-470.

Tembe, E.T., Otache, P.O. and Ekhuemelo, D.O., 2017. Density, Shatter index, and Combustion

properties of briquettes produced from groundnut shells, rice husks and saw dust of Daniellia oliveri. Journal of Applied Biosciences 82, pp.7372 – 7378.

Toledo Filho, R. D., Ghavami, K., and England, G. L., 2005. "Free, restrained and drying shrinkage of cement mortar composites reinforced with vegetable fibres." Cement and Concrete Composites, 27(5), 537-546.

UNDP / CEDRO, 2016. *Biomass briquetting process*. A guideline report.

Veer-Ramjeawon P., Chan M., 2010. Use of coconut oil as a substitute to diesel in Agalega, UNEP, Partnership for Clean Fuel and Vehicles, available from http://www.unep.org/transport/PCFV/PDF/Mauritius_%20MChan_%20Autocheck.pdf, accessed in October 2014.

Wahyuningrum, D., Achmad, S., Syah, Y.M., Buchari, B. and Ariwahjoedi, B., 2008. The Synthesis of Imidazoline Derivative Compounds as Corrosion Inhibitor towards Carbon Steel in 1% NaCl Solution. *Journal of Mathematical and Fundamental Sciences*, *40*(1), pp.33-48.

Yahya M.A, Al-Qodah Z., and Ngah C.W.Z., 2015. *Agricultural bio-waste materials as potential sustainable precursors used for activated carbon production: A review*, Elsevier Science & Technology.

Yusufu, M.I., Ariahu, C.C. and Igbabul, B.D., 2012. Production and characterization of activated carbon from selected local raw materials.*African Journal of Pure and Applied Chemistry*, *6*(9), pp.123-131.

Yusufu, M.I., Ariahu, C.C. and Igbabul, B.D., 2012. Production and characterization of activated carbon from selected local raw materials.*African Journal of Pure and Applied Chemistry*, *6*(9), pp.123-131.

APPENDIX

Annex 1: Potential corrosion inhibitors for mild steel

Proposed inhibitors	Metal used	Type of inhibitor	Corrosive medium	Methodology	Result	Reference
Polyaniline (PAni)	Stainless steel coupons of 2 x 3 cm			PAni was synthesised by miniemulsion polymerisation. Spin coating technique was for applied on metal coupons. ASTM 610-01 was used to determine efficiency of coating.	PAni retards corrosion to a great extent by accelerating the formation of a passive Fe_2O_3 layer	Bhadra et al., 2011
Coconut coir dust	Mild steel, 0.09 cm x 5 cm 4 cm (surface area = 20 cm^2) dimensions, for weight loss study and 3 cm x 3 cm dimensions for hydrogen evolution measurements.	Mixed	0.5M H_2SO_4	1kg of the coconut coir dust was extracted in **Soxhlet apparatus** using **methanol** for 48 h. The extract was concentrated initially using **rotary evaporator** and finally by evaporation to dryness on a **steam bath** to obtain a solid residue devoid of methanol. The water extract was obtained by soaking the coir dust in **deionised water** for 72 h. It was then filtered and the filtrate evaporated to dryness on a steam bath to obtain a solid residue. The solid residues of both extracts were stored in a refrigerator prior to use in corrosion studies. Chemical and electrochemical techniques used.	Max. inhibition efficiency = 87% for methanol coconut coir dust extract and 45% for water coconut coir dust extract The adsorption of the extracts' components onto the mild steel surface follow Temkin and Freundlich adsorption isotherms for methanol and water extracts respectively.	Umoren et al., 2014
Coconut petiole	Mild steel, 5 cm x 1 cm coupons with 2	Mixed	0.5M H_2SO_4	200 g of air dried coconut palm petiole pieces were transferred to a 2000 mL	Max. inhibition efficiency = 95.24% in	Vijayalaks hmi et al.,

Proposed inhibitors	Metal used	Type of inhibitor	Corrosive medium	Methodology	Result	Reference
extract	mm thickness		and 1M HCl	round bottomed flask, directly heated in a mantle with water condenser at about 80^{o}C in the absence of air and without a carrier solvent (destructive distillation). The products obtained were: i) a gaseous mixture or wood gas; ii) 95 mL of the aqueous distillate obtained which was used as inhibitor; iii) 5 mL of a thick black liquid or wood tar which was separated from the aqueous distillate using a separating funnel; iv) 71 g of a solid residue or wood charcoal were left in a round bottle flask	0.5 M H_2SO_4 and 90.35% in 1 M HCl The corrosion process is inhibited by adsorption of the coconut palm petiole extract on the mild steel surface following the Langmuir adsorption isotherm. This indicates that the inhibition effect of the extract is due to adsorption of some or all of the listed phytochemical constituents. Adsorption is spontaneous and occurs by physical adsorption.	2011
Crude methanolic extract of Artemisia pallens (Asteraceae)	Mild steel	Mixed	1.0 M HCL	Weight loss Electrochemical technique	Max. inhibition efficiency = 98% Adsorption due to Fe-inhibitor complex at iron oxide layer	Garai et al., 2012
Bark of Ochrosia oppositifolia (OOB)	Mild steel, exposed area of 3.14 cm^2 for electrochemical study, and specimens	Mixed	1.0 M HCL	Electrochemical techniques (potentiodynamic polarization measurements and electrochemical impedance spectroscopy, EIS) and	Max. inhibition efficiency = 96% Adsorption due to the formation of protective	Raja et al., 2013

Proposed inhibitors	Metal used	Type of inhibitor	Corrosive medium	Methodology	Result	Reference
	with a size of 2.3 × 0.2 × 2.3 cm for SEM analysis.			scanning electron microscopy (SEM)	layer of corrosion inhibitor Isoreserpiline (ISR) responsible corrosion inhibition	
2-((5-mercapto-1,3,4-thiadiazol-2-ylimino) methyl) phenol Schiff base (MTMP)	Mild steel disc, 0.50 cm^2 surface area exposed	Mixed type, with predominant control of cathodic reaction.	0.5 M HCL	Electrochemical techniques such as potentiodynamic polarization curves, weight loss (WL), electrochemical impedance spectroscopy (EIS) and linear polarization resistance (LPR) were used.	Max. inhibition efficiency = 97% Chemisorption	Solmaz et al., 2011
(NE)-N-(thiophen-3-ylmethylidene	Mild steel X52 specimens of 3.0 x 2.4 x 0.6 cm	Mixed	1.0 M HCl	Weight loss, potentiodynamic polarization and electrochemical impedance spectroscopy (EIS)	Max. inhibition efficiency = 88.9% Chemisorption	Daoud et al., 2013
Bis-Schiff bases of isatin	Mild steel, 2.5 cm x 2 cm x 0.025 cm for gravimetric and 8 cm x 1 cm x 0.025 cm for electrochemical experiments.	Mixed	1.0 M HCl	Gravimetric measurements, electrochemical impedance spectroscopy (EIS), potentiodynamic polarization and quantum chemical study.	- Physical/Chemical Adsorption	Ansari & Quraishi, 2013
Pyridine derivatives (Pyridine-2-thiol (P2T) and 2-Pyridyl disulfide	1.5 cm^2 mild steel exposed	Mixed	1.0M HCl	Potentiodynamic polarization and electrochemical impedance spectroscopy (EIS) techniques were employed. To explore inhibitors adsorption mechanism, Langmuir isotherm and quantum chemical studies were used.	- Physisorption/Chemisorption	Kosari et al., 2014.

Proposed inhibitors	Metal used	Type of inhibitor	Corrosive medium	Methodology	Result	Reference
(2PD))						
Murraya koenigii leaves extract	Metal strips (2.5 cm x 2.0 cm x 0.025 cm)	Mixed	1.0M HCl	5g dried leaves soaked in 500 mL deionized water Reflux for 5h, solution filtered and concentrated to 100mL. Weight loss, electrochemical impedance spectroscopy (EIS), linear polarization and potentiodynamic polarization techniques were used.	97.02% Adsorption of the inhibitor molecules on the metal surface	Quraishi et al., 2010
Caffeic Acid	Metal sheet (1.0 x 2.0 x 0.1 cm) ASTM G31 used	Mixed	0.1M H_2SO	Open-circuit potential (OCP) versus time and potentiodynamic polarization curves were recorded in agreement with ASTM G5 norm. Weight loss, electrochemical impedance spectroscopy and polarization techniques were used.	96% Adsorption of organic molecules by blocking the cathodic site of electrode surface	de Souza & Spinelli, 2009
Murraya koenigii leaves extract		Mixed	0.5M H_2SO_4	Weight loss, electrochemical impedance spectroscopy (EIS), linear polarization and potentiodynamic polarization techniques were used.	94.66% Adsorption of inhibitor molecules on surface due to protonation of amino group	Quraishi et al., 2010
Black pepper extract	Mild steel specimens of size 3.0 × 1.0 × 0.21 cm	Mixed	1.0 M H_2SO_4	Conventional weight loss studies (303–323 K), electrochemical studies viz., Tafel polarization, ac impedance and scanning electron microscope (SEM) studies.	90% Adsorption of phyto constituents of black peppers forming a protective layer on surface	Raja & Sethuraman, 2008
Carboxymethyl cellulose (CMC)	Mild steel 0.09 cm in thickness Coupons of 5 cm x 4 cm (surface area =		2.0 M H_2SO_4	Weight loss, hydrogen evolution, thermometric, Langmuir adsorption isotherm model and Dubinin-Radushkevich adsorption isotherm	60.8% Physical adsorption mechanism by blocking the surface	Solomon et al., 2010

Proposed inhibitors	Metal used	Type of inhibitor	Corrosive medium	Methodology	Result	Reference
	20 cm^2) dimension for weight loss study and 3 cm x 3 cm dimension for thermometric and hydrogen evolution methods.			model were used.		
Spirulina platensis	Mild steel specimens of the size 1.5 x 5.0 x· 0.2 cm were used for weight loss studies, while coupons of size 1 cm2 were used for electrochemical studies and SEM analysis	Mixed	1.0M H_2SO_4	Powdered form of S. platensis (100 g) was extracted with absolute ethanol using Soxhlet apparatus. The ethanolic extract was distilled to obtain a solid residue, which was used as the inhibitor Weight loss method, potentiodynamic polarization method, electrochemical impedance spectroscopy measurements and SEM analysis were conducted.	82% Physical Adsorption of inhibitor molecules on active site	Kamal & Sethuraman, 2012
Nauclea Latifolia (Ethanol Extract)	The hydrogen evolution experiments were conducted on mild steel coupons of dimension 2.0 x 0.08 x 5.0 cm (with a surface area of 21.12 cm^2) and for the weight loss study, mild steel specimens of size 4.0 x 0.08 x 5.0 cm (with a surface area of 41.44		5.0M H_2SO_4	The parts (bark (BK), leaves (LV) and root (RT)) of N. latifolia were collected, cut into small chips, dried in an N53C – Genlab laboratory oven at 50 C, and ground into powder form. 80.0 g of the powder was extracted continually with 250 cm^3 of absolute ethanol in a soxhlet extractor for 24 h. After recovering most of the ethanol, the extract was heated on a water bath (at 60 C) until most of the ethanol evaporated. 4.0 g of the ethanol extract was digested in 1.0 liter of 5.0 M H_2SO_4 and 1.0 M H_2SO_4 solutions for hydrogen evolution and weight loss	94.26% Physical adsorption of the extracts on the surface by simply blocking the active corrosion site The presence of alkaloids in the root and leaves extracts is assumed to be responsible for the observed inhibition trend	Uwah et al., 2013

Proposed inhibitors	Metal used	Type of inhibitor	Corrosive medium	Methodology	Result	Reference
	cm^2) were used			measurements, respectively. The resultant solution was kept for 24 h, filtered and stored. From the stock solution (4.0 g/l), inhibitor test solutions (concentrations of 0.1, 0.5, 1.0, 2.0 and 4.0 g/l) were prepared.		
Synthesized glycine derivative (GlyD1)	Cylindrical discs cut from a mild steel rod fitted by Teflon on a glass tube as a holder, leaving 0.20 cm^2 of the surface area exposed	Mixed	4.0M H_2SO_4	The new glycine derivative (GlyD1) was synthesized in the laboratory Tafel extrapolation, linear polarization resistance (LPR) and impedance methods were used to test corrosion inhibitor efficiency	98% Physical adsorption	Amin & Ibrahim, 2011
Oxo-triazole derivative (DTP)	Mild steel, 3.00 x 1.50 x 1.50 cm (in the weight loss experiment) and 1.05 x 1.05 x 1.20 cm (in the electrochemical experiment) dimensions.	Mixed	0.5M H_2SO_4	Weight loss, potentiodynamic polarization, EIS and SEM were conducted.	89.9% typical chemisorption at the interface by shearing of electron	Tao et al., 2009
Alizarin yellow GG (AYGG) (an azo dye) in the presence of iodide ions		Cathodic	2.0 M H_2SO_4	Weight loss and hydrogen evolution methods were used.	85% Physisorption of dye molecules forming a protective film	Ebenso et al., 2008
Lavandula dentata aqueous	Mild steel pieces of lxbt [1,5x1,5x0,2 cm]	Mixed	1M HCL	Chemical (weight loss) and electrochemical (potentiodynamic and electrochemical impedance	The results from these techniques show that the inhibition efficiency	Bouammal i et al., 2013

Proposed inhibitors	Metal used	Type of inhibitor	Corrosive medium	Methodology	Result	Reference
extract				spectroscopy, EIS) measurement were conducted. Aerial parts of Lavandula dentata were air-dried at room temperature and essential oil was discarded by **hydro distillation** for 3 h using a **Clevenger-type apparatus**. The aqueous extract was centrifuged at 1000rd/min for 10 min and filtered to eliminate the undissolved materials. The aqueous solution obtained was concentrated by **vacuum evaporation** and dried with a **sand bath** to constant weight before use	increases with increase in the percentage of LD extract to attain 95% at 2wt%.	
Aloe vera	Mild steel sheets		2.4 M H_2SO_4	Samples of Aloe vera obtained were dried, grounded and soaked in a solution of **ethanol** for 48 h. After 48 h, the samples were cooled and filtered. The filtrates were further subjected to evaporation at 352 K in order to leave the sample free of the ethanol. The stock solutions of the extract so obtained were used in preparing 1,000, 2,000, 3,000 and 4,000 ppm of the samples by dissolving 0.1, 0.2, 0.3 and 0.4 g of the extract in 1 L of **2.5M H_2SO_4**, respectively. Infra red spectrophotometer. Thermodynamic adsorption theories and Gasometric (Hydrogen evolution)	Chemical adsorption isotherm	Eddy and Odoemelam, 2009

Proposed inhibitors	Metal used	Type of inhibitor	Corrosive medium	Methodology	Result	Reference
				methods The study was conducted at 303 and 333 K		
Pennyroyal Mint (Mentha pulegium, PM)		Cathodic	1M HCl	Weight loss measurements, electrochemical polarisation and EIS methods were used.	Adsorption isotherm	Bouyanzer et al., 2006
Thyme	Steel rod cross section = 1.25 cm^2	Mixed	0.1M H_2SO_4	a.c , d.c electrochemical techniques and potentiodynamic polarization were used. 50g of substance were added to 500mL **methanol**, then refluxed for 3 h. The extract was then filtered and completed to 100mL MeOH. Difference volumes of the filtrate were then taken and diluted to 100mL of 0.1M **H_2SO_4** solutions. All test solutions contained 10vol% MeOH to keep the extract completely soluble.	Max. Inhibition efficiency = 89.6%	Khamis and Alandis, 2002
Four different types of essential oils, including rosemary, eucalyptus, jojoba and mugwort (i.e. Artemisia)	2205 and 2507 duplex stainless steels Stainless steel plates were cut into pieces of 1 cm^2.		HCl and H_2SO_4	Electrochemical technique used	For 2507 steel eucalyptus oil –anodic inhibitor El-Etre and Abdallah found that natural honey exhibited a very good inhibition performance towards steel corrosion in chloride containing water. However, none	Potgieter et al., 2012

Proposed inhibitors	Metal used	Type of inhibitor	Corrosive medium	Methodology	Result	Reference
and two types of honey (Honey from orange blossoms [honey OB] and honey from blue gum trees [honey BG])					of this claimed effect was observed for the duplex stainless steel alloys in the acidic chloride solution investigated. Of all the plant extracts used in this investigation, Mugwort oil shows the most promise for further detailed evaluations. Its inhibitory effect on the corrosion behaviour of the alloys could be the result of an increase in the transfer resistance of the system through the adsorption of mugwort on the alloy surface.	
Natural honey	Copper strips Surface area=1.0cm^2		0.5M NaCl	-Weight loss measurement -Cathodic polarisation technique	Maximum inhibition effiency = 89.0% (with 1000ppm honey for 4 days) Lowest inhibition efficiency = 1.98% (200ppm honey for 30 days) Growth of microorganisms after	El-Etre, 1998

Proposed inhibitors	Metal used	Type of inhibitor	Corrosive medium	Methodology	Result	Reference
					several days Obeys Langmuir isotherm	
Trefoil flower honey	Carbon steel Surface area=1.0cm^2		Saline water	-Weight loss measurement -Potentiostatic polarisation technique	Maximum inhibition effiency = 91.23% (with 400ppm honey for 1 day) Lowest inhibition efficiency = 29.34% (100ppm honey for 3 days) Follows Langmuir isotherm	El-Etre and Abdallah, 2000
Musa Sapientum peels extracts	Five mild steel bars each of weight 35.50g were mechanically cut and washed with ethanol to remove any form of grease or oxide		2.0M H_2SO_4	2 kg of fresh samples of Musa Sapientum peels were washed carefully with distill water to remove any form of dirt from the peels. The peels were dried under the sun and weighed at intervals until a constant weight of 1.20kg was attained. This was to ensure complete removal of water from the peels. The dried Musa Sapientum peels were grounded using an **industrial scale grinder** to powdered form. The powdered Musa Sapientum peels was then run through **wire mesh sifter** to obtain very fine powdered samples and to separate the shaft of the peels. The fine powdered were completely soaked in **ethanol solution** for 96 hours after which the mixture was stirred properly	Concentration of corrosion inhibitor is directly proportional to inhibitor efficiency and surface coverage but inversely proportional to weight loss of mild steel bar. Freundlich Isotherm and Kinetic – Thermodynamic model predicted the kinetics adsorption of the ethanol extract of Musa Sapientum peels used as a corrosion inhibitor of mild steel bar to 96.59 and 89 % confidence level	Salami et al., 2015

Proposed inhibitors	Metal used	Type of inhibitor	Corrosive medium	Methodology	Result	Reference
				in order to have homogenous solution and then filtered. The filtrate was subjected to **evaporation process** to remove the ethanol in the filtrate. The inhibitor was obtained in its pure form at the end of the evaporation process. The stock solution of the extract obtained were used in preparing different concentrations of the extract by dissolving 0.2, 0.4, 0.6 and 0.8g of the extract in 1 litre of **2.0M H_2S0_4** respectively.	respectively while Langmuir and Linear isotherm did not.	

Annex 2: Composites with coconut husk

Coconut husk	Method used	Parameters	Purpose	Results	Reference
Green coconut fibre -NaOH (2, 3 and 4%) treatment -1 h under constant stirring and 24h at room temperature -dried for 6-7days	Taguchi's design of experiments (DoE) -L9 orthogonal array concept Mathematical model – response surface methodology (RSM) for tensile strength (using MINITAB software)	Matrix – HDPE Fibre lengths – 3, 6 and 9 mm Mix – 30, 40 and 50%wt Arrangement – random orientation Processing technique – Hand injection moulding	Textile industry	Experiment values: -Max. tensile strength of 17.86MPa at 40% fibre volume fraction, 3 mm fibre length RSM prediction: -Max. tensile strength of 17.81MPa at 40% fibre volume fraction, 3 mm fibre length Tensile strength decreased with increase in fibre length	Reddy, 2013
Coir fibre and rice husk -Ripe coconut husks soaked for 5 months (retting process) -Husks hammered -Fibres separated with comb -Impurities and shorter fibres were removed -Alkali treatment (6% NaOH)	Tensile strength- ASTM D3039 Flexural strength- ASTM D709	Matrix used –Epoxy resin (Araldite LY 556) Hardener – HY951 (for epoxy resin) Fibre length – 15mm Processing technique – Hand layup, compression under room temperature with natural curing	Industrial applications	Max. tensile strength = 20.21MPa Max. flexural strength = 58.27MPa Max. strengths at 80% coir fibre and 20% rice husk	Gopinath et al., 2014
Coconut coir	Tensile test – ASTM D3039/ASTM D3039M Flexural test- ASTM D790-03 Impact test- ASTM	Matrix – Epoxy (CY205) (density: 1.15-1.20g/cm^3) Hardener – HY951 (density: 0.97-0.99g/cm^3) Releasing agent – wax Coir length- 0.03-0.1cm		Tensile strength = 17.86MPa Flexural strength = 11.49kJ/m^2 Impact strength = 11.49kJ/m^2	Harish et al., 2009

Coconut husk	Method used	Parameters	Purpose	Results	Reference
	D256-05	Coir diameter- 12-24µm Arrangement-Uniform Processing technique – Hand layup			
Coconut coir fibre -Washed with distilled water -Dried at 80^{o}C -NaOH (6%) treatment	Tests conducted were: Fourier Transform Infrared spectroscopic (FTIR) analysis Tensile strength Impact strength Flexural strength	Reinforcement material – Glass fibre (25%) Matrix – Unsaturated polyester (Catalyst- Cobalt naphenate ($C_{22}H_{14}O_4Co$), Hardener-Methyl ethyl ketone peroxide (MEKP)) Fibre length – 10mm (whickers) Mix – 0-20wt% Processing technique – hand layup Cured at constant load of 4kg for 24h at room temperature		Tensile strength decreased with increasing fibre content (due to fibre brittleness, lack of interfacial adhesion between matrix and fibres). Flexural strength increased with increasing fibre content. Impact strength increased with increasing fibre content. Max. tensile strength at 5%wt fibre and flexural and impacts strengths max. at 20%wt. fibre.	Nasif, 2015
Coir -5% NaOH treatment, 72h, room temperature -Washed with water and distilled water -Air dried, 2 days	Tensile and flexural strengths tested Specimen dimension for tensile test – 120 x 10 x 2mm Surface morphology – Scanning Electron Microscope	Polyester matrix - poly(butylene succinate) (PBS, 1.26g/cm^3) Mix – 10-50% Fibres-dried at 60^{o}C, 8h Fibre length – 10-20mm Mixing – Brabender mixer at 140^{o}C Composite –laminated and cut into 5mm long pieces. Further pelletized into smaller pellets using a Strand Pelletiser Processing technique – Compression molded at 140^{o}C using hydraulic molding test press		Mechanical properties of treated coir/PBS composites were higher than those of untreated coir/PBS composites. Mechanical strength of the composites increased with increasing fibre content up to 20 wt%, but decreased over 20 wt%.	Tran et al., 2012
Coconut fibre -200ml of 10% NaOH, for 1h -Washed with	Tensile test (ASTM D638) Micro-hardness test	Matrix – Unsaturated polyester Mould releasing agent – Poly Vinyl Alcohol (PVA) Fibre length before treatment – 5-		Alkali treatment of fibres improved tensile properties and hardness of composite For tensile properties, 10% fibre	Onuegbu et al., 2013

Coconut husk	Method used	Parameters	Purpose	Results	Reference
distilled water -Dried at 80^{o}C, 3h		10mm Mix – 5, 10, 15 and 20%wt.		load gave the best reinforcing property for treated fibre composites 15% fibre load samples exhibited the best micro-hardness.	
Coconut fibre -Dried (moisture content, 2-3%)	Particle board dimensions: 40mm x 40mm x 10mm NMR 14810:2006-Plywood sheets standard was used Thickness swelling, water absorption, modulus of rupture, modulus of elasticity, internal bond and accelerated aging test were evaluated.	Matrix 1-castor oil based polyurethane adhesive Matrix 2- Urea formaldehyde Fibre length- 7mm Panel density – 0.8-1.0g/cm^{3} Processing technique – Heated automatic (hydraulic) press, 100-140^{o}C Compression pressure – 50kg/cm^{2} for 10min.	Civil and agricultural construction	Castor oil-based bi-component polyurethane resin presented superior results when compared to the urea-formaldehyde Scanning microscopy electronic images (SEM) indicated that castor oil-based polyurethane adhesive occupies gaps between particles (improved physical and mechanical properties of the panels).	Fiorelli et al., 2012
Coconut coir -Moisture content-1-2% -Chopped fibres dried at 100^{o}C, 36h		Matrix – Used polypropylene drinking straws Fibre length – 12-15mm	Thermal insulator		Ganiron, 2013
Coconut husk -30%fibres and 70% pith		Binderless Processing technique – Hot press (180^{o}C) Compression pressure – 300-750kN (3-30min)	Substitute building materials and timber	Density = 1.3 to 1.4g/cm^{3} Strength = 50MPa Stiffness = 5GPa Thickness swelling in water = 8% after 24h soaking in water Water absorption – 8%	Van Dam et al., 2004

Annex 3: Composites with coconut shell

Coconut shell	Method used	Parameters	Purpose	Results	Reference
Coconut shell -dried in open air, -grinded using pulverising machine, and -sieved according to BS 1377:1990	Chemical analysis – Absorption Spectrometer Density, ρ = m/v Water absorption %Weight gained=(Final weight initial - initial weight)/initial weightx100 Hardness –Hardness tester Tensile strength-Tensometer tensile machine Impact energy-Charpy impact machine and ductility Composite morphology - SEM	Matrix - pelletized polyethylene (PE) waste (sundried and shredded) Particle size = 100µm Mix - 5-25% vol. CS PE and CS were blended using a two-roll rheomixer at 50^{o}C, 60 rpm Processing technique - Hydraulic pressing machine (Compression)	Engineering applications	Hardness increased with increasing CS particles mix Tensile strength decreases with increasing volume fraction of CS particles (may be due to imperfect interfacial bonding between CS particles and PE). Microstructural analysis-homogeneity between the coconut shell particles and the matrix decreases with increase in the coconut shell particles content. Porosity increased as percentage of CS particles increased.	Olumuyiwa et al., 2012
Coconut shell -dried 5 days and cleaned -grinded by: 1. manual hammering 2. hammer milling machine, then 3. ball milling machine -Sieved using 80BSS (British standard size) sieve bowl	Tensile testing – Instron universal testing machine Impact test- Impact testing machine Hardness test – Brinell hardness testing machine Flexural test – Testometric universal testing machine	Matrix - Unsaturated polyester resin (matrix) Mix – 5-30% weight Weight of Polyester – 95-70g For homogenous interfacial interaction – 1g methyl ethyl ketone peroxide (catalyst) and 0.5g cobalt Naphthante (accelerator) were added to the mixture Processing technique - Mould (wooden) casting Mould release agent –	Industrial application	Ultimate tensile strength = 70MPa Highest impact strength = 4.76J Highest hardness = 208BHN Max. strength to withstand stretching was at 10% mix	Durowaye et al., 2014

Coconut shell	Method used	Parameters	Purpose	Results	Reference
		Masking tape			
Coconut shell powder (CSP) -Cleaned -Crushed and powdered using hammer -Sieved (600, 425, 300, and 212 micron) using sieve shaker	Density of composite determined using equation: $\rho_{comp} = 1/(w_{csp}/\rho_{csp} + w_{mat}/\rho_{mat})$ Tensile strength Flexural strength Hydrophilic behaviour-Absorption test	Matrix – Epoxy resin (Hardener-MH 933) Mix – 20, 30 and 40%wt Cure time – 24h Processing technique – mould casting Composite shape – dog-bone	Application in interior part of aircraft, motor car and automobile with 20-30% vol. CSP	Max. tensile strength with 20%vol. CSP Max. flexural strength with 30%vol. CSP Min. water absorption with 20%vol. CSP	Singh et al., 2013
Coconut shell powder (CSP) -Cleaned -Dried in open air -Powdered using pulverised machine	Tensile, bending and impact tests were conducted Dimensions: -Tensile test:12.4cm (length), 3mm (thickness), 1.85cm (edges width) and 1.3cm (middle width) -Bending test: 9.5cm (length) x 3mm (thickness) x 1cm (width) -Impact test: 6.2cm (length) x 1cm (width) x 9mm (thickness)	Matrix – High Density Polyethylene Mix – 0-40% Different mesh sizes Processing technique – Injection molding and casting	Applications in aerospace and automobile industry	Max. tensile strength with 10% vol CSP Bending strength same for 10,20,30 and 40%vol. CSP Max. impact strength with 20%vol. CSP	Vasu et al., 2015
Coconut shell powder	Tensile and flexural strengths – Universal Testing Machine (as per ASTM D3039)	Matrix – High density polyethylene (HDPE) Mix – 0-30% wt Roll mill for mixing HDPE and coconut shell powder Processing technique – Hot press, 170^{o}C			Nor, 2007

Coconut shell	Method used	Parameters	Purpose	Results	Reference
		Compression pressure – 142kg/cm^2 for 5 min			
Barley husk (BH) and coconut shell (CS) -Conditioned for 4h at 45^{o}C with 20% moisture content to reduce fibre damage during grinding -before mixing: dried at 80^{o}C for 24h (Moisture content < 0.5%)	Thermal property - Thermal gravimetric analysis by thermal gravimetric analyser Physical property - Particle morphology and particle size was investigated by Scanning Electron Microscopy (SEM) and water absorption (EN ISO 62) to evaluate viability as reinforcements. Chemicals content Elementary analysis Fourier-Transform Infrared Spectroscopy Tensile test – EN ISO 527 Charpy impact strength test – EN 179	Binding material – Polypropylene (PP) Coupling agent – Maleic anhydride polypropylene BH and CS mixed with PP by high speed cascade mixer Mix- 40% fibres Test sample at 160-180^{o}C Moulding process- Injection at 80^{o}C, 20 kN/mm^2	Substitution for wood floor in wood plastic composites	Thermally stable at 195^{o}C. Coconut shell had high moisture uptake Low O/C ratio indicated high proportion of aliphatic and aromatic carbons Addition of coupling agent increased tensile strength (from about 23 to 29MPa) by 30% (via ester linkage formation between cellulosic filler and PP molecule) but slightly reduced elongation at break () due to increase in rigidity/	Bledzki et al., 2010

Annex 4: Activated carbon from coconut husk and shell

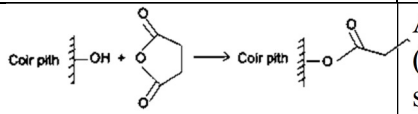
Coconut processing	Method used	Results	Purpose	Reference
Coconut shell -Cleaned -Particle size: G2 -Acid concentration: 24.5% H_2SO_4 -Soak time: 24h at room temperature -Filtered -Heat in oven at 200^oC for 24h -Allow to cool to room temperature -Washed with distilled water -Soaked in $NaHCO_3$ -pH:6 -Dried in oven at 105^oC, 3h -Crushed using electric grinder (<1.14mm)	Acid treatment (H_2SO_4) **Operating variables:** -pH -Initial dye concentration -Dosage of adsorbent	Pretreated coconut shell yield = 89.378 ± 0.027% **Characteristics:** Particle size ≤ 1.14 mm Bulk density = 795 ± 14.34 g/L Ash content = 4.478 ± 0.211% Moisture content = 4.335 ± 0.237% pH = 6.00 ± 0.01	Adsorption of reactive red 158 dye by chemically activated coconut shell	Beekaroo, 2011
Coconut shell -Washed with water -Dried in oven -Sieved into 500µm	Standard method used: SMEWW 1992 Activating agents: $FeCl_3$, $CaCl_2$, $ZnCl_2$ and K_2CO_3	$ZnCl_2$-activated carbon most effectively adsorbed 92.2% colour of the molasses while the $FeCl_3$-activated was most effective in adsorbing 94.3% of oil/grease, 46.2% of dissolved oxygen, 71.9% of BOD, 72.1% of COD and 96% each of dissolved solids (DS), suspended solids (SS) and total solids (TS).	Study of adsorption efficiency of $FeCl_3$, $CaCl_2$ and K_2CO_3-activated carbon for the 500µm particle size produced from carbonized coconut shell on adsorbates obtained from industrial effluent and wastewaters as well as colour of molasses.	Gimba and Turoti, 2006
Coconut shell -Crushed into 1.0-0.8cm chips	Activating agent: Heat and acid Iodine values- as per Okuo et al. (2008) Carbon hardness-ASTM (2002)	**Heat activation**: 850^oC for 2 ½ h Heat activation yield=36.30-41.10%	Home and industrial purposes	Yusufu et al., 2012

Coconut processing	Method used	Results	Purpose	Reference
	method Ash-as per AOAC (1994) Bulk density as per Okaka and Potter (1976) Moisture-air-oven method as per AOAC (1994) Surface area- by adsorption of N_2 at 77K using micrometric surface area analyser (ASAP2010) Porosity- Barrett, Joyner, Halenda (BJH) method	Iodine value: 840.18mg/g Hardness: 96.5% Ash: 2.4% Bulk density: 0.66g/cm^3 Moisture:5.1% Surface area: 895m^2/g Porosity,V_{meso}: 0.040cm^3/g **Acid activation:** Acid: Conc. Phosphoric Acid (H_3PO_4) Carbon:Acid - 1:4 Acid activation: 600^oC, 2h Acid activation yield=40.40-46.21% Iodine value: 848.69mg/g Hardness: 81.0% Ash: 2.8% Bulk density: 0.68g/cm^3 Moisture:6.4% Surface area: 912m^2/g Porosity,V_{meso}: 0.035cm^3/g		

Coconut processing	Method used	Results	Purpose	Reference
Coconut shell -Cleaned, fibre-free and soil-free -Milled to 2.4mm diameter (mesh size 8) -10g of the coconut shells were used per sample -Soaking time- 12 h -Continuous supply of N_2 (inert	Response surface methodology Activating agent: Phosphoric acid (H_3PO_4) **Variables:** -Impregnation ratio- 1.0, 1.5 and 2.0 (wt basis H_3PO_4:coconut shell) (as cited in Molina-Sabio et al., 1995) -Activation time-10, 20 and 30 min	The optimum range identified for impregnation ratio starts from 1.345 to 2, while for the activation time it was from 14.9 to 23.9 min. The optimum range for activation temperature is from 394 to 416^oC. The		Gratuito et al., 2008

Coconut processing	Method used	Results	Purpose	Reference
environment) during activation time -Washed with distilled water (6-7 washings) -Washed with 0.1M NaOH -Washed with distilled water -Dried in oven at 105^{o}C	-Activation temperature- 400, 450 and 500^{o}C **Responses evaluated (dependent variables):** Yield Bulk density as per Lima and Marshall (2005) Average pore diameter Small pore diameter Number of pores per unit area- Scanning Electron Microscope (SEM) Image Pro Plus version 5.1 was used for digital image analysis of pores	optimum points are 1.725, 19.5 min, and 416^{o}C for impregnation ratio, activation time, and activation temperature, respectively.		
Coconut husk -washed -dried at 105 ^{o}C -Crushed to mesh size (1–2 mm) -Carbonised at 700 ^{o}C under purified N_2 (99.995%), 150 cm^3/min, 2 h in a stainless steel vertical tubular reactor placed in a tube furnace, heating rate fixed at 10 ^{o}C/min -Char soaked in KOH -Mixture dehydrated in oven overnight at 105 ^{o}C -and then activated under the same condition as carbonisation, but to a different final temperature. -N_2 switched to carbon dioxide (CO_2)	Response surface methodology Analysis of variance (ANOVA) Activated carbon preparation variables: -Activation temperature, -Activation time, and -Chemical impregnation (KOH:char) ratio	Optimum conditions: - Activation temperature: 816^{o}C, - Activation time of 1 h, and - KOH:char ratio of 3.9.	Adsorption capacity on methylene blue dye and carbon yield were investigated.	Tan et al., 2008

Coconut processing	Method used	Results	Purpose	Reference
-Cooled to room temperature -Washed with hot deionized water and 0.1 M HCl, pH 6–7				
Coconut husk -Pre-treated coconut husk loaded in stainless steel vertical tubular reactor placed in a tube furnace -Carbonisation -ramping the temperature from room temperature to 700^{o}C, heating rate of 10 °C/min for 2 h -Purified N_2 (99.995%) at flow rate of 150 cm^3/min -KOH:char impregnation ratio (IR) of 2.91 -Activation temperature up to 750^{o}C -N_2 gas flow switched to CO_2 -Activation held for 2.29 h -Cooled to room temperature under N_2 flow -Washed with hot deionized water and 0.1 M HCl until the pH of the washing solution reached 6–7.	Adsorption parameters: -Initial concentration -Agitation time -pH	-Adsorption of TCP increased with increase in agitation time and initial concentration while acidic pH was more favourable for the adsorption of TCP -Equilibrium data were fitted to non-linear models of Langmuir, Freundlich, Temkin and Redlich–Peterson, and the equilibrium data were best described by the Langmuir isotherm model, with maximum monolayer adsorption capacity of 716.10mg/g at 30^{o}C.	Adsorption of 2,4,6-trichlorophenol (TCP)	Hameed et al., 2008a
Coir pith -Dried in sunlight for 5 h -Grinded and sieved to 250–500 mm -Carbonization at 700^{o}C for 1 h using a muffle furnace under closed condition -Carbonized material sieved to 250–500 mm again	Adsorption parameters: -Agitation time -Dye concentration -Adsorbent dose -pH -Temperature -Desorption (Re-generation)	Acidic pH was favourable for the adsorption of Congo Red		Namasivaya and Kavitha, 2002

Coconut processing	Method used	Results	Purpose	Reference
Esterified coir pith preparation: -Coir pith was washed with distilled water -Air dried and ground to diameter 300–600 um -Soxhlet extraction used with a mixture of toluene, acetone and methanol (4:1:1, v/v/v) for 12 h -Dried at 105^{o}C for 15 h and cooled to ambient temperature in a desiccators -Esterification (Clave et al., 2004; Marchetti et al., 2000) was carried out by stirring 7.5 g of coir pith prepared above with 7.5 g of succinic anhydride, in 100 mL of N,N-dimethyl formamide (DMF) at 80^{o}C for 2 h in the presence of a catalyst, triethylamine (0.1 eq.) -Esterification was carried out in a round bottom flask equipped with a condenser and a calcium chloride drying tube -After the reaction, the unreacted anhydride and DMF were removed by Soxhlet extraction with acetone for 15 h -Esterified coir pith was treated with a 1 N $NaHCO^{3}$ solution (50 ml, 1 h, 20^{o}C), washed with distilled water (50 ml) and dried for 12 h at 105^{o}C.	Varying conditions to assess the kinetic and equilibrium parameters: - agitation time - metal ion concentration	 Fig. 1. Reaction between coir pith and succinic anhydri Adsorption capacity was enhanced as indicated by the increased uptake of Co from aqueous solutions Possibility for reuse of the biomaterial	Adsorption of cobalt (II) ions from aqueous solution	Parab et al., 2008
Coconut bunch waste	-Scanning electron microscopy	Equilibrium isotherms were	Removal of methylene	Hameed et

Coconut processing	Method used	Results	Purpose	Reference
-Washed with distilled water -Sliced, spread on trays and oven dried at 70^{o}C for 48 h -Grinded and sieved to particle size 1–2 mm	(SEM) analysis was carried out on the CBW, to study its surface texture before and after MB adsorption -Fourier Transform Infrared (FTIR) (FTIR- 2000, Perkin Elmer) analysis was applied on the CBW and dye adsorbed CBW to determine the surface functional groups, where the spectra were recorded from 4000 to 400 cm−1.	well described by the Langmuir equation, giving maximum adsorption capacity of 70.92 mg/g at 30^{o}C	blue dye from aqueous solution by adsorption	al., 2008b
Coconut copra meal -Washed with hot water to remove excess oil -Sun dried -Sieved to <250µm -Soaked in 0.02mol/dm^3 HCl overnight -Washed, pH neutral -Dried at 373K, 24h	Adsorption parameters: -Biosorbent dose -pH	Biosorption process is pH dependent and maximum removal of cadmium from aqueous solution occurred at pH 6.	As biosorbent	Ho and Ofomaja, 2006
Babassu **coconut mesocarp** -Crushed to 0.0088-0.177mm particle size	Adsorption parameters: -Stirring time -pH -Temperature	Max. adsorption at pH 1.0		Vieira et al., 2009

Annex 5: Measured diameter of coconut fibres

Untreated coconut fibres						
Sample No.	**d1, µm**	**d2, µm**	**d3, µm**	**d4, µm**	**d5, µm**	**Average diameter, µm**
1	300	297	292	308	295	298
2	303	286	281	278	270	284
3	322	355	325	322	333	331
4	593	524	509	407	404	487
5	126	145	153	150	142	143
6	311	281	292	287	292	293
7	284	273	284	293	290	285
8	268	276	271	273	284	274
9	109	87	87	107	112	100
10	229	224	246	230	241	234
11	134	134	153	159	147	145
12	167	167	83	175	164	151
13	270	270	268	265	268	268
14	218	221	221	216	208	217
15	303	295	320	295	270	297
16	178	189	189	188	186	186
17	399	432	492	443	440	441
18	156	164	150	161	161	158
19	156	145	153	140	145	148
20	191	186	199	219	213	202
21	167	164	164	153	150	160
22	145	134	142	148	153	144
23	145	145	158	139	150	147
24	175	158	158	164	169	165
25	150	161	158	142	156	153
26	183	186	194	183	186	186
27	147	142	134	128	126	135
28	150	164	156	156	156	156
29	208	183	189	219	208	201
30	388	385	377	391	377	384
31	145	158	167	164	158	158
32	224	205	188	227	249	219

33	158	167	158	161	167	162
34	139	128	123	134	123	129
35	380	388	382	391	391	386
36	139	126	123	137	128	131
37	279	295	290	282	290	287
38	147	142	142	150	145	145
39	289	289	317	295	309	300
40	276	257	259	243	249	257
41	175	169	169	191	170	175
42	355	380	366	339	334	355
43	161	169	167	147	158	160
44	142	145	158	148	161	151
45	232	249	235	224	257	239
46	322	323	336	323	322	325
47	352	333	336	361	355	347
48	161	178	169	161	167	167
49	208	194	227	224	219	214
50	243	238	221	208	216	225
51	218	232	238	243	232	233
52	156	158	150	161	158	157
53	257	270	260	268	262	263
54	287	284	281	284	273	282
55	150	161	156	145	156	154
56	197	161	175	178	170	176
57	134	131	126	126	120	127
58	150	161	169	161	161	160
59	172	161	167	164	161	165
60	363	363	391	358	350	365
61	314	328	317	348	331	328
62	188	208	221	227	216	212
63	404	393	377	386	382	388
64	434	453	443	426	412	434
65	145	137	131	150	156	144
66	179	158	167	160	170	167
67	273	273	273	325	273	283
68	240	238	257	241	227	241
69	350	350	352	333	330	343

70	202	208	205	213	208	207
71	396	388	393	410	399	397
72	147	131	131	123	117	130
73	339	374	344	336	358	350
74	123	126	126	137	150	132
75	178	172	170	153	167	168
76	218	243	213	227	208	222
77	262	243	230	235	227	239
78	186	186	199	178	186	187
79	156	176	169	167	183	170
80	325	309	336	333	306	322
81	164	159	156	169	142	158
82	172	178	188	188	197	185
83	418	399	434	418	415	417
84	500	543	535	538	513	526
85	178	180	167	175	183	177
86	336	336	350	339	336	339
87	147	145	142	142	150	145
88	175	150	161	172	180	168
89	292	295	328	325	317	311
90	363	339	355	350	344	350
					Total Average Diameter, µm	236
					Minimum Diameter, µm	100
					Maximum Diameter, µm	526
					Standard Deviation	95
Alkaline treated coconut fibres						
Sample No.	**d1, µm**	**d2, µm**	**d3, µm**	**d4, µm**	**d5, µm**	**Average diameter, µm**
1	112	117	104	109	90	106
2	262	262	273	282	263	268
3	421	421	424	422	421	422
4	186	189	194	202	202	195
5	213	216	208	211	222	214
6	289	279	289	284	296	287
7	342	323	347	292	320	325
8	96	101	104	93	109	101
9	330	309	303	287	304	307

10	115	96	112	123	109	111
11	210	249	216	197	208	216
12	268	270	284	298	311	286
13	156	164	156	167	167	162
14	175	169	150	158	158	162
15	167	158	142	158	153	156
16	112	118	117	120	128	119
17	109	140	153	186	246	167
18	109	142	107	107	107	114
19	126	123	115	123	118	121
20	126	90	90	90	93	98
21	158	153	145	142	143	148
22	164	175	180	180	167	173
23	142	189	126	137	134	146
24	306	312	301	392	314	325
25	249	273	273	273	397	293
26	104	112	115	104	101	107
27	202	202	202	186	197	198
28	85	74	87	102	93	88
29	331	254	268	246	265	273
30	93	98	101	82	93	93
31	104	101	104	110	101	104
32	289	279	303	300	301	294
33	137	117	109	128	127	124
34	112	115	98	126	107	112
35	172	164	202	186	208	186
36	287	339	295	281	284	297
37	183	170	164	186	175	176
38	112	131	107	107	107	113
39	229	260	266	264	264	257
40	192	197	197	188	191	193
41	169	151	148	132	150	150
42	101	112	126	115	128	116
43	137	167	145	142	156	149
44	142	137	137	145	123	137
45	142	175	164	170	167	164
46	112	101	98	96	120	105

47	235	230	235	232	232	233
48	112	96	85	98	109	100
49	202	199	200	186	205	198
50	489	434	432	467	451	455
51	134	156	161	142	148	148
52	219	213	229	232	243	227
53	109	116	126	93	96	108
54	183	161	167	158	161	166
55	115	123	134	131	137	128
56	79	66	49.2	68	68	66
57	142	137	131	123	123	131
58	109	93	79	82	85	90
59	153	134	118	107	107	124
60	193	192	205	173	182	189
61	186	208	202	218	208	204
62	360	289	279	282	399	322
63	98	77	82	85	109	90
64	221	227	295	244	213	240
65	238	232	221	227	211	226
66	79	98	82	76	76	82
67	268	232	235	232	222	238
68	274	257	219	219	216	237
69	243	240	218	301	221	245
70	221	218	209	217	202	213
71	219	220	216	203	208	213
72	142	134	153	139	158	145
73	434	443	426	423	385	422
74	219	224	243	203	239	226
75	206	222	200	202	199	206
76	224	199	224	202	198	209
77	304	262	249	257	216	258
78	145	115	120	117	132	126
79	120	139	110	118	116	121
80	115	115	104	104	115	111
81	555	566	593	598	568	576
82	120	126	109	98	93	109
83	314	325	330	330	314	323

84	74	90	96	101	85	89
85	213	235	221	202	213	217
86	90	93	90	96	98	93
87	232	202	224	210	213	216
88	120	128	128	115	120	122
89	243	240	218	229	213	229
90	303	298	287	274	270	286
					Total Average Diameter, μm	191
					Minimum Diameter, μm	66
					Maximum Diameter, μm	576
					Standard Deviation	93

Annex 6: Tensile strength of coconut fibres

Untreated coconut fibres:

Sample No.	Average Diameter at Fracture, mm	Cross Sectional Area at Fracture, mm^2	Elongation at Break, mm	Force at Break, N	Time to Failure, S	Strain at Break, %	Stress at Break, N/mm^2	Tensile strength, Mpa	Calculated Young's Modulus, Mpa
1	0.126	0.050	9.482	2.172	22.789	37.331	30.331	43.826	0.812
2	0.112	0.039	7.507	0.995	18.064	29.555	14.072	25.430	0.476
3	0.185	0.107	6.036	1.117	14.525	23.764	15.801	10.434	0.665
4	0.198	0.123	7.690	1.910	18.513	30.276	27.025	15.508	0.893
5	0.104	0.034	8.745	0.933	21.033	34.429	13.199	27.458	0.383
6	0.101	0.032	7.567	1.277	18.199	29.791	18.064	39.690	0.606
7	0.127	0.051	8.873	1.805	21.335	34.933	25.530	35.735	0.731
8	0.248	0.193	10.699	4.910	25.714	42.122	69.462	25.452	1.649
9	0.118	0.044	4.761	2.509	11.475	18.744	35.495	57.357	1.894
10	0.195	0.120	7.601	2.015	18.287	29.925	28.502	16.799	0.952
11	0.150	0.071	6.069	2.072	14.614	23.894	29.313	29.235	1.227
12	0.148	0.068	3.513	0.488	8.482	13.831	6.898	7.130	0.499
13	0.099	0.031	5.853	0.837	14.091	23.043	11.844	27.404	0.514
14	0.176	0.098	6.931	3.114	16.683	27.287	44.054	31.855	1.614
15	0.250	0.196	10.797	6.353	25.953	42.508	89.877	32.407	2.114
16	0.114	0.041	5.399	1.163	13.009	21.256	16.460	28.386	0.774
17	0.135	0.058	8.959	1.731	21.545	35.272	24.483	30.055	0.694
18	0.108	0.037	3.319	1.037	8.025	13.067	14.673	28.300	1.123
19	0.244	0.187	13.469	8.098	32.358	53.028	114.563	43.225	2.160
20	0.159	0.079	4.847	3.211	11.687	19.083	45.426	40.633	2.380
21	0.135	0.057	6.384	0.926	15.375	25.134	13.096	16.221	0.521
22	0.190	0.114	10.065	5.542	24.198	39.626	78.403	48.764	1.979
23	0.249	0.194	13.926	6.490	33.465	54.827	91.815	33.373	1.675
24	0.296	0.275	11.597	5.843	27.873	45.657	82.662	21.285	1.811
25	0.223	0.156	6.113	5.308	14.718	24.067	75.093	34.037	3.120
26	0.173	0.094	9.234	3.803	22.206	36.354	53.801	40.447	1.480
27	0.126	0.050	11.010	2.393	26.462	43.346	33.854	48.132	0.781
28	0.141	0.062	6.963	2.266	16.760	27.413	32.057	36.384	1.169

29	0.115	0.041	7.713	1.281	18.557	30.366	18.128	30.940	0.597
30	0.121	0.046	9.194	2.136	22.103	36.197	30.218	46.439	0.835
31	0.121	0.046	3.233	1.345	7.817	12.728	19.022	29.436	1.495
32	0.136	0.058	10.527	2.040	25.308	41.445	28.860	35.211	0.696
33	0.142	0.063	5.420	0.656	13.063	21.339	9.282	10.385	0.435
34	0.107	0.036	6.267	1.714	15.090	24.673	24.245	47.653	0.983
35	0.137	0.059	8.376	1.493	20.137	32.976	21.129	25.320	0.641
36	0.267	0.224	4.324	5.879	10.429	17.024	83.171	26.250	4.886
37	0.246	0.191	8.856	7.853	21.291	34.866	111.097	41.172	3.186
38	0.351	0.388	10.796	11.328	25.943	42.504	160.258	29.201	3.770
39	0.378	0.450	7.126	8.408	17.149	28.055	118.949	18.691	4.240
40	0.105	0.035	4.417	1.336	10.651	17.390	18.903	38.426	1.087
41	0.253	0.200	11.732	5.345	28.190	46.189	75.616	26.664	1.637
42	0.253	0.200	11.278	5.575	27.108	44.402	78.870	27.812	1.776
43	0.131	0.054	6.182	1.758	14.882	24.339	24.868	32.410	1.022
44	0.117	0.043	4.738	1.816	11.420	18.654	25.695	42.227	1.377
45	0.117	0.043	8.411	2.198	20.227	33.114	31.095	51.285	0.939
46	0.259	0.210	14.710	7.600	35.333	57.913	107.518	36.119	1.857
47	0.287	0.258	12.248	3.487	29.423	48.220	9.331	13.494	0.194
48	0.134	0.056	6.674	1.895	16.066	26.276	26.809	33.694	1.020
49	0.147	0.068	10.196	2.795	24.511	40.142	39.541	41.284	0.985
50	2.261	16.060	11.180	2.678	26.877	44.016	37.886	0.167	0.861
51	0.202	0.129	11.987	2.807	28.803	47.193	39.711	21.811	0.841
52	0.136	0.058	6.385	1.838	15.374	25.138	25.997	31.539	1.034
53	0.165	0.086	11.394	4.464	27.379	44.858	63.153	52.192	1.408
54	0.177	0.099	14.249	6.139	34.232	56.098	86.849	62.093	1.548
55	0.095	0.028	7.999	1.420	19.235	31.492	20.085	50.083	0.638
56	0.150	0.071	6.613	1.286	15.919	26.035	18.197	18.145	0.699
57	0.116	0.042	4.301	1.621	10.380	16.933	22.935	38.214	1.354
58	0.160	0.080	10.389	2.420	24.732	40.508	34.236	30.090	0.845
59	0.119	0.044	6.323	1.311	15.227	24.894	18.553	29.469	0.745
60	0.250	0.197	14.022	7.059	33.691	55.205	99.864	35.836	1.809
61	0.196	0.121	10.361	5.175	24.903	40.791	73.211	42.792	1.795
62	0.125	0.049	11.089	2.684	26.657	43.657	37.971	55.030	0.870
63	0.266	0.222	7.926	2.435	19.066	31.205	34.448	10.987	1.104

64	0.354	0.395	14.637	11.765	35.158	57.626	166.441	29.816	2.888
65	0.143	0.064	5.198	1.475	12.519	20.465	20.873	22.896	1.020
66	0.140	0.061	6.846	1.117	16.471	26.953	15.797	18.245	0.586
67	0.339	0.361	5.565	4.076	13.399	21.909	57.664	11.290	2.632
68	0.149	0.070	9.484	2.239	22.802	37.339	31.675	32.188	0.848
69	0.263	0.218	12.666	7.060	30.434	49.866	99.879	32.391	2.003
70	0.190	0.113	8.409	1.784	20.222	33.106	25.234	15.797	0.762
71	0.311	0.303	8.195	3.980	19.712	32.264	56.305	13.132	1.745
72	0.153	0.073	7.076	1.305	17.026	27.858	18.458	17.792	0.663
73	0.243	0.186	12.238	5.433	29.404	48.181	76.861	29.191	1.595
74	0.175	0.097	3.464	1.841	8.361	13.638	26.050	19.048	1.910
75	0.137	0.059	7.688	1.777	18.496	30.268	25.137	30.225	0.830
76	0.179	0.100	8.093	1.610	19.469	31.862	22.774	16.066	0.715
77	0.191	0.114	9.700	2.996	23.326	38.189	42.385	26.196	1.110
78	0.161	0.081	7.195	2.375	17.314	28.327	33.599	29.238	1.186
79	0.144	0.065	9.450	1.435	22.725	37.205	20.305	21.967	0.546
80	0.163	0.083	8.027	3.642	19.305	31.602	51.524	43.633	1.630
81	0.099	0.031	6.181	0.994	14.883	24.335	14.064	32.545	0.578
82	0.171	0.092	8.382	2.206	20.162	33.000	31.209	23.902	0.946
83	0.285	0.254	8.768	4.291	21.091	34.520	60.705	16.863	1.759
84	0.284	0.253	12.116	5.801	29.116	47.701	82.067	22.894	1.720
85	0.148	0.069	5.893	2.292	14.194	23.201	32.425	33.218	1.398
86	0.300	0.283	7.203	2.128	17.329	28.358	30.105	7.516	1.062
87	0.126	0.050	7.768	1.112	18.694	30.583	15.730	22.295	0.514
88	0.139	0.061	4.390	0.967	10.593	17.283	13.687	15.977	0.792
89	0.212	0.141	11.680	6.957	28.068	45.984	98.421	49.365	2.140
90	0.279	0.245	10.587	8.116	25.443	41.681	114.818	33.188	2.755
Minimum	0.095	0.028	3.233	0.488	7.817	12.728	6.898	0.167	0.194
Maximum	2.261	16.060	14.710	11.765	35.333	57.913	166.441	62.093	4.886
Mean	0.205	0.296	8.410	3.249	20.226	33.108	45.508	30.049	1.336
Standard Deviation	0.230	1.683	2.834	2.446	6.794	11.154	34.816	12.424	0.853
C. of V.	1.121	5.686	0.337	0.753	0.336	0.337	0.765	0.413	0.639
L.C.L.	-0.484	-4.753	-0.091	-4.089	-0.156	-0.355	-58.941	-7.222	-1.224
U.C.L	0.894	5.345	16.912	10.586	40.608	66.570	149.958	67.320	3.896

Alkaline treated coconut fibres:

Sample No.	Average Diameter at Fracture, mm	Cross Sectional Area at Fracture, mm^2	Elongation at Break, mm	Force at Break, N	Time to Failure, S	Strain at Break, %	Stress at Break, N/mm^2	Tensile strength, MPa	Calculated Young's Modulus, MPa
1	0.217	0.147	12.771	4.372	30.680	50.280	61.851	29.663	1.230
2	0.230	0.166	15.291	4.258	36.724	60.201	60.238	25.666	1.001
3	0.220	0.152	13.009	6.631	31.252	51.217	93.809	43.769	1.832
4	0.263	0.218	12.318	9.502	29.597	48.496	134.426	43.661	2.772
5	0.099	0.031	7.236	0.634	17.406	28.488	8.975	20.674	0.315
6	0.086	0.023	8.982	1.124	21.591	35.362	15.896	48.828	0.450
7	0.134	0.056	1.381	0.441	3.366	5.437	6.233	7.841	1.146
8	0.318	0.318	15.152	8.658	36.392	59.654	122.486	27.219	2.053
9	0.139	0.060	9.538	1.589	22.935	37.551	22.481	26.330	0.599
10	0.289	0.262	7.033	4.584	16.923	27.689	64.850	17.470	2.342
11	0.086	0.023	9.808	0.746	23.582	38.614	10.558	31.958	0.273
12	0.225	0.159	11.129	3.096	26.747	43.815	43.799	19.501	1.000
13	0.267	0.224	10.982	1.934	26.399	43.236	27.355	8.635	0.633
14	0.212	0.141	9.823	2.787	23.623	38.673	39.428	19.813	1.020
15	0.112	0.039	9.736	1.391	23.412	38.331	19.681	35.297	0.513
16	0.082	0.021	8.545	0.961	20.555	33.642	13.598	45.493	0.404
17	0.187	0.109	9.254	2.057	22.256	36.433	29.101	18.804	0.799
18	0.120	0.045	8.546	1.026	20.553	33.646	14.516	22.832	0.431
19	0.140	0.061	8.666	1.204	20.841	34.118	17.039	19.666	0.499
20	0.868	2.367	7.390	1.128	17.780	29.094	15.064	0.477	0.518
21	0.280	0.246	11.391	2.125	27.374	44.846	30.063	8.628	0.670
22	0.134	0.056	10.996	3.335	26.427	43.291	47.181	59.475	1.090
23	0.282	0.251	6.758	1.009	16.266	26.606	14.280	4.027	0.537
24	0.176	0.098	7.406	3.682	17.822	29.157	52.090	37.750	1.787
25	0.143	0.064	11.739	4.568	28.203	46.217	64.624	70.907	1.398
26	0.091	0.026	4.842	0.319	11.671	19.063	4.519	12.316	0.237
27	0.157	0.077	10.774	3.239	25.895	42.417	45.822	41.934	1.080
28	0.078	0.019	8.259	0.974	19.864	32.516	13.782	51.486	0.424
29	0.268	0.226	7.432	2.847	17.882	29.260	40.277	12.580	1.377

30	0.100	0.032	3.483	0.362	8.416	13.713	5.117	11.477	0.373
31	0.073	0.017	8.056	1.023	19.382	31.717	14.474	61.442	0.456
32	0.268	0.226	9.280	5.206	22.313	36.535	73.650	23.038	2.016
33	0.074	0.017	6.840	0.766	16.472	26.929	11.311	44.049	0.420
34	0.085	0.022	6.227	0.654	14.993	24.516	9.252	29.086	0.377
35	0.172	0.093	10.122	1.955	24.332	39.850	27.659	20.986	0.694
36	0.226	0.160	11.601	2.186	27.875	45.673	30.926	13.623	0.677
37	0.162	0.083	7.857	2.386	18.902	30.933	33.755	28.797	1.091
38	0.080	0.020	6.228	0.586	14.989	24.520	8.286	29.292	0.338
39	0.298	0.280	9.745	2.961	23.433	38.366	41.890	10.585	1.092
40	0.108	0.037	6.102	2.040	14.701	24.024	28.860	55.878	1.201
41	0.092	0.027	8.318	1.007	20.009	32.748	14.240	37.871	0.435
42	0.084	0.022	8.752	1.266	21.048	34.457	17.909	56.572	0.520
43	0.090	0.026	8.032	1.398	19.318	31.622	19.782	54.453	0.626
44	0.125	0.049	7.884	1.334	18.973	31.039	18.872	27.351	0.608
45	0.126	0.050	9.204	2.868	22.131	36.236	40.574	57.139	1.120
46	0.101	0.032	6.664	0.820	16.038	26.236	11.605	25.689	0.442
47	0.221	0.154	7.363	3.100	17.718	28.988	43.856	20.167	1.513
48	0.081	0.021	5.473	0.461	13.187	21.547	6.520	22.476	0.303
49	0.153	0.074	9.210	3.375	22.143	36.260	47.746	45.892	1.317
50	0.257	0.207	11.879	3.911	28.547	46.768	55.329	18.907	1.183
51	0.102	0.033	4.699	0.540	11.327	18.500	7.645	16.586	0.413
52	0.122	0.047	8.904	1.839	21.418	35.055	26.011	39.200	0.742
53	0.072	0.016	8.834	0.942	21.242	34.780	13.329	58.489	0.383
54	0.116	0.042	5.863	1.095	14.119	23.083	15.485	25.903	0.671
55	0.137	0.059	8.955	1.172	21.530	35.256	16.578	19.993	0.470
56	0.056	0.010	1.554	0.208	3.784	6.118	2.950	20.888	0.482
57	0.109	0.037	7.765	1.131	18.677	30.571	15.995	30.413	0.523
58	0.079	0.019	7.006	0.715	16.861	27.583	10.110	36.839	0.367
59	0.087	0.024	6.931	0.925	16.674	27.287	13.089	39.080	0.480
60	0.181	0.103	12.769	2.802	30.676	50.272	39.640	27.165	0.789
61	0.091	0.026	9.476	1.163	22.787	37.307	16.459	44.901	0.441
62	0.378	0.449	6.749	5.510	16.248	26.571	77.951	12.275	2.934
63	0.256	0.206	17.435	9.838	41.867	68.642	139.179	47.709	2.028
64	0.184	0.106	11.797	6.738	28.353	46.445	95.323	63.488	2.052

65	0.276	0.239	14.958	3.898	35.928	58.890	55.145	16.312	0.936
66	0.076	0.018	2.733	0.312	6.617	10.760	4.415	17.194	0.410
67	0.106	0.035	9.910	1.175	23.833	39.016	16.617	33.162	0.426
68	0.087	0.024	7.018	0.834	16.890	27.630	11.804	34.753	0.427
69	0.139	0.060	11.669	3.328	28.040	45.941	47.082	55.145	1.025
70	0.139	0.061	8.296	2.591	19.952	32.661	36.655	42.564	1.122
71	0.224	0.157	11.484	4.368	27.591	45.213	61.785	27.760	1.367
72	0.114	0.041	8.867	1.167	21.392	34.909	16.510	28.583	0.473
73	0.230	0.166	13.923	6.150	33.442	54.815	87.005	36.942	1.587
74	0.155	0.076	11.747	2.825	28.220	46.248	39.966	37.332	0.864
75	0.160	0.081	11.655	4.412	28.009	45.886	62.417	54.585	1.360
76	0.084	0.022	5.776	1.425	13.911	22.740	20.155	64.901	0.886
77	0.137	0.059	10.782	2.499	25.909	42.449	35.354	42.630	0.833
78	0.244	0.188	7.145	4.201	17.192	28.130	59.432	22.387	2.113
79	0.285	0.256	15.683	3.889	37.665	61.744	55.018	15.198	0.891
80	0.096	0.029	7.509	0.936	18.065	29.563	13.239	32.194	0.448
81	0.295	0.273	12.166	5.511	29.237	47.898	77.965	20.185	1.628
82	0.279	0.245	13.543	3.068	32.537	53.319	43.403	12.510	0.814
83	0.192	0.115	10.582	6.447	25.431	41.661	91.206	55.901	2.189
84	0.215	0.145	11.444	6.194	27.503	45.055	87.627	42.573	1.945
85	0.140	0.061	11.456	3.381	27.529	45.102	47.831	55.224	1.061
86	0.149	0.069	10.139	3.807	24.370	39.917	53.858	54.878	1.349
87	0.190	0.113	12.915	6.286	31.027	50.846	88.929	55.543	1.749
88	0.195	0.119	15.046	5.732	36.140	59.236	81.091	47.983	1.369
89	0.074	0.017	7.759	0.851	18.665	30.547	12.035	48.937	0.394
90	0.196	0.120	11.808	3.537	28.371	46.488	50.038	29.427	1.076
Minimum	0.056	0.010	1.381	0.208	3.366	5.437	2.950	0.477	0.237
Maximum	0.868	2.367	17.435	9.838	41.867	68.642	139.179	70.907	2.934
Mean	0.170	0.126	9.325	2.704	22.422	36.713	38.244	33.058	0.964
Standard Deviation	0.105	0.255	3.060	2.150	7.338	12.049	30.421	16.456	0.610
C. of V.	0.619	2.030	0.328	0.795	0.327	0.328	0.795	0.498	0.633
L.C.L.	-0.146	-0.639	0.144	-3.747	0.408	0.567	-53.018	-16.311	-0.867
U.C.L	0.486	0.890	18.506	9.154	44.435	72.859	129.506	82.427	2.795

Annex 7: Coconut Fibre Lignocellulosic contents

Neutral Dertergent Fibre (NDF)					
	Before		After		
	Mass of sample (g)	Mass of filter paper (g)	Mass of sample + filter paper (g)	Mass of sample (g)	NDF (%)
Shell					
1	1.015	0.88	1.776	0.896	88.28
2	1.009	0.868	1.768	0.9	89.20
3	1.004	0.876	1.783	0.907	90.34
Average Neutral Dertergent Fibre (NDF) (%)					89.27
Husk					
1	1.01	0.888	1.648	0.76	75.25
2	1.002	0.852	1.608	0.756	75.45
3	1.005	0.849	1.608	0.759	75.52
Average Neutral Dertergent Fibre (NDF) (%)					75.41
Treated fibre					
1	1.011	0.871	1.725	0.854	84.47
2	1.008	0.882	1.74	0.858	85.12
3	1.003	0.868	1.729	0.861	85.84
Average Neutral Dertergent Fibre (NDF) (%)					85.14
Untreated fibre					
1	1.006	0.866	1.727	0.861	85.59
2	1.002	0.841	1.705	0.864	86.23
3	1.001	0.852	1.721	0.869	86.81
Average Neutral Dertergent Fibre (NDF) (%)					86.21

Acid Dertergent Fibre (ADF) (%)					
	Before		After		
	Mass of sample (g)	Mass of filter paper (g)	Mass of sample + filter paper (g)	Mass of sample (g)	ADF (%)
Shell					
1	1.02	0.843	1.622	0.779	76.37
2	1.005	0.861	1.631	0.77	76.62
3	1.002	0.847	1.619	0.772	77.05
Average Acid Dertergent Fibre (ADF) (%)					76.68
Husk					
1	1.01	0.879	1.582	0.703	69.60
2	1.004	0.838	1.544	0.706	70.32
3	1	0.851	1.564	0.713	71.30
Average Acid Dertergent Fibre (ADF) (%)					70.41
Treated fibre					
1	1.019	0.885	1.652	0.767	75.27
2	1.002	0.873	1.638	0.765	76.35

3	1.001	0.853	1.614	0.761	76.02
Average Acid Dertergent Fibre (ADF) (%)					75.88
Untreated fibre					
1	1	0.839	1.626	0.787	78.70
2	1.002	0.883	1.68	0.797	79.54
3	1.026	0.848	1.674	0.826	80.51
Average Acid Dertergent Fibre (ADF) (%)					79.58

Acid Dertergent Lignin (ADL)							
	Before		After h2so4		After Ashing		
	Mass of sample (g)	Mass of crucible (g)	Mass of sample + crucible (g)	Mass of sample (g)	Mass of sample + crucible (g)	Mass of sample (g)	ADL (%)
Shell							
1	1.021	135.315	135.684	0.369	135.319	0.004	35.75
2	1.005	94.923	95.301	0.378	94.925	0.002	37.41
3	1.002	88.207	88.563	0.356	88.208	0.001	35.43
Average Acid Dertergent Lignin (ADL) (%)							36.20
Husk							
1	0.991	88.211	88.587	0.376	88.218	0.007	37.24
2	1.004	72.652	73.025	0.373	72.655	0.003	36.85
3	1	94.922	95.296	0.374	94.925	0.003	37.10
Average Acid Dertergent Lignin (ADL) (%)							37.06
Treated fibre							
1	0.85	94.924	95.158	0.234	94.929	0.005	26.94
2	1.003	88.209	88.488	0.279	88.212	0.003	27.52
3	1.001	72.655	72.946	0.291	72.658	0.003	28.77
Average Acid Dertergent Lignin (ADL) (%)							27.74
Untreated fibre							
1	0.83	94.922	95.176	0.254	94.928	0.006	29.88
2	1.002	107.875	108.181	0.306	107.883	0.008	29.74
3	0.913	88.212	88.482	0.27	88.214	0.002	29.35
Average Acid Dertergent Lignin (ADL) (%)							29.66

	Formula	**Shell**	**Husk**	**Treated fibre**	**Untreated fibre**
Cellulose	*(ADF - ADL)*	40.48	33.34	48.14	49.92
Hemi-cellulose	*(NDF - ADF)*	12.59	5.00	9.26	6.63
Lignin	*(ADL)*	36.20	37.06	27.74	29.66

Annex 8: Corrosion inhibitor trials

Trial 1;-

Four mild steel samples were coated on both sides (front and back) using a flat brush. Honey was used as additive in coconut oil. The specimens' coating applied are as such:

- Sample A1: Control
- Sample A2: Coconut oil
- Sample A3: 95% by weight coconut oil + 5% honey
- Sample A4: 50% by weight coconut oil + 50% honey

The coated samples were then placed on an exposure rack as shown in Figure xx. Nylon supports, bolts and nuts were used to attach the specimens firmly on the rack.

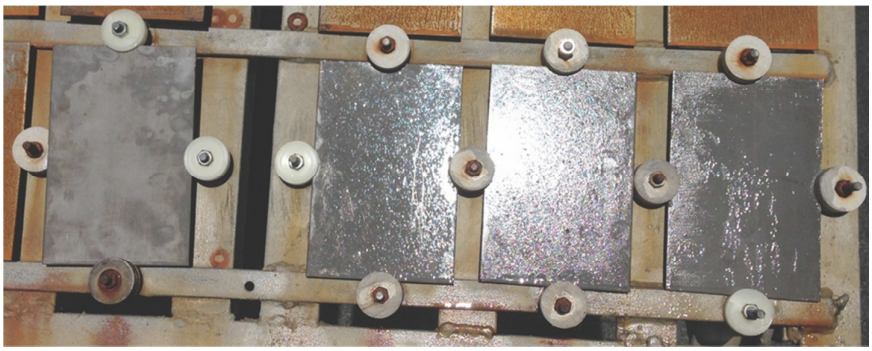


Figure A.8.1: Mild steel samples exposed on rack

The exposed mild steel specimens were monitored every 48 hours. To avoid loss of coating on the samples, photographs were taken instead of scanning with a flatbed scanner. ImageJ software was then used to analyse the area corroded.

Figure xxx represents the results obtained from imageJ as percentage area corroded versus hours exposed in the atmosphere. It is seen that the sample A4 rusted at a slowest rate compared to the other samples A1, A2 and A3. Hence, a second batch of four mild steel specimens were cleaned and coconut oil to honey coating ratio was varied from 25% to 75% by weight.

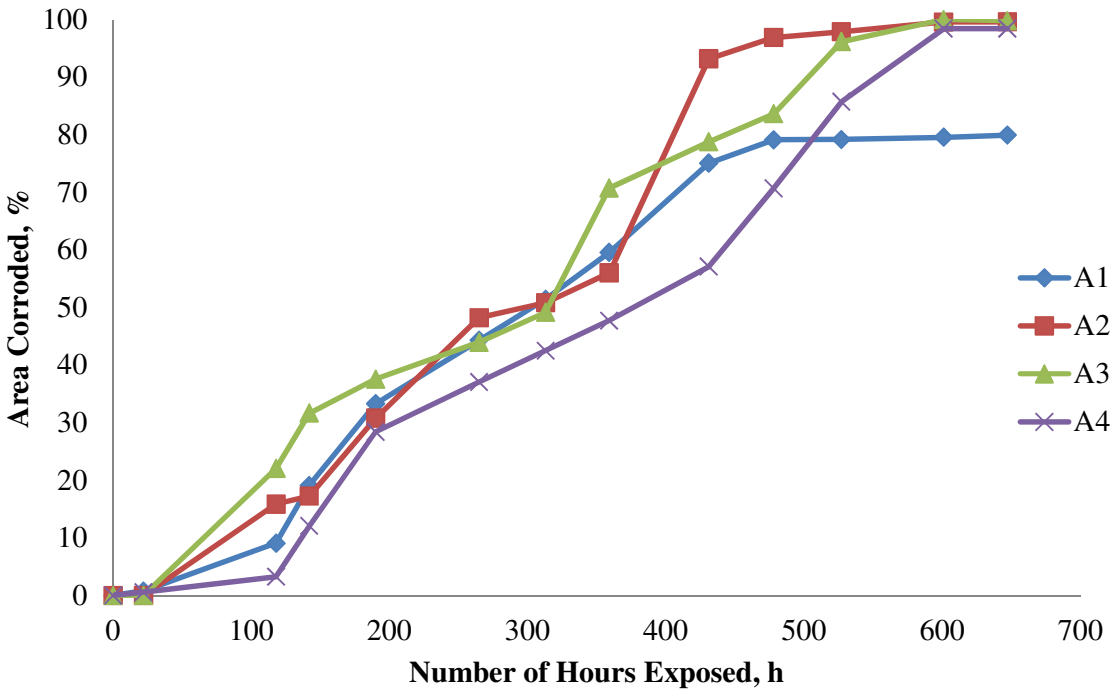


Figure A.8.2: Graph of percentage area corroded against number of hours exposed in the atmosphere for A samples

Trial 2;-

For the second batch of four mild steel specimens (B samples), coating was applied on both sides (front and reverse) of mild steel specimens as follows:

- Sample B1: Control
- Sample B2: 75% coconut oil + 25% honey
- Sample B3: 50% coconut oil + 50% honey
- Sample B4: 25% coconut oil + 75% honey

Figure 2.15 represents the percentage area corroded obtained from imageJ analysis against hours of atmospheric exposure. It is seen that the coconut oil and honey coatings have a significant corrosion inhibition effect compared to the referenced sample, B1. Specimen B2, with 75% by mass of coconut oil and 25% by mass of honey has the lowest area of corrosion on its surface than B3 and B4.

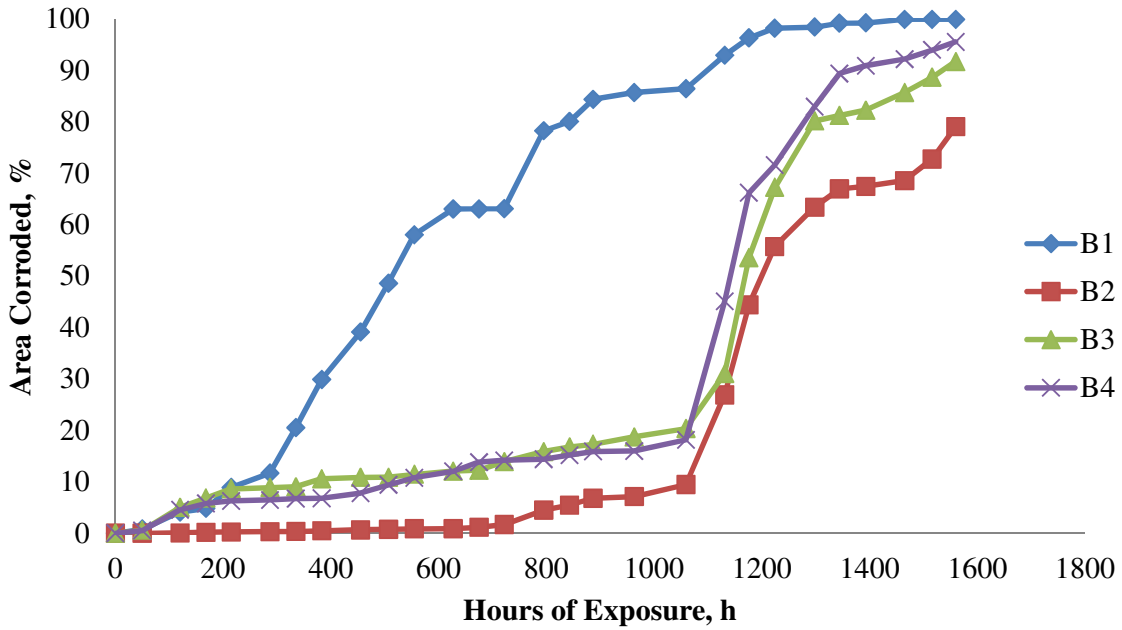


Figure A.8.3: Graph of percentage area corroded against number of hours exposed in the atmosphere for B samples

From the trials, it was determined that the coating's optimum mix of coconut oil and honey was 75% and 25% respectively. It was noted that the coconut oil and honey mixture were melting with the outdoor temperature. Thus, there was a significant decrease in thickness of the coatings applied. A potential solution is to increase the viscosity of the coconut oil.

Annex 9: Caramelisation of honey

3% by weight EVA was blend with the optimum coconut oil and honey mixture. The blend was prepared by stirring 3g EVA, 75g coconut oil and 25g honey, at a rotational speed of 300 rpm for 5h at 125 ^{o}C. Afterward, the mixture was cooled to room temperature. It was observed that caramelisation of honey was occurred.

So, EVA should be heated only with coconut oil, then after cooling the honey can be added to the mixture.

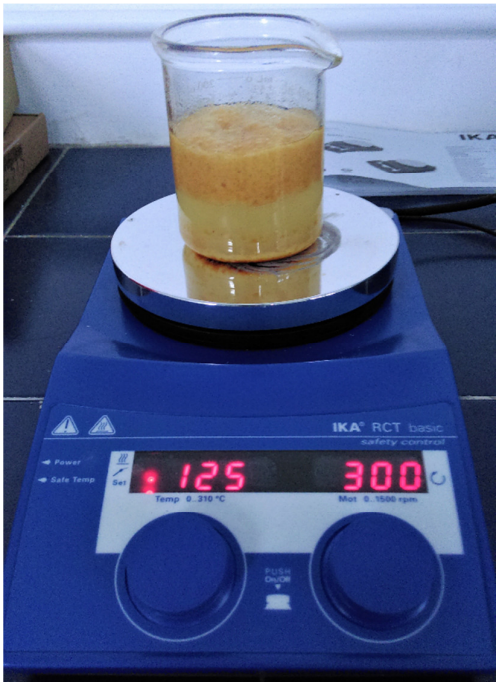


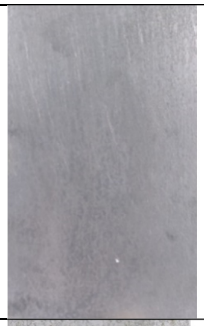
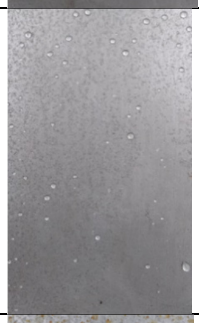
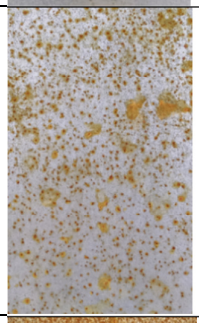
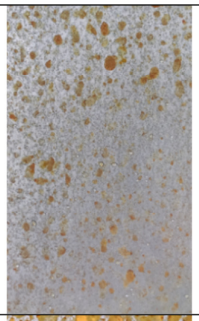
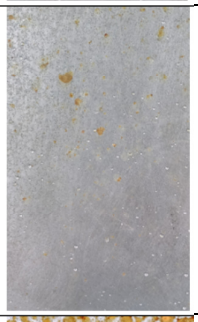
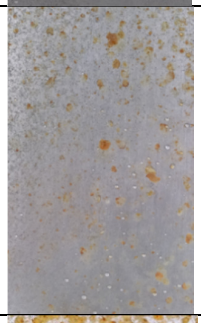
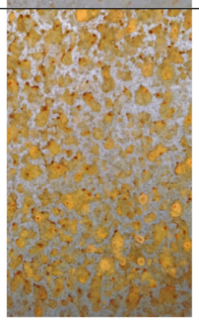
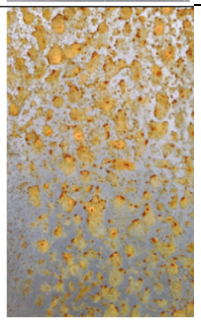
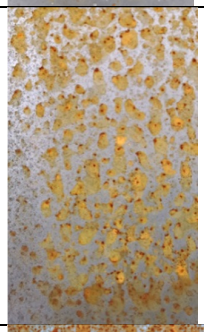
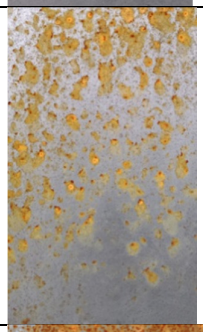
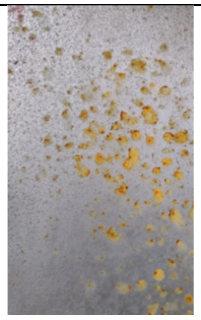
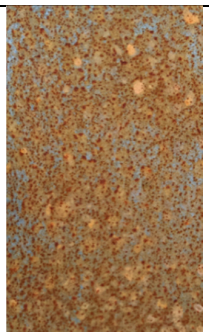
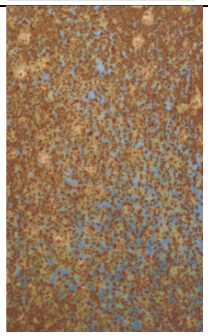
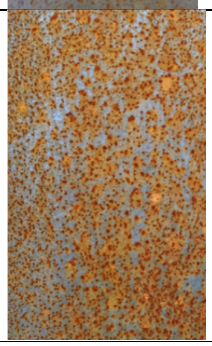
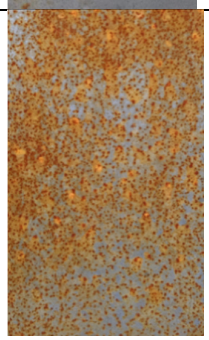
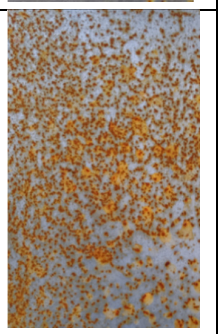
Figure A.9.1: Thermal treatment of EVA in coconut oil and honey



Figure A.9.2: Caramelisation of honey

Annex 10: Mild steel samples and ImageJ analysis

Table A.10.1; Outdoor Exposure samples

Day	OR1	OR2	OR3	O2	O3	O4
0						
1						
2						
5						
6						

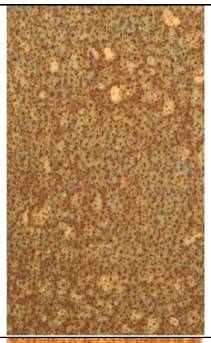
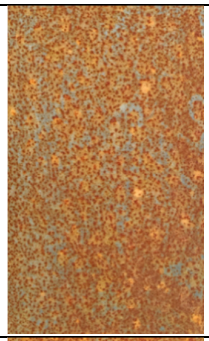
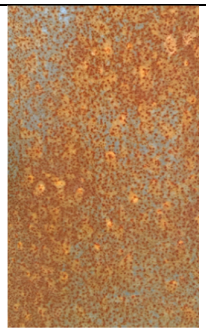
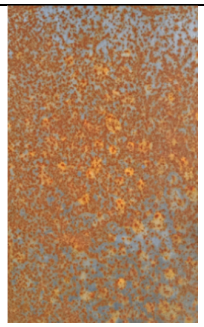
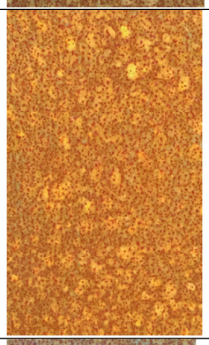
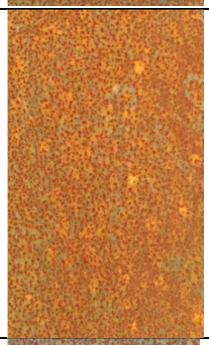
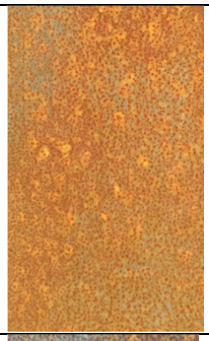
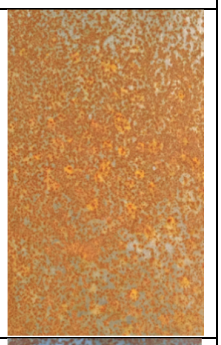
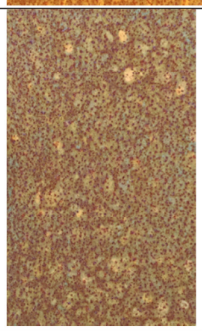
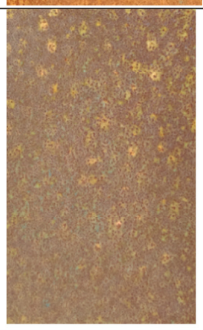
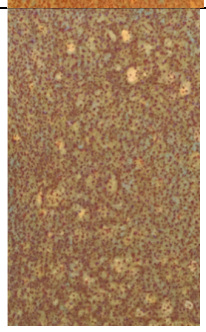
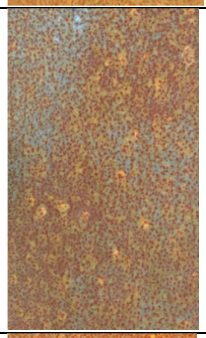
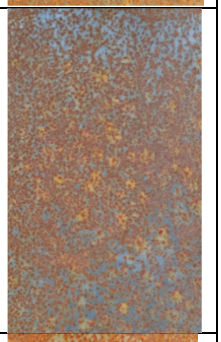
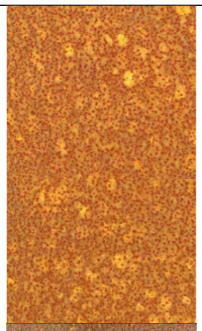
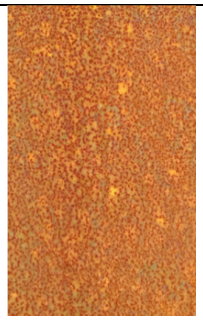
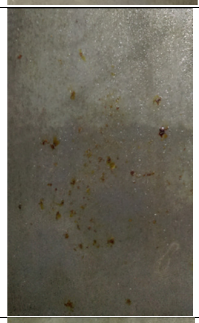
7						
8						
9						
13						
19						

Table A.10.2; Sheltered Exposure sample

Day	SR1	SR2	SR3	S2	S3	S4
0						
7						
15						
22						
31						

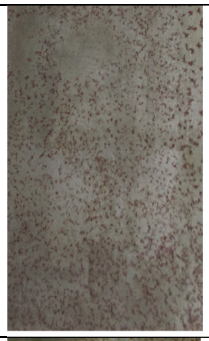
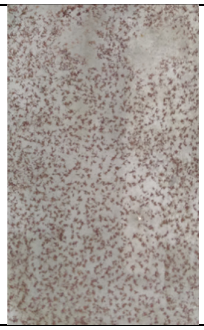
37						
45						
53						
66						
92						

Table A.10.3; Percentage area corroded from image analysis of Outdoor Exposure

Outdoor Exposure						
Time of exposure (day)	Percentage area corroded (%)					
	OR1	OR2	OR3	O2	O3	O4
0	0.000	0.000	0.000	0.000	0.000	0.000
1	0.481	0.316	0.202	0.092	0.017	0.000
2	17.221	7.812	0.759	3.198	0.297	0.028
5	50.560	37.060	31.128	24.254	15.368	2.227
6	53.021	48.914	40.710	38.018	35.881	21.397
7	59.201	50.611	45.919	43.820	39.653	30.007
8	73.714	66.999	48.520	46.002	44.080	37.295
9	78.608	68.340	57.132	53.053	47.921	42.730
13	81.854	73.892	66.756	60.171	57.013	51.055
19	98.911	87.614	79.013	70.004	67.689	62.025

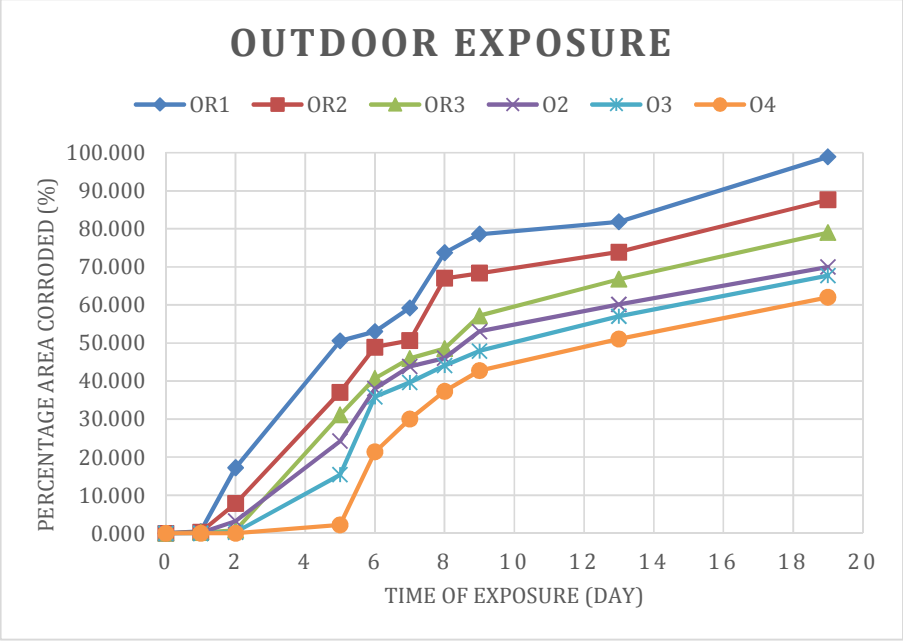


Figure A.10.1: Graph of percentage area corroded against number of days exposed in the atmosphere

Table A.10.4; Percentage area corroded from image analysis of Sheltered Exposure

Sheltered Exposure						
Time of exposure (day)	Percentage area corroded (%)					
	SR1	SR2	SR3	S2	S3	S4
0	0.000	0.000	0.000	0.000	0.000	0.000
7	0.342	0.330	0.301	0.257	0.219	0.193
15	1.594	1.187	0.711	0.863	0.481	0.205
22	3.013	1.848	1.577	0.998	0.516	0.255
31	4.343	3.381	2.562	2.008	1.267	0.640
37	5.622	4.015	3.200	2.894	1.889	1.050
45	9.886	5.566	4.713	3.909	2.817	1.521
53	12.562	6.798	5.293	5.621	3.407	1.755
66	14.799	8.239	5.684	6.634	3.744	2.449
92	19.110	9.110	7.621	8.002	4.801	3.584

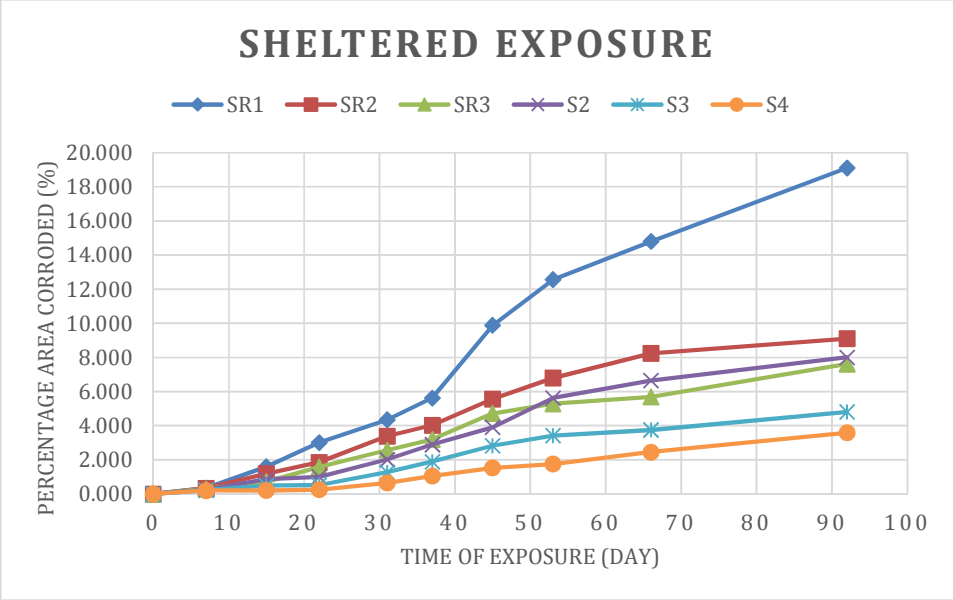
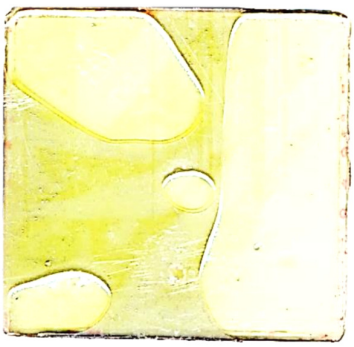
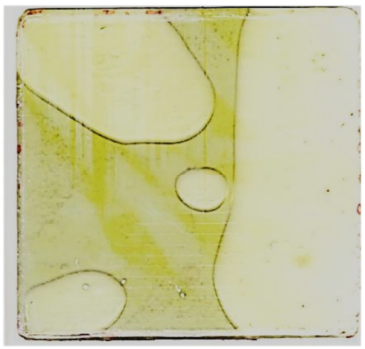


Figure A.10.2: Graph of percentage area corroded against number of days exposed in sheltered place

Annex 11: Problems encountered and solution in Resin injection and vacuum infused

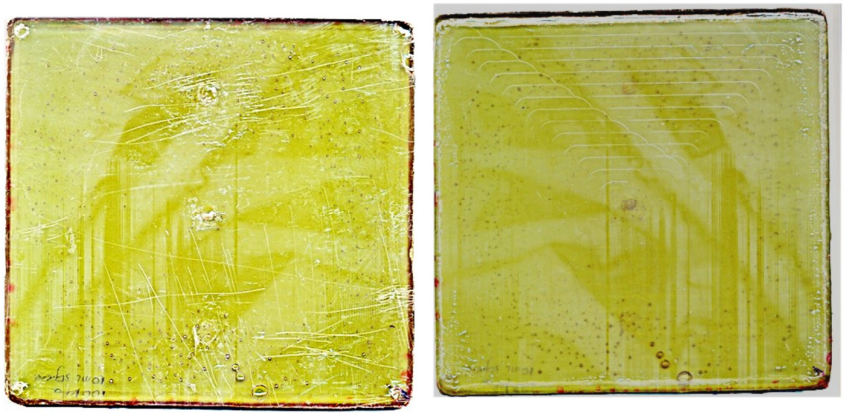
Trial No.	Date	Results
1	13/07/2016	Methodology: 230 g (100%) resin with 2.3 g (1%) MEKP used At atmospheric pressure, i.e injection pressure was at room pressure Observations: -While pouring resin into container for mixing, uneven viscosity of resin was observed (like presence of partially cured resin) -Amount of resin insufficient => Consequence: Air was injected into mould creating uneven surface -Bubbles present in cured resin, which may be due to high viscosity of resin -Thinner thickness of catalyst did not cure after 1 day -After 2 days of curing, sample was cured (by touch) -Cured resin sample is shown below, with top and bottom surfaces. Solution: To decrease viscosity, styrene is to be added To increase amount of resin used by 30 g and to use a higher ratio of catalyst  

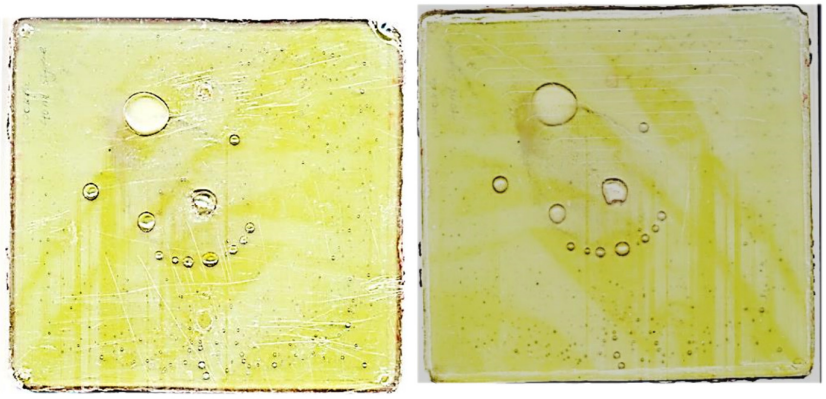
Trial No.	Date	Results
2	19/07/2016	Methodology: 260 g (100%) resin, 3.139 g (1.2%) MEKP, 5 mL (4.718g, 1.8%) styrene Atmospheric pressure Observations: -Loss of vacuum pressure, may be from cracked flexible tube -Bubbles still present -Resin still insufficient -Cured after 1 day -Cured resin sample is shown below, with top and bottom surfaces. Solution: 300 g of resign to be used 10 mL styrene to be used To check for cracked flexible tubes, and to replace same with new ones. To try using seal tape, instead of silicone as gasket at tune and connector joints to reduce time consumed for silicone to dry 
3	22/07/2016	Methodology: Resin = 300.352g (100% by mass) MEKP = 3.385g (1.127% of rein by mass) Styrene = 10 mL (9.088g, 3% of resin by mass)

Trial No.	Date	Results
		Atmospheric pressure Seal tape used instead of silicone Cracked flexible tubes were replaced Resin was filtered Tests done with Universal Testing Machine. Observations: Fully cured during weekend A few air bubbles trapped in resin Solution: To use 15 mL styrene to next trial
4	26/07/2016	Methodology: Resin = 300.488g (100%) MEKP = 3.340 g (1.1 % by mass) Styrene = 13.506 g (15 mL, 4.5% by mass) Injection pressure = 80 kPa Seal tape used Tests done with Universal Testing Machine. Observations: -Slow flow rate of resin in mould => Vacuum pressure lost and pump had to be switched on -Bubbles observed in mould -When pump was switched back on, bubbles in resin rose and popped -Pressure loss at resin tank inlet while injecting pressure Solution: Tilt resin tank while pouring resin A pressure gage is to added to control vacuum pressure such that the pump may

Trial No.	Date	Results
		be kept on when used Clean inlet resin tank to reduce air loss
5	17/08/2016	Methodology: Resin = 308.580g (100%) MEKP = 3.241g (1.05% by mass) Styrene = 8.972g (10 mL, 2.9% by mass) Injection pressure = 80 kPa Seal tape used Observations: -Pump was left on to keep vacuum -Resin flows faster than in previous trials -Bubbles negligible at centre of cured resin but present at surrounding -Cured resin sample is shown below, with top and bottom surfaces. Solution: Use magnetic stirrer to remove bubbles formed in resin  
6	19/08/2016	Methodology: Resin = 309.613 g (100%) MEKP = 3.032g (0.98% by mass)

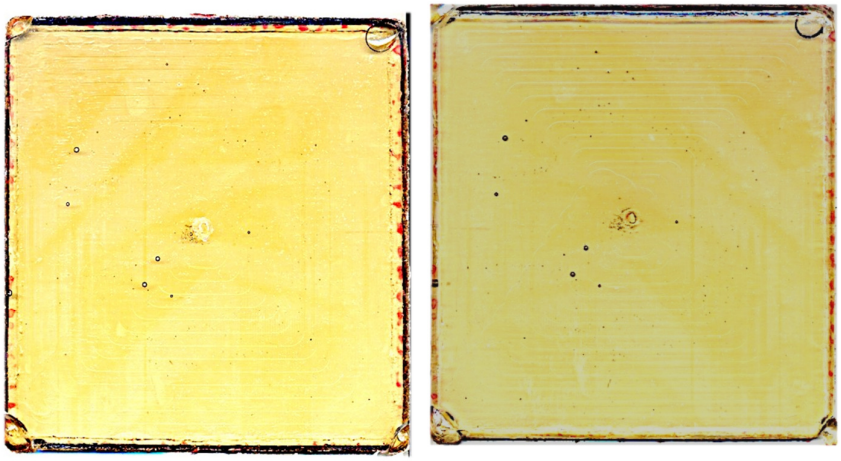
Trial No.	Date	Results
		Styrene = 9.062 g (10 mL, 2.9% by mass) Injection pressure = 100 kPa -Seal tape used. -Magnetic stirrer from chemical engineering lab used. -Styrene and resin mixed for over an hour. -Catalyst added and mixed with magnetic stirrer -Mixture transported from chemical engineering lab to mechanical workshop Observations: -Negligible bubbles from use of magnetic stirrer -While vacuum infusing resin, the latter was allowed to flow slowly Problem: due to prolonged mixing with magnetic stirrer, transportation and slow flow, resin started to cure resulting in uneven distribution of matrix in mould. -Air injected when using pressure which may be due to lack of resin. -Cured resin sample is shown below, with top and bottom surfaces. Solution: -Use manual mixing as magnetic stirrer is time consuming and resin has a gel time of around 10-15 min after mixing with catalyst. 
7	24/08/2016	Methodology: Resin = +300 g (100%) Note: electronic balance couldn't measure as weight of resin+weight of can exceeded the balance's limit of 410g.

Trial No.	Date	Results
		MEKP = 3.007 g (1% by mass) Styrene = 9.199 g (10mL, 3% by mass) Injection pressure = 100 kPa Observations: -Bubbles may be forming from narrowed resin tank outlet with G-clamp - Cured resin sample is shown below, with top and bottom surfaces. Solution: -Check viscosity, add more styrene to reduce viscosity as it is expected that bubbles will be eliminated consequently. -To keep resin tank outlet's diameter constant (leaving tube open without altering diameter with G-clamp to regulate resin flow). 
8	01/09/2016	Methodology: Resin = 333.420 g (100%) MEKP = 3.195 g (0.96% by mass) Styrene = 36.54 g (40mL, 10.96% by mass) Viscosity = 1,750 cP at 22^{o}C Injection pressure = 100 kPa Observations: -Brookefield viscometer used to measure viscosity of resin. Spindle number 3 at rotating speed of 50 r.p.m. gave a dial reading of 87.5. Therefore, the viscosity obtained was 1,750 cP (dial reading x factor, 87.5 x 20) at 22^{o}C.

Trial No.	Date	Results
		-Connector got disconnected with mould - Cured resin sample is shown below, with top and bottom surfaces. Solution: -Add more styrene to reduce viscosity to fit range of 100-1,000 cP -Increase size of hole to fit connector such that it's tightly fitted with the mould. 
9	08/09/2016	Methodology: New resin used from unsealed bottle Resin =327.524 g (100%) MEKP = 3.085 g (0.94 % by mass) Styrene = 35.744 g (40 mL, 16.37% by mass) Injection pressure = 100 kPa Viscosity = 990 cP (Spindle number 3, speed 100 rpm, dial reading 99, factor 10) Observations: -Bubbles still present: may be due to moisture or low vacuum pressure or rough surface of mould cover - Cured resin sample is shown below, with top and bottom surfaces. Solution: -Try with fresh resin

Trial No.	Date	Results
		
10	19/09/2016	Methodology: Fresh resin (Pink) used. Resin = 320.346g (100%) MEKP = 3.142 g (0.98 % by mass) Styrene = 0 g Injection pressure = 100 kPa Viscosity = 450 cP (spindle number 3, speed 100, dial reading 45, factor 10) Observations: -Bubbles still present - Cured resin sample is shown below, with top and bottom surfaces. Solution: -Use degassing chamber to eliminate bubbles before moulding -change Perspex cover

Trial No.	Date	Results
		 
11	24/11/2016	Methodology: Fresh resin (Pink) used. Resin = 310.152g (100%) MEKP = 3.081g (1 % by mass) Styrene = 0 g Injection pressure = 80 kPa Viscosity = 450 cP (spindle number 3, speed 100, dial reading 45, factor 10) Resin was degassed for 5 min before and after addition of catalyst. Observations: -Resin in container was clearer after the degassing process. - During vacuum infusion of resin, fewer bubbles were present. - Cured resin sample is shown below, with top and bottom surfaces. Solution: -Degassing time is to be increased and a container with a larger surface area is to be used to increase efficiency of degassing resin.

Trial No.	Date	Results
		

Annex 12: Details on composite making for Agalega and Mauritius fibres

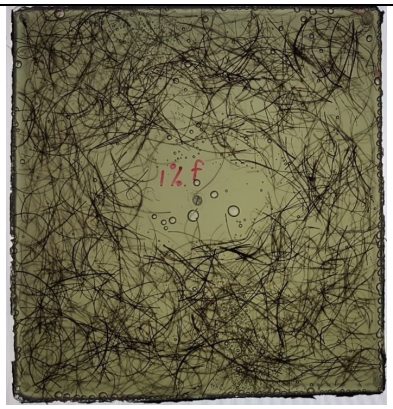
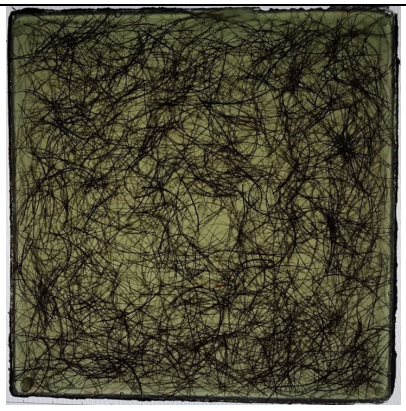
A fresh resin was used for the experiment and the conditions were as follows,

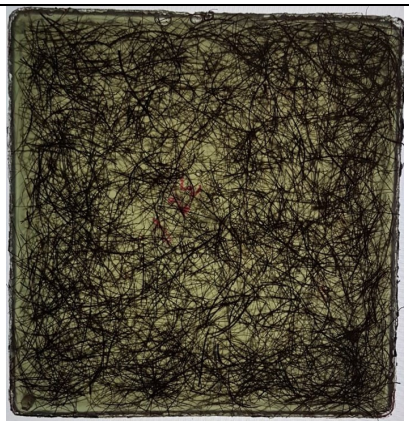
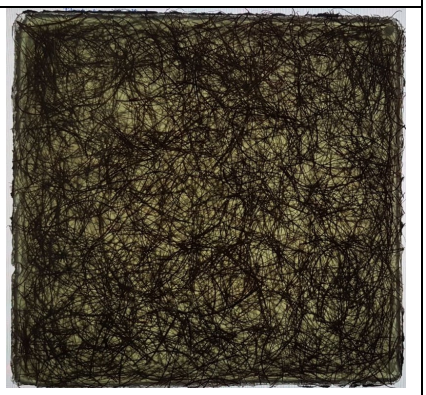
Coconut fibre: alkaline treatment (6% w/w NaOH)

Resin viscosity; 1880 cP (Spindle No. = 2, Spindle speed = 20 rpm, Dial reading = 94, dial factor = 20)

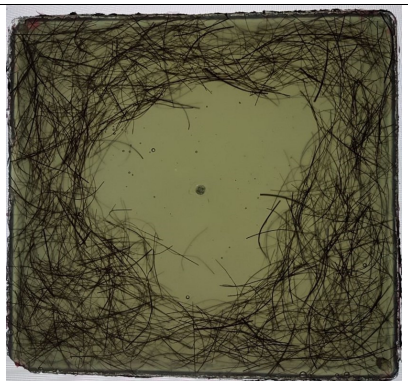
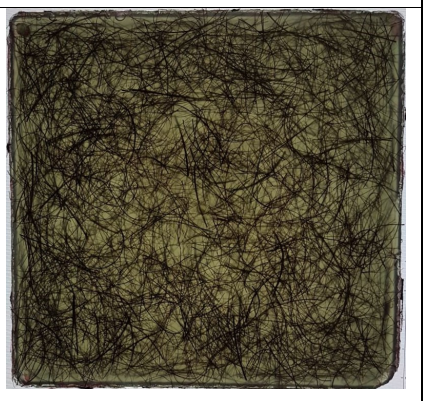
Degassing time: 5 min before adding catalyst + 10 min after mixing in catalyst

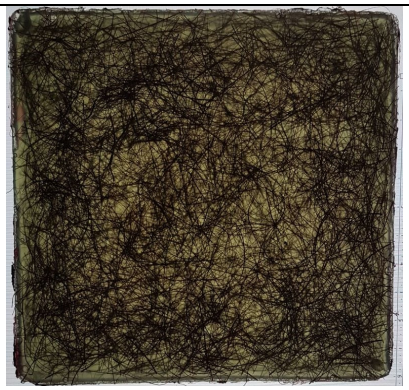
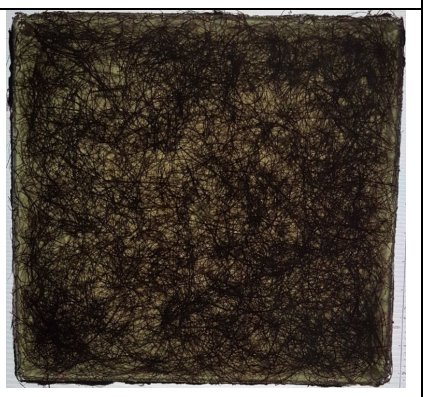
Injection pressure: 80 kPa

Trial No.	Date		Agalega
1	04/10/2017	Coconut fibre = 3.302g (1% by volume) Resin = 300.095g (100%) MEKP = 3.022g (1 % by mass) Note: Fibres displace during injection and some air bubbles.	
2	11/10/2017	Coconut fibre = 6.680g (2% by volume) Resin = 300.15g (100%) MEKP = 3.009g (1 % by mass) Note: No air bubbles	

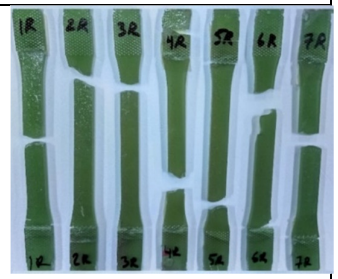
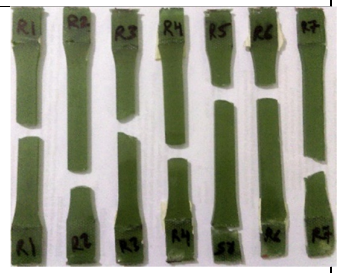
Trial No.	Date		Agalega
3	13/10/2017	Coconut fibre = 10.138g (3% by volume) Resin = 300.206g (100%) MEKP = 3.017g (1 % by mass) Note: No air bubbles	
4	16/10/2017	Coconut fibre = 13.630g (4% by volume) Resin = 300.024g (100%) MEKP = 3.031g (1 % by mass) Note: No air bubbles	
5	18/10/2017	Coconut fibre =17.222g (5% by volume) Resin = 300.132g (100%) MEKP = 3.033g (1 % by mass) Note: No air bubbles	

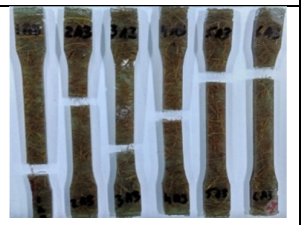
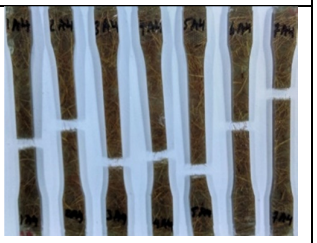
Trial No.	Date		Agalega
6	20/10/2017	Control Resin = 326.418g (100%) MEKP = 3.245g (1 % by mass) Note: No air bubbles	

Trial No.	Date		Mauritius
1	25/10/2017	Coconut fibre = 3.308g (1% by volume) Resin = 308.904g (100%) MEKP = 3.151g (1 % by mass) Note: Fibres displace during injection	
2	30/10/2017	Coconut fibre = 6.689g (2% by volume) Resin = 303.215g (100%) MEKP = 3.015g (1 % by mass) Note: No air bubbles	

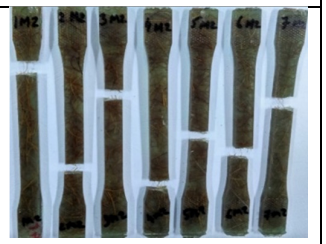
Trial No.	Date		Mauritius
3	31/10/2017	Coconut fibre = 10.123g (3% by volume) Resin = 300.310g (100%) MEKP = 3.095g (1 % by mass) Note: No air bubbles	
4	08/11/2017	Coconut fibre = 13.641g (4% by volume) Resin = 300.031g (100%) MEKP = 3.030g (1 % by mass) Note: No air bubbles	
5	07/11/2017	Coconut fibre = 17.228g (5% by volume) Resin = 300.434g (100%) MEKP = 3.058g (1 % by mass) Note: No air bubbles	

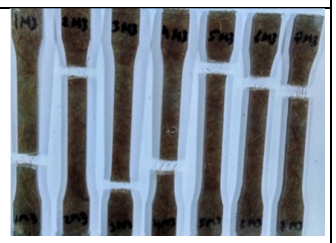
Annex 13: Tensile strength result for Agalega and Mauritius fibres composites

Sample	Average thickness T, mm	Average width W, mm	Force at Break, N	Elongation at Break, mm	Stress at Break, MN/m2	Strain at Break, %	Youngs Modulus, MN/m2	Time to Failure, s	Tensile Strength at Break, MPa	Percentage Elongation at Break, %	Calculated Young's Modulus, MPa	
1R	7.10	13.10	5695.702	5.974	58.119	3.621	1896.699	238.825	61.238	11.948	1605.054	
3R	7.02	13.10	5155.356	7.448	52.606	4.514	2010.389	297.732	56.086	14.896	1165.397	
4R	6.77	13.13	5514.279	6.019	56.268	3.648	1888.733	240.570	62.050	12.038	1542.434	
5R	7.07	13.10	5799.653	5.717	59.180	3.465	2199.754	228.565	62.649	11.434	1707.937	
6R	6.88	13.07	5026.889	7.486	51.295	4.537	2092.318	299.273	55.890	14.972	1130.593	
7R	7.00	13.17	5060.231	4.398	51.635	2.665	2000.090	175.812	54.903	8.796	1937.523	
Average	6.97	13.11	5375.35		56.967	3.742	2014.664		58.803	12.347	1514.823	
Standard deviation	0.13	0.03	337.96			0.71	118.57			2.33	314.52	
2R; Defective (did not break in narrow section)												
1R2	6.62	13.00	3306.018	8.888	33.735	5.387	1888.003	355.264	38.435	17.776	626.230	
2R2	6.57	12.97	3552.949	4.971	36.255	3.013	1860.349	198.714	41.727	9.942	1203.286	
3R2	6.47	12.92	3524.118	5.679	35.960	3.442	1851.711	227.022	42.191	11.358	1044.741	
4R2	6.38	13.52	3562.658	6.442	36.354	3.904	1883.355	257.530	41.291	12.884	931.199	
5R2	6.35	13.53	3630.912	5.106	37.050	3.095	1848.593	204.131	42.251	10.212	1197.092	
6R2	6.40	13.63	3215.110	3.900	32.807	2.364	1986.497	155.927	36.848	7.800	1387.775	
7R2	6.35	12.93	3236.881	6.693	33.029	4.056	1802.974	267.503	39.413	13.386	814.324	
Average	6.45	13.21			35.926	3.609	1874.497		40.308	11.908	1029.235	
Standard deviation	0.11	0.33	173.56			0.97	56.73			3.20	259.96	
1A2	6.92	13.07	1641.633	1.219	16.751	0.739	2737.659	48.753	18.164	2.438	2266.712	
2A2	6.92	13.12	1479.725	0.949	15.099	0.575	2959.857	37.968	16.310	1.898	2625.913	
3A2	6.90	13.05	2332.218	1.929	23.798	1.169	2562.731	77.133	25.901	3.858	2035.757	
4A2	6.90	13.10	1388.622	0.949	14.170	0.575	2884.706	37.992	15.363	1.898	2464.348	
5A2	6.83	13.10	2347.418	1.824	23.953	1.105	2703.158	72.974	26.223	3.648	2167.692	

6A2	6.82	13.12	2154.717	1.619	21.987	0.981	2735.010	64.753	24.099	3.238	2241.284	
Average	6.88	13.09	1890.72		19.293		2763.854		21.010	2.830	2300.284	
Standard deviation	0.04	0.03	437.32				140.48			0.87	212.19	
	7A2; Defective (did not break in narrow section)											
2A3	6.82	13.20	1934.362	1.484	19.738	0.899	2674.237	59.372	21.498	2.968	2195.551	
4A3	6.92	13.18	1860.125	1.290	18.981	0.782	2859.049	51.590	20.400	2.580	2427.238	
5A3	6.92	13.15	1582.695	1.081	16.150	0.655	2871.118	43.236	17.401	2.162	2465.649	
6A3	6.92	13.22	2346.633	1.759	23.945	1.066	2776.766	70.349	25.670	3.518	2246.248	
Average	6.89	13.19	1930.95		19.704	0.851	2795.293		21.242	2.807	2333.671	
Standard deviation	0.05	0.03	315.75			0.17	90.94		3.422	0.58	132.78	
	1A3; Defective (did not break in narrow section) 3A3; Defective (broken at air bubbles)											
1A4	6.87	13.17	1954.171	1.364	19.941	0.827	2919.968	54.573	21.614	2.728	2411.245	
2A4	7.02	13.18	1649.871	1.128	16.835	0.684	2936.435	45.137	17.836	2.256	2461.257	
3A4	7.10	13.17	1571.025	0.970	16.031	0.588	3135.620	38.776	16.805	1.940	2726.361	
4A4	7.18	13.18	1942.305	1.235	19.819	0.748	3150.320	49.455	20.510	2.470	2649.599	
5A4	7.20	13.17	1953.387	1.229	19.933	0.745	3194.598	49.171	20.605	2.458	2675.570	
6A4	7.13	13.18	1916.416	1.225	19.555	0.742	3115.161	49.021	20.378	2.450	2635.445	
7A4	7.05	13.18	1782.457	1.174	18.188	0.712	2990.560	46.954	19.178	2.348	2554.494	
Average	7.14	13.18	1898.641		19.374		3112.660		19.561	2.432	2628.777	
Standard deviation	0.07	0.01	78.99				87.65		0.666	0.06	45.24	
2A5	7.12	13.18	1432.163	0.870	14.614	0.527	3091.821	34.797	15.265	1.740	2773.055	
3A5	7.25	13.20	1720.479	1.045	17.556	0.633	3198.096	41.785	17.978	2.090	2773.460	
4A5	7.15	13.18	1971.627	1.254	20.119	0.760	3225.851	50.189	20.917	2.508	2647.237	
5A5	7.28	13.15	1660.952	0.987	16.948	0.598	3205.459	39.521	17.342	1.974	2834.114	
7A5	7.15	13.17	1754.214	1.097	17.900	0.665	3017.449	43.907	18.634	2.194	2691.729	
Average	7.19	13.17	1795.598		18.417		3149.586		18.027	2.225	2724.360	
Standard deviation	0.08	0.02	159.42				114.89		1.810	0.27	79.70	
	1A5; Defective (did not break in narrow section)											

	6A5; Defective (did not break in narrow section)										
2M2	6.80	13.15	2212.675	1.639	22.578	0.993	2780.398	65.565	24.745	3.278	2273.716
3M2	7.00	13.22	2152.658	1.519	21.966	0.921	2888.807	60.730	23.268	3.038	2385.016
5M2	7.22	13.15	2301.032	1.602	23.480	0.971	2979.247	64.086	24.247	3.204	2418.126
6M2	7.18	13.18	2149.618	1.547	21.935	0.938	2834.071	61.891	22.699	3.094	2338.486
7M2	7.05	13.20	2122.159	1.481	21.655	0.898	2910.596	59.252	22.804	2.962	2411.470
Average	7.05	13.18	2187.628		22.323		2878.624		23.553	3.115	2365.363
Standard deviation	0.17	0.03	71.49				75.64		0.905	0.13	53.70
	1M2; Defective (did not break in narrow section) 4M2; Defective (did not break in narrow section)										
1M3	7.03	13.13	2355.067	1.618	24.031	0.981	3022.995	64.726	25.496	3.236	2449.643
2M3	7.05	13.12	2214.047	1.581	22.592	0.958	2884.705	63.284	23.943	3.162	2358.246
4M3	7.15	13.15	2309.662	1.585	23.568	0.961	2922.327	63.420	24.565	3.170	2452.445
6M3	6.95	13.15	2151.187	1.496	21.951	0.907	2938.706	59.862	23.538	2.992	2420.176
7M3	6.77	13.18	1798.834	1.225	18.355	0.742	2910.411	49.013	20.165	2.450	2473.720
Average	6.99	13.15	2165.759		22.099		2935.829		23.541	3.002	2430.846
Standard deviation	0.14	0.02	220.07				52.56		2.027	0.32	44.84
	3M3; Defective (did not break in narrow section) 5M3; Defective (did not break in narrow section)										
2M4	7.18	13.17	2264.257	1.602	23.105	0.971	2929.497	64.049	23.940	3.204	2379.506
3M4	7.25	13.13	2521.682	1.944	25.731	1.178	2560.862	77.749	26.484	3.888	2184.295
4M4	7.22	13.15	2442.052	1.932	24.919	1.171	2519.683	77.282	25.733	3.864	2128.010
5M4	7.08	13.17	2200.122	1.676	22.45	1.016	2783.972	67.081	23.590	3.352	2209.646
7M4	6.87	13.18	2427.832	2.044	24.774	1.239	2408.443	81.765	26.819	4.088	1999.516
Average	7.12	13.16	2371.189		24.196		2640.491		25.313	3.679	2180.195
Standard Deviation	0.15	0.02	133.77				211.48		1.472	0.38	137.82
	1M4; Defective (did not break in narrow section) 6M4;Defective (did not break in narrow section)										
1M5	7.17	13.22	2375.955	1.801	24.244	1.092	2852.264	72.052	25.084	3.602	2220.147
2M5	7.28	13.17	2562.183	1.918	26.145	1.162	2839.961	76.699	26.718	3.836	2250.000
3M5	7.37	13.18	2258.864	1.707	23.05	1.035	2839.358	68.279	23.259	3.414	2227.053



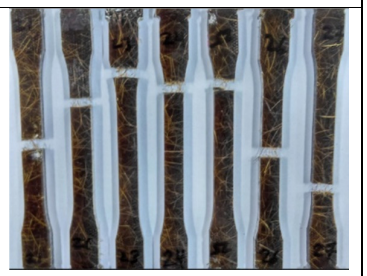
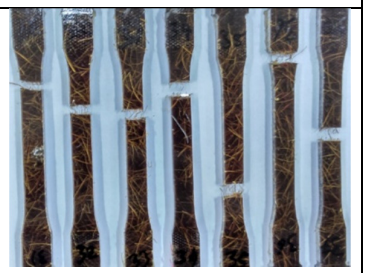
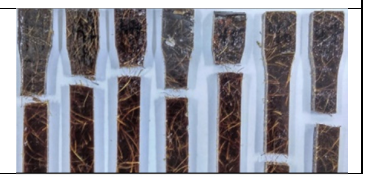






4M5	7.42	13.18	1949.072	1.35	19.888	0.818	2979.278	54.034	19.934	2.700	2431.296	
5M5	7.27	13.18	2230.032	1.602	22.755	0.971	2897.859	64.068	23.278	3.204	2343.460	
6M5	7.13	13.17	2225.129	1.668	22.705	1.011	2810.325	66.706	23.691	3.336	2245.796	
7M5	6.90	13.13	2114.51	1.705	22.567	1.033	2766.17	68.191	23.332	3.410	2184.608	
Average	7.22	13.18	2245.106		23.051		2855.031		23.614	3.357	2271.766	
Standard Deviation	0.17	0.03	192.86				67.88		2.068	0.35	85.63	

Annex 14: Tensile strength result for fibre-shell composites

Sample	Average thickness T, mm	Average width W, mm	Force at Break, N	Elongation at Break, mm	Stress at Break, MN/m2	Strain at Break, %	Youngs Modulus, MN/m2	Time to Failure, s	Tensile Strength at Break, MPa	Percentage Elongation at Break, %	Calculated Young's Modulus, MPa	
1S2	6.70	13.06	2104.507	1.639	21.475	0.993	2748.887	65.566	24.045	3.278	2162.638	
2S2	6.84	13.16	2234.151	1.775	22.797	1.076	2720.683	70.982	24.808	3.550	2118.680	
4S2	6.67	13.07	2241.506	1.784	22.873	1.081	2669.115	71.357	25.693	3.568	2115.911	
5S2	6.56	13.05	2473.041	2.491	25.235	1.510	2246.073	99.644	28.873	4.982	1671.192	
6S2	6.91	13.19	2171.879	1.554	22.162	0.942	2841.666	62.173	23.818	3.108	2352.654	
7S2	6.81	13.07	1882.190	1.436	19.206	0.870	2727.296	57.478	21.152	2.872	2207.586	
Average	6.75	13.10	2184.55		22.291	1.079	2658.953		24.731	3.560	2104.777	
Standard deviation	0.13	0.06	193.35			0.23	210.01			0.75	229.64	
3S2; Defective (did not break in narrow section)												
1S3	6.75	13.23	1911.610	1.353	19.506	0.820	2904.448	54.135	21.390	2.706	2378.780	
2S3	6.84	13.20	1987.023	1.429	20.276	0.866	2848.872	57.135	21.997	2.858	2341.339	
3S3	6.64	13.36	2197.180	1.580	22.420	0.958	2821.922	63.203	24.768	3.160	2340.292	
4S3	6.90	13.48	2526.487	2.067	25.780	1.253	2653.749	82.672	27.170	4.134	2057.462	
5S3	6.69	13.44	1955.838	1.417	19.958	0.859	2767.798	56.703	21.747	2.834	2323.399	
7S3	6.80	13.21	1786.772	1.232	18.232	0.747	2907.628	49.292	19.886	2.464	2440.696	
Average	6.77	13.32			21.052	0.917	2817.403		22.826	3.026	2313.662	
Standard deviation	0.10	0.12	264.30			0.18	95.89			0.59	132.35	
6S3; Defective (did not break in narrow section)												
1S4	6.61	14.06	2619.258	2.540	26.727	1.539	2396.470	101.554	28.177	5.080	1736.647	
2S4	6.87	13.57	2031.055	1.456	20.725	0.882	2801.635	58.277	21.802	2.912	2349.773	
4S4	6.66	13.64	2040.862	1.613	20.825	0.978	2583.804	64.534	22.483	3.226	2129.346	
6S4	6.64	13.57	2165.406	1.719	22.096	1.042	2572.855	68.807	24.038	3.438	2120.537	
7S4	6.68	13.53	1590.344	1.212	16.228	0.735	2661.596	48.510	17.596	2.424	2207.891	

Average	6.69	13.67	2089.39		21.320		2603.272		22.819	3.416	2108.839	
Standard deviation	0.10	0.22	367.88				147.33			1.01	227.46	
3S4; Defective (did not break in narrow section) 5S4; Defective (did not break in narrow section)												

Annex 15: Characterisation of raw materials for briquettes

Before producing briquettes from coconut husk and shell, it is necessary to find out the factors affecting the characteristics of the product. Coconut husk and shell were characterised in term of moisture content, ash content, volatile matter, fixed carbon and calorific value.

I. Moisture Content

The ASABE Standards S358.2 (Moisture Measurement-Forages) was used to determine the moisture content of the husk and shell. To calculate the moisture content of both coconut husk and shell, 100g of each sample were weighed as shown in Figure A.15.1. They were placed in an oven at 60^{o}C for 24 hours. The change in mass was recorded and the samples were left in the oven for another 24 hours. The experiment was carried out in triple and an average of the results was used. Moisture content was calculated as shown below:

$$\text{Moisture content} = \frac{(\text{mass of plate + sample}) - (\text{mass of plate + dry sample})}{(\text{mass of plate + sample}) - \text{mass of plate}} \times 100$$



Figure A.15.1: Coconut husk and shell used to determine moisture content

The results obtained are shown in Table A.15.1. The average moisture content of coconut husk was 20.2% and that of coconut shell was 11.8%.

Table A.15.1: Moisture content of coconut husk and shell

Moisture content of coconut husk	Experiment 1	Experiment 2	Experiment 3
Mass of plate, g	114.8	112.3	120.4
Mass of plate + husk, g	215.5	212.6	213.9
Mass of plate + dry husk at 1st removal, g	195.4	192.3	193.8
Mass of plate + dry husk at 2nd removal, g	195.2	192.0	193.8
Mass of plate + dry husk at 3rd removal, g	195.2	192.0	193.8
Mass loss, g	20.3	20.6	20.1
(Mass of plate + husk) – mass of plate	100.7	100.3	100.5
Moisture content, %	20.2	20.5	20.0
Moisture content of coconut shell			

Mass of plate, g	109.5	105.3	108.8
Mass of plate + shell, g	209.8	206.0	209.2
Mass of plate + dry shell at 1st removal, g	198.1	194.5	197.9
Mass of plate + dry shell at 2nd removal, g	197.8	194.1	197.6
Mass of plate + dry shell at 3rd removal, g	197.8	194.1	197.6
Mass loss, g	12.0	11.9	11.6
(Mass of plate + shell) – mass of plate	100.3	100.7	100.4
Moisture content, %	12.0	11.8	11.6

II. Ash content

The ASTM E1755 – 01 (Standard Test Method for Ash in Biomass) determine the ash content expressed as a percentage of residue remaining after dry oxidation of sample at 550 – 600 ^{o}C. To calculate the ash content of both coconut husk and shell, 4g of each sample were weighed in crucibles shown in Figure A.15.2. They were placed in a furnace at 550^{o}C for 3 hours. The change in mass was recorded. The experiment was carried out in triple and an average of the results was taken as the ash content. Ash content was calculated as shown below:

$$\text{Ash content} = \frac{\text{(mass of crucible + ash) – mass of crucible}}{\text{(mass of crucible + sample) – mass of crucible}} \times 100$$



Figure A.15.2: Coconut husk and shell used to determine ash content

The results obtained are shown in Table A.15.2. The average ash content of coconut husk was 1.982% and that of coconut shell was 0.125%.

Table A.15.2: Ash content of coconut husk and shell

Ash content of coconut husk	Experiment 1	Experiment 2	Experiment 3
Mass of crucible, g	120.592	108.683	111.828
Mass of crucible + husk, g	124.593	112.686	115.530
Mass of crucible + ash, g	120.688	108.755	111.895
Mass of ash, g	0.096	0.072	0.070
(Mass of crucible + husk) – mass of crucible	4.001	4.003	4.002
Ash content, %	2.399	1.799	1.749
Ash content of coconut shell			

Mass of crucible, g	126.642	119.360	120.867
Mass of crucible + shell, g	130.655	123.362	124.906
Mass of crucible + ash, g	126.647	119.364	120.873
Mass of ash, g	0.005	0.004	0.006
(Mass of crucible + shell) – mass of crucible	4.013	4.002	4.017
Ash content, %	0.125	0.100	0.149

III. Volatile Matter

The ASTM E872-82 (Standard Test Method for Volatile Matter in the Analysis of Particulate Wood Fuels) determines the percentage of gaseous products, exclusive of moisture vapour in the analysis. The volatile matter is determined by incinerating the sample at 950 ± 20 ^{o}C in a furnace for 7 minutes. The volatile matter of both coconut husk and shell, were determined separately as follows;

1. The mass of a dry crucible was weighed using an electronic mass balance and recorded as m1 (mass of crucible).
2. Then 4g of dry sample (moist free) was added in the dry crucible and was recorded as m2 (mass of crucible + sample).
3. The crucible containing the sample was covered with a lid, then placed in a furnace and heated at 950 ± 20 ^{o}C in the absent of air for 7 minutes and the char obtained was left to cool.
4. The crucible and its content were weighed carefully and recorded as m3 (mass of crucible + char).
5. The volatile matter was calculated using the following formula:-

$$\text{Volatile matter} = \frac{(m2 - m1) - (m3 - m1)}{(m2 - m1)} \times 100$$

Where,

m1 - mass of crucible

m2 - mass of crucible + sample

m3 - mass of crucible + char

The results obtained are shown in Table A.15.3. The average volatile matter of coconut husk was 82.27% and that of coconut shell was 74.56%.

Table A.15.3: volatile matter of coconut husk and shell

volatile matter of coconut husk	Experiment 1	Experiment 2	Experiment 3
Mass of crucible, g	120.697	117.438	126.647
Mass of crucible + husk, g	124.698	121.439	130.647
Mass of crucible + char, g	122.019	118.714	127.941
Mass of char, g	1.322	1.276	1.294
(Mass of crucible + husk) – mass of crucible	4.001	4.001	4.000
volatile matter, %	66.96	68.11	67.65
volatile matter of coconut shell			
Mass of crucible, g	119.446	118.924	107.880
Mass of crucible + shell, g	123.446	122.925	111.882
Mass of crucible + char, g	120.449	120.066	108.974
Mass of char, g	1.003	1.142	1.094
(Mass of crucible + shell) – mass of crucible	4.000	4.001	4.002
volatile matter, %	74.93	71.46	72.66

IV. Fixed Carbon

The fixed carbon of the sample was calculated by using the following equation;

Fixed carbon = 100 – (Moisture content + Ash content + Volatile content)

The calculated average fixed carbon of coconut husk was 10.25% and that of coconut shell was 15.06%. The fixed carbon values of each sample was calculated by replacing the average values of moisture, ash and volatile contents in the above equation follows;

Material	Average Moisture content, %	Average Ash content, %	Average Volatile matter, %	Average Fixed carbon, %
Coconut husk	20.2	1.982	67.57	10.25
Coconut shell	11.8	0.125	73.02	15.06

V. Calorific Value

The calorific value is one of the most important parameter in the evaluation of materials to be used as fuels. The higher heating value of coconut husk, coconut shell and waste oil were determined by the use of an oxygen bomb calorimeter and in accordance with the ASTM D2015 (Standard Test Method for Gross Calorific Value of Coal and Coke by the Adiabatic Bomb Calorimeter).

Procedure

- A volumetric flask was used to fill the calorimeter bucket with 2 L of water. The bucket was then placed in the calorimeter container.

- Approximately 10 cm of fuse wire was attached to the electrodes of the bomb head through the eyelet holes.
- Around 1.000 g of pulverised coconut sample was compressed by the use of a pelletizer and the mass of the pellet was recorded.
- The pellet was placed in a capsule and was then placed under the fuse wire which has been attached previously. The wire should neither be in contact with the sample nor with the capsule. It must be just above the sample.
- The bomb head was then carefully placed in the bomb cylinder and screw cap of the cylinder tightened.
- The thumb screw on the bomb head was closed and the bomb was filled with oxygen until the regulator read a pressure of 25 atm.
- The bomb was then placed in the calorimeter bucket and the two electrodes were connected to the terminals of the bomb head.
- The calorimeter was covered with lid and the belt was attached to the stirrer and motor.
- The stirrer was switch on and the temperature of the water was allowed to stabilise for about 5 minutes.
- After stabilisation the initial temperature of the water was recorded, then the ignition button was pressed to start the combustion of the sample.
- The peak temperature was recorded as the final temperature.
- The temperature of the water was noted every 30 seconds and a graph was plotted so as to find the peak temperature, which was recorded as the final temperature.

Calculations

<u>Standardization (Calibration)</u>

Benzoic acid was used for the calibration, because it burns without leaving any residue.

Calorific value of Benzoic acid = 6318 cal/g

Energy released per degree Celsius temperature rise = 10.253 kJ/^{o}C.

ΔT = Difference in stabilization temperature

Difference in stabilization temperature = Final temperature – Initial temperature

Energy released during combustion of sample, = 10.253 kJ/^{o}C $\times \Delta T$

Gross calorific value = $\frac{Energy\ released\ by\ sample}{Mass\ of\ sample}$

The results obtained are shown in Table A.15.4. The average Gross Calorific Value of the raw materials used are as follows;

Raw material	Average GCV (MJ/kg)
Non-carbonised husk	17.372
Non-carbonised shell	18.925
Charcoal husk	22.801
Charcoal shell	32.271
Waste oil	39.547

Table A.15.4: Gross Calorific Value of raw materials

Non-carbonised raw materials				
Mass of pellet (g)	***Initial temperature (^oC)***	***Final temperature (^oC)***	***Change in temperature***	***GCV (MJ/kg)***
Husk				
0.560	25.803	26.768	0.965	17.668
0.861	26.225	27.674	1.449	17.255
0.987	24.937	26.592	1.655	17.192
Average Gross Calorific Value (GCV)				17.372
Shell				
1.134	26.712	28.796	2.084	18.842
0.994	26.566	28.403	1.837	18.948
0.997	25.951	27.797	1.846	18.984
Average Gross Calorific Value (GCV)				18.925
Charcoal raw materials				
Husk				
0.973	26.721	28.868	2.147	22.624
0.988	27.006	29.208	2.202	22.851
0.970	27.070	29.239	2.169	22.927
Average Gross Calorific Value (GCV)				22.801
Shell				
1.033	26.911	30.171	3.260	32.357
0.998	27.527	30.668	3.141	32.269
0.927	27.260	30.170	2.910	32.186
Average Gross Calorific Value (GCV)				32.271
Waste oil				
0.725	26.197	28.975	2.778	39.287
0.414	26.333	27.938	1.605	39.749
0.518	26.343	28.344	2.001	39.607
Average Gross Calorific Value (GCV)				39.547

Annex 16: Characterisation of briquettes

Part I: Density of briquettes

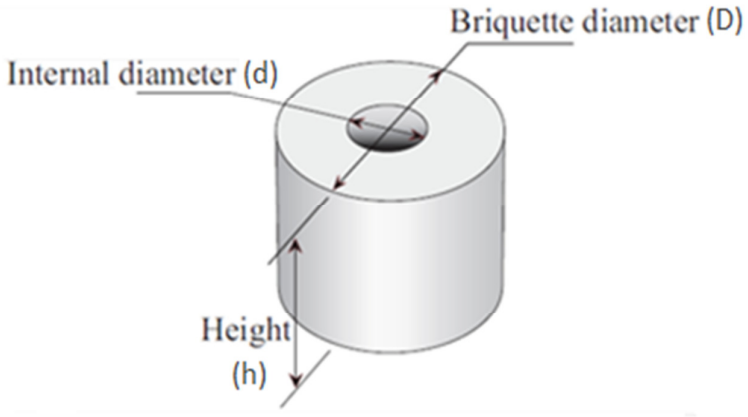


Figure A.16.1: Cylindrical holey type briquette

Volume of briquette (V) is calculated using the following formula: -

$$V = \frac{\pi h\,(D^2 - d^2)}{4}$$

Where

D = External diameter of briquette, m

d = Internal diameter of briquette, m

h = Height of briquette, m

The external diameter, D was set at 3 cm, which is the outer diameter of the mould and the internal diameter, d was fixed at 1 cm.

From definition of density,

$$\rho = \frac{m}{V} \qquad [kg/m^3]$$

Where

ρ = density of briquette, kg/m^3

m = mass of briquette, kg

v = volume of briquette, m^3

Table A.16.1: Density of non-carbonised briquettes

Non-carbonised briquette													
Husk : Shell ratio	***Optimum oil used (%)***	***Exp. No.***	***Mass of husk used (g)***	***Mass of shell used (g)***	***Mass of oil used (g)***	***Total mass (g)***	***Mass of briquette (g)***	***Briquette height (mm)***			***Average height (mm)***	***Briquette Volume (cm3)***	***Briquette Density (kg/m3)***
								h1	***h2***	***h3***	***<h>***		
100 : 0	40	1	20.030	0.000	8.009	28.039	25.580	45.21	45.35	45.12	45.23	28.42	900.1
		2	20.019	0.000	8.025	28.044	26.320	47.06	46.96	47.02	47.01	29.54	890.9
		3	20.036	0.000	8.056	28.092	27.107	49.38	49.45	49.41	49.41	31.05	873.0
	Average Briquette Density												***888.0***
75 : 25	38	1	15.053	5.064	7.618	27.735	26.850	44.09	43.89	44.11	44.03	27.67	970.4
		2	15.010	5.054	7.626	27.690	26.211	43.50	43.52	43.61	43.54	27.36	957.9
		3	15.016	5.028	7.621	27.665	25.623	47.64	47.46	47.16	47.42	29.80	859.9
	Average Briquette Density												***929.4***
50 : 50	35	1	10.055	10.021	7.075	27.151	25.805	41.65	41.73	41.77	41.72	26.21	984.4
		2	10.053	10.036	7.064	27.153	25.932	43.22	43.28	42.97	43.16	27.12	956.2
		3	10.044	10.023	7.048	27.115	25.677	41.10	41.31	41.37	41.26	25.93	990.3
	Average Briquette Density												***977.0***
25 : 75	33	1	5.011	15.004	6.622	26.637	24.674	36.16	36.13	35.93	36.07	22.67	1088.5
		2	5.033	15.056	6.623	26.712	24.990	36.85	37.00	36.87	36.91	23.19	1077.5
		3	5.027	15.030	6.628	26.685	24.761	37.52	37.45	37.36	37.44	23.53	1052.3
	Average Briquette Density												***1072.8***
0 : 100	30	1	0.000	20.056	6.008	26.064	23.864	-	-	-	-	-	-
		2	0.000	20.012	6.059	26.071	23.984	-	-	-	-	-	-
		3	0.000	20.091	6.083	26.174	24.017	-	-	-	-	-	-

Note; - For composition 100% shell, the briquettes were broken while handling, thus the height of briquettes were not obtained.

Table A.16.2: Density of charcoal briquettes

Charcoal briquette													
Husk : Shell ratio	***Optimum oil used (%)***	***Exp. No.***	***Mass of husk used (g)***	***Mass of shell used (g)***	***Mass of oil used (g)***	***Total mass (g)***	***Mass of briquette (g)***	***Briquette height (mm)***			***Average height (mm)***	***Briquette Volume (cm3)***	***Briquette Density (kg/m3)***
								h1	***h2***	***h3***	***<h>***		
100 : 0	35	1	20.050	0.000	7.008	27.058	24.254	35.92	36.01	35.85	35.93	22.58	1074.3
		2	20.014	0.000	7.004	27.018	23.675	36.24	36.07	36.18	36.16	22.73	1041.8
		3	20.006	0.000	7.032	27.038	23.842	36.32	36.07	36.12	36.17	22.73	1049.0
	Average Briquette Density												***1055.0***
75 : 25	33	1	15.016	5.028	6.617	26.661	24.051	33.59	33.30	33.33	33.41	20.99	1145.7
		2	15.014	5.022	6.636	26.672	24.753	34.87	34.51	34.54	34.64	21.77	1137.1
		3	15.028	5.022	6.617	26.667	24.284	33.24	33.38	33.43	33.35	20.96	1158.7
	Average Briquette Density												***1147.2***
50 : 50	30	1	10.005	10.008	6.012	26.025	23.978	32.22	32.35	32.40	32.32	20.31	1180.5
		2	10.010	10.001	6.030	26.041	24.066	31.21	31.36	31.40	31.32	19.68	1222.6
		3	10.032	10.034	6.013	26.079	24.131	30.48	30.64	30.52	30.55	19.20	1257.1
	Average Briquette Density												***1220.1***
25 : 75	28	1	5.042	15.016	5.623	25.681	24.448	30.45	30.22	30.25	30.31	19.04	1283.7
		2	5.014	15.020	5.628	25.662	24.212	30.13	30.03	30.17	30.11	18.92	1279.6
		3	5.001	15.003	5.629	25.633	24.198	30.58	30.42	30.38	30.46	19.14	1264.2
	Average Briquette Density												***1275.8***
0 : 100	25	1	0.000	20.045	5.033	25.078	24.336	29.07	29.20	29.09	29.12	18.30	1329.9
		2	0.000	20.083	5.025	25.108	24.514	29.57	29.43	29.38	29.46	18.51	1324.2
		3	0.000	20.031	5.012	25.043	24.187	29.06	29.04	29.03	29.04	18.25	1325.3
	Average Briquette Density												***1326.4***

Part II: Gross Calorific Value of briquettes

The same standard test method and apparatus used in appendix B, were used in the determination of the calorific value of the difference briquette composition. Two type of briquettes were produced in different husk to shell ratio, with waste oil as binder namely;

- Non-carbonised briquette
- Charcoal briquette

Table 18.3 and table 18.4 show the results obtained from the GCV test of the two types of briquettes with theirs corresponding husk to shell compositions. The gross calorific value of each type of briquettes and compositions are summarised below;

Non-carbonised composition (%)		Optimum oil used (%)	Average GCV (MJ/kg)
Coconut Husk	Coconut Shell		
100	0	40	21.872
75	25	38	22.327
50	50	35	22.648
25	75	33	22.179
0	100	30	21.890
Charcoal composition (%)		**Optimum oil used (%)**	**Average GCV (MJ/kg)**
Coconut Husk	**Coconut Shell**		
100	0	35	28.979
75	25	33	29.691
50	50	30	30.941
25	75	28	31.832
0	100	25	32.743

Table A.16.3: Gross Calorific Value of non-carbonized briquette

Non carbonized Briquette				
Mass of pellet (g)	***Initial temperature (oC)***	***Final temperature (oC)***	***Change in temperature***	***GCV (MJ/kg)***
100% husk; 0% shell				
1.065	26.080	28.367	2.287	22.017
1.026	25.964	28.087	2.123	21.216
0.988	26.114	28.271	2.157	22.384
Average Gross Calorific Value (GCV)				21.872
75% husk; 25% shell				
0.993	26.149	28.262	2.113	21.817
1.061	26.413	28.780	2.367	22.874
1.040	26.556	28.817	2.261	22.290
Average Gross Calorific Value (GCV)				22.327
50% husk; 50% shell				
1.077	26.392	28.819	2.427	23.105
0.993	27.266	29.414	2.148	22.179
1.056	26.424	28.758	2.334	22.661

Average Gross Calorific Value (GCV)				22.648
25% husk; 75% shell				
1.045	27.442	29.684	2.242	21.997
0.990	26.562	28.721	2.159	22.360
0.937	26.476	28.503	2.027	22.180
Average Gross Calorific Value (GCV)				22.179
0% husk; 100% shell				
1.099	26.525	28.881	2.356	21.980
1.018	26.416	28.580	2.164	21.795
0.975	26.602	28.684	2.082	21.894
Average Gross Calorific Value (GCV)				21.890

Table A.16.4: Gross Calorific Value of charcoal briquette

Charcoal Briquette				
Mass of pellet (g)	***Initial temperature (oC)***	***Final temperature (oC)***	***Change in temperature***	***GCV (MJ/kg)***
100% husk; 0% shell				
1.100	26.613	29.730	3.117	29.053
1.061	26.173	29.170	2.997	28.962
0.982	26.496	29.266	2.770	28.921
Average Gross Calorific Value (GCV)				28.979
75% husk; 25% shell				
0.964	26.390	29.186	2.796	29.738
0.985	26.569	29.417	2.848	29.645
0.996	26.364	29.248	2.884	29.688
Average Gross Calorific Value (GCV)				29.691
50% husk; 50% shell				
1.013	26.282	29.341	3.059	30.961
0.958	26.327	29.218	2.891	30.941
0.982	26.278	29.240	2.962	30.922
Average Gross Calorific Value (GCV)				30.941
25% husk; 75% shell				
0.972	26.568	29.575	3.007	31.719
0.997	26.569	29.677	3.108	31.962
1.041	26.552	29.782	3.230	31.815
Average Gross Calorific Value (GCV)				31.832
0% husk; 100% shell				
1.034	25.735	29.045	3.310	32.821
1.078	26.222	29.653	3.431	32.633
0.961	26.469	29.541	3.072	32.775
Average Gross Calorific Value (GCV)				32.743

Part III: Drop shatter test

The drop shatter test of the briquettes was performed in accordance with the ASTM D440 (standard test method of drop shatter test for coal). This test method is used to measure the relative resistance to breakage of briquettes when handled.

Procedure

- Weigh and record the initial mass of the sample
- Place sample in a resealable polythene bag and drop it freely from a distance of 6 ft (1.8m) onto a concrete floor.
- Carefully return and level the bag to the initial height (6 ft) and again drop it.
- After the second drop, separate the fragments into sized portion by using the sieve openings size of 1, 0.75 and 0.5 in., during sieving care should be taken so as to prevent further breakage of sample. When using 1 in. sieve openings, pieces which do not pass through readily shall be tried by hand to determine whether they will pass through in any position without forcing. For sieves 0.75 in. and 0.5 in., the pieces shall be sieved either by shaking or rolling by hand without upending the individual pieces.
- Weigh the fragments remaining on each sieve and at bottom of sieve.
- Make at least two test per category to obtain size stability and find their average.

Calculation

- Determine the weight percents of the sample prior to and again after the test. Calculate to the nearest 0.1 %
- Multiply the appropriate weight percents by their respective average sieve size openings.
- The sum of these products before testing is designated as ***S***. The sum of these products after testing is designated as ***s***.
- The size stability is calculated as a percent by dividing ***s*** by ***S*** and multiplying by 100 %.
- The friability is expressed as 100 % minus the size stability, i.e. the size stability and the friability sum to 100 %.
- Calculate the size stability and the friability to the nearest 0.5 %.

The table below show a summary of the drop shatter test for the 2 types of briquettes with their corresponding composition variations.

Non-carbonised composition (%)		Average size stability (%)	Average friability (%)
Coconut Husk	Coconut Shell		
100	0	99	1
75	25	96	4
50	50	77	23
25	75	36	64
0	100	20	80
Charcoal composition (%)		**Average size stability (%)**	**Average friability (%)**
Coconut Husk	**Coconut Shell**		
100	0	43	57
75	25	46	54
50	50	50	50
25	75	57	43
0	100	66	34

Non-carbonised Briquette						
Sieves, inches		Weight, g	Weight, % (1)	Average of sieve opening, in.		Product of (1) * (2)
Retained on	Passing			Inches	Normalizing factor (2)	
Sample 1 (100% husk)						
1	1.5	27.480	100	1.25	1	100 : S
dropped sample						
1	1.5	26.895	97.871	1.25	1	97.871
0.75	1	0.000	0.000	0.875	0.7	0.000
0.5	0.75	0.000	0.000	0.625	0.5	0.000
	0.5	0.577	2.100	0.25	0.2	0.420
Total (sum of products (1) * (2) for dropped sample)						98.291 : s
Size stability, % = (100 * s)/S = (100 *s)/100 = s = 98.3						
Size stability = 98 %						
Friability = (100 - s) = 2 %						

Non-carbonised Briquette						
Sieves, inches		Weight, g	Weight, % (1)	Average of sieve opening, in.		Product of (1) * (2)
Retained on	Passing			Inches	Normalizing factor (2)	
Sample 2 (100% husk)						
1	1.5	25.946	100	1.25	1	100 : S
dropped sample						
1	1.5	25.618	98.736	1.25	1	98.736
0.75	1	0.000	0.000	0.875	0.7	0.000
0.5	0.75	0.000	0.000	0.625	0.5	0.000
	0.5	0.321	1.237	0.25	0.2	0.247
Total (sum of products (1) * (2) for dropped sample)						98.983 : s
Size stability, % = (100 * s)/S = (100 *s)/100 = s = 99.0						
Size stability = 99 %						
Friability = (100 - s) = 1 %						

Non-carbonised Briquette						
Sieves, inches		Weight, g	Weight, % (1)	Average of sieve opening, in.		Product of (1) * (2)
Retained on	Passing			Inches	Normalizing factor (2)	
Sample 3 (100% husk)						
1	1.5	26.661	100	1.25	1	100 : S
dropped sample						
1	1.5	26.410	99.059	1.25	1	99.059
0.75	1	0.000	0.000	0.875	0.7	0.000
0.5	0.75	0.000	0.000	0.625	0.5	0.000
	0.5	0.211	0.791	0.25	0.2	0.158
Total (sum of products (1) * (2) for dropped sample)						99.217 : s
Size stability, % = (100 * s)/S = (100 *s)/100 = s = 99.2						
Size stability = 99 %						
Friability = (100 - s) = 1 %						

Non-carbonised Briquette						
Sieves, inches		Weight, g	Weight, % (1)	Average of sieve opening, in.		Product of (1) * (2)
Retained on	Passing			Inches	Normalizing factor (2)	
Sample 1 (75% husk; 25% shell)						
1	1.5	26.485	100	1.25	1	100 : S
dropped sample						
1	1.5	25.243	95.311	1.25	1	95.311
0.75	1	0.000	0.000	0.875	0.7	0.000
0.5	0.75	0.000	0.000	0.625	0.5	0.000
	0.5	1.239	4.678	0.25	0.2	0.936
Total (sum of products (1) * (2) for dropped sample)						96.246 : s
Size stability, % = (100 * s)/S = (100 *s)/100 = s = 96.2						
Size stability = 96 %						
Friability = (100 - s) = 4 %						

Non-carbonised Briquette						
Sieves, inches		Weight, g	Weight, % (1)	Average of sieve opening, in.		Product of (1) * (2)
Retained on	Passing			Inches	Normalizing factor (2)	
Sample 2 (75% husk; 25% shell)						
1	1.5	27.136	100	1.25	1	100 : S
dropped sample						
1	1.5	25.840	95.224	1.25	1	95.224
0.75	1	0.000	0.000	0.875	0.7	0.000
0.5	0.75	0.000	0.000	0.625	0.5	0.000
	0.5	1.292	4.761	0.25	0.2	0.952
Total (sum of products (1) * (2) for dropped sample)						96.176 : s
Size stability, % = (100 * s)/S = (100 *s)/100 = s = 96.2						
Size stability = 96 %						
Friability = (100 - s) = 4 %						

Non-carbonised Briquette						
Sieves, inches		Weight, g	Weight, % (1)	Average of sieve opening, in.		Product of (1) * (2)
Retained on	Passing			Inches	Normalizing factor (2)	
Sample 3 (75% husk; 25% shell)						
1	1.5	25.881	100	1.25	1	100 : S
dropped sample						
1	1.5	23.731	91.693	1.25	1	91.693
0.75	1	0.851	3.288	0.875	0.7	2.302
0.5	0.75	0.097	0.375	0.625	0.5	0.187
	0.5	1.200	4.637	0.25	0.2	0.927
Total (sum of products (1) * (2) for dropped sample)						95.109 : s
Size stability, % = (100 * s)/S = (100 *s)/100 = s = 95.1						
Size stability = 95 %						
Friability = (100 - s) = 5 %						

Non-carbonised Briquette						
Sieves, inches		Weight, g	Weight, % (1)	Average of sieve opening, in.		Product of (1) * (2)
Retained on	Passing			Inches	Normalizing factor (2)	
Sample 1 (50% husk; 50% shell)						
1	1.5	25.910	100	1.25	1	100 : S
dropped sample						
1	1.5	17.558	67.765	1.25	1	67.765
0.75	1	2.852	11.007	0.875	0.7	7.705
0.5	0.75	1.984	7.657	0.625	0.5	3.829
	0.5	2.954	11.401	0.25	0.2	2.280
Total (sum of products (1) * (2) for dropped sample)						81.579 : s
Size stability, % = (100 * s)/S = (100 *s)/100 = s = 81.6						
Size stability = 82 %						
Friability = (100 - s) = 18 %						

Non-carbonised Briquette						
Sieves, inches		Weight, g	Weight, % (1)	Average of sieve opening, in.		Product of (1) * (2)
Retained on	Passing			Inches	Normalizing factor (2)	
Sample 2 (50% husk; 50% shell)						
1	1.5	26.152	100	1.25	1	100 : S
dropped sample						
1	1.5	15.783	60.351	1.25	1	60.351
0.75	1	2.881	11.016	0.875	0.7	7.711
0.5	0.75	1.107	4.233	0.625	0.5	2.116
	0.5	6.242	23.868	0.25	0.2	4.774
Total (sum of products (1) * (2) for dropped sample)						74.953 : s
Size stability, % = (100 * s)/S = (100 *s)/100 = s = 75.0						
Size stability = 75 %						
Friability = (100 - s) = 25 %						

Non-carbonised Briquette						
Sieves, inches		Weight, g	Weight, % (1)	Average of sieve opening, in.		Product of (1) * (2)
Retained on	Passing			Inches	Normalizing factor (2)	
Sample 3 (50% husk; 50% shell)						
1	1.5	26.042	100	1.25	1	100 : S
dropped sample						
1	1.5	14.739	56.597	1.25	1	56.597
0.75	1	2.693	10.341	0.875	0.7	7.239
0.5	0.75	3.866	14.845	0.625	0.5	7.423
	0.5	4.183	16.063	0.25	0.2	3.213
Total (sum of products (1) * (2) for dropped sample)						74.471 : s
Size stability, % = (100 * s)/S = (100 *s)/100 = s = 74.5						
Size stability = 74 %						
Friability = (100 - s) = 26 %						

Non-carbonised Briquette						
Sieves, inches		Weight, g	Weight, % (1)	Average of sieve opening, in.		Product of (1) * (2)
Retained on	Passing			Inches	Normalizing factor (2)	
Sample 1 (25% husk; 75% shell)						
1	1.5	24.906	100	1.25	1	100 : S
dropped sample						
1	1.5	3.280	13.170	1.25	1	13.170
0.75	1	3.746	15.041	0.875	0.7	10.528
0.5	0.75	1.481	5.946	0.625	0.5	2.973
	0.5	16.043	64.414	0.25	0.2	12.883
Total (sum of products (1) * (2) for dropped sample)						39.554 : s
Size stability, % = (100 * s)/S = (100 *s)/100 = s = 39.6						
Size stability = 40 %						
Friability = (100 - s) = 60 %						

Non-carbonised Briquette						
Sieves, inches		Weight, g	Weight, % (1)	Average of sieve opening, in.		Product of (1) * (2)
Retained on	Passing			Inches	Normalizing factor (2)	
Sample 2 (25% husk; 75% shell)						
1	1.5	24.858	100	1.25	1	100 : S
dropped sample						
1	1.5	5.810	23.373	1.25	1	23.373
0.75	1	0.000	0.000	0.875	0.7	0.000
0.5	0.75	1.409	5.668	0.625	0.5	2.834
	0.5	17.536	70.545	0.25	0.2	14.109
Total (sum of products (1) * (2) for dropped sample)						40.316 : s
Size stability, % = (100 * s)/S = (100 *s)/100 = s = 40.3						
Size stability = 40 %						
Friability = (100 - s) = 60 %						

Non-carbonised Briquette						
Sieves, inches		Weight, g	Weight, % (1)	Average of sieve opening, in.		Product of (1) * (2)
Retained on	Passing			Inches	Normalizing factor (2)	
Sample 3 (25% husk; 75% shell)						
1	1.5	25.081	100	1.25	1	100 : S
dropped sample						
1	1.5	0.000	0.000	1.25	1	0.000
0.75	1	2.845	11.343	0.875	0.7	7.940
0.5	0.75	1.843	7.348	0.625	0.5	3.674
	0.5	20.245	80.718	0.25	0.2	16.144
Total (sum of products (1) * (2) for dropped sample)						27.758 : s
Size stability, % = (100 * s)/S = (100 *s)/100 = s = 27.8						
Size stability = 28 %						
Friability = (100 - s) = 72 %						

Non-carbonised Briquette						
Sieves, inches		Weight, g	Weight, % (1)	Average of sieve opening, in.		Product of (1) * (2)
Retained on	Passing			Inches	Normalizing factor (2)	
Sample 1 (100% shell)						
1	1.5	24.016	100	1.25	1	100 : S
dropped sample						
1	1.5	0.000	0.000	1.25	1	0.000
0.75	1	0.000	0.000	0.875	0.7	0.000
0.5	0.75	0.000	0.000	0.625	0.5	0.000
	0.5	24.002	99.942	0.25	0.2	19.988
Total (sum of products (1) * (2) for dropped sample)						19.988 : s
Size stability, % = (100 * s)/S = (100 *s)/100 = s = 20.0						
Size stability = 20 %						
Friability = (100 - s) = 80 %						

Non-carbonised Briquette						
Sieves, inches		Weight, g	Weight, % (1)	Average of sieve opening, in.		Product of (1) * (2)
Retained on	Passing			Inches	Normalizing factor (2)	
Sample 2 (100% shell)						
1	1.5	23.860	100	1.25	1	100 : S
dropped sample						
1	1.5	0.000	0.000	1.25	1	0.000
0.75	1	0.000	0.000	0.875	0.7	0.000
0.5	0.75	0.000	0.000	0.625	0.5	0.000
	0.5	23.846	99.941	0.25	0.2	19.988
Total (sum of products (1) * (2) for dropped sample)						19.988 : s
Size stability, % = (100 * s)/S = (100 *s)/100 = s = 20.0						
Size stability = 20 %						
Friability = (100 - s) = 80 %						

Non-carbonised Briquette						
Sieves, inches		Weight, g	Weight, % (1)	Average of sieve opening, in.		Product of (1) * (2)
Retained on	Passing			Inches	Normalizing factor (2)	
Sample 3 (100% shell)						
1	1.5	23.974	100	1.25	1	100 : S
dropped sample						
1	1.5	0.000	0.000	1.25	1	0.000
0.75	1	0.000	0.000	0.875	0.7	0.000
0.5	0.75	0.000	0.000	0.625	0.5	0.000
	0.5	23.967	99.971	0.25	0.2	19.994
Total (sum of products (1) * (2) for dropped sample)						19.994 : s
Size stability, % = (100 * s)/S = (100 *s)/100 = s = 20.0						
Size stability = 20 %						
Friability = (100 - s) = 80 %						

Charcoal Briquette						
Sieves, inches		Weight, g	Weight, % (1)	Average of sieve opening, in.		Product of (1) * (2)
Retained on	Passing			Inches	Normalizing factor (2)	
Sample 1 (100% husk)						
1	1.5	23.516	100	1.25	1	100 : S
dropped sample						
1	1.5	0.000	0.000	1.25	1	0.000
0.75	1	7.381	31.387	0.875	0.7	21.971
0.5	0.75	6.818	28.993	0.625	0.5	14.497
	0.5	9.281	39.467	0.25	0.2	7.893
Total (sum of products (1) * (2) for dropped sample)						44.361 : s
Size stability, % = (100 * s)/S = (100 *s)/100 = s = 44.4						
Size stability = 44 %						
Friability = (100 - s) = 56 %						

Charcoal Briquette						
Sieves, inches		Weight, g	Weight, % (1)	Average of sieve opening, in.		Product of (1) * (2)
Retained on	Passing			Inches	Normalizing factor (2)	
Sample 2 (100% husk)						
1	1.5	23.910	100	1.25	1	100 : S
dropped sample						
1	1.5	0.000	0.000	1.25	1	0.000
0.75	1	5.717	23.910	0.875	0.7	16.737
0.5	0.75	7.755	32.434	0.625	0.5	16.217
	0.5	10.402	43.505	0.25	0.2	8.701
Total (sum of products (1) * (2) for dropped sample)						41.655 : s
Size stability, % = (100 * s)/S = (100 *s)/100 = s = 41.7						
Size stability = 42 %						
Friability = (100 - s) = 58 %						

Charcoal Briquette						
Sieves, inches		Weight, g	Weight, % (1)	Average of sieve opening, in.		Product of (1) * (2)
Retained on	Passing			Inches	Normalizing factor (2)	
Sample 3 (100% husk)						
1	1.5	23.512	100	1.25	1	100 : S
dropped sample						
1	1.5	0.000	0.000	1.25	1	0.000
0.75	1	6.642	28.249	0.875	0.7	19.775
0.5	0.75	7.132	30.333	0.625	0.5	15.167
	0.5	9.730	41.383	0.25	0.2	8.277
Total (sum of products (1) * (2) for dropped sample)						43.218 : s
Size stability, % = (100 * s)/S = (100 *s)/100 = s = 43.2						
Size stability = 43 %						
Friability = (100 - s) = 57 %						

Charcoal Briquette						
Sieves, inches		Weight, g	Weight, % (1)	Average of sieve opening, in.		Product of (1) * (2)
Retained on	Passing			Inches	Normalizing factor (2)	
Sample 1 (75% husk; 25% shell)						
1	1.5	24.502	100	1.25	1	100 : S
dropped sample						
1	1.5	0.000	0.000	1.25	1	0.000
0.75	1	9.832	40.127	0.875	0.7	28.089
0.5	0.75	4.441	18.125	0.625	0.5	9.063
	0.5	10.216	41.695	0.25	0.2	8.339
Total (sum of products (1) * (2) for dropped sample)						45.491 : s
Size stability, % = (100 * s)/S = (100 *s)/100 = s = 45.5						
Size stability = 45 %						
Friability = (100 - s) = 55 %						

Charcoal Briquette						
Sieves, inches		Weight, g	Weight, % (1)	Average of sieve opening, in.		Product of (1) * (2)
Retained on	Passing			Inches	Normalizing factor (2)	
Sample 2 (75% husk; 25% shell)						
1	1.5	23.789	100	1.25	1	100 : S
dropped sample						
1	1.5	0.000	0.000	1.25	1	0.000
0.75	1	5.263	22.124	0.875	0.7	15.487
0.5	0.75	11.128	46.778	0.625	0.5	23.389
	0.5	7.305	30.707	0.25	0.2	6.141
Total (sum of products (1) * (2) for dropped sample)						45.017 : s
Size stability, % = (100 * s)/S = (100 *s)/100 = s = 45.0						
Size stability = 45 %						
Friability = (100 - s) = 55 %						

Charcoal Briquette						
Sieves, inches		Weight, g	Weight, % (1)	Average of sieve opening, in.		Product of (1) * (2)
Retained on	Passing			Inches	Normalizing factor (2)	
Sample 3 (75% husk; 25% shell)						
1	1.5	24.004	100	1.25	1	100 : S
dropped sample						
1	1.5	0.000	0.000	1.25	1	0.000
0.75	1	9.586	39.935	0.875	0.7	27.955
0.5	0.75	6.781	28.249	0.625	0.5	14.125
	0.5	7.595	31.641	0.25	0.2	6.328
Total (sum of products (1) * (2) for dropped sample)						48.407 : s
Size stability, % = (100 * s)/S = (100 *s)/100 = s = 48.4						
Size stability = 48 %						
Friability = (100 - s) = 52 %						

Charcoal Briquette						
Sieves, inches		Weight, g	Weight, % (1)	Average of sieve opening, in.		Product of (1) * (2)
Retained on	Passing			Inches	Normalizing factor (2)	
Sample 1 (50% husk; 50% shell)						
1	1.5	24.023	100	1.25	1	100 : S
dropped sample						
1	1.5	0.000	0.000	1.25	1	0.000
0.75	1	13.082	54.456	0.875	0.7	38.119
0.5	0.75	5.885	24.497	0.625	0.5	12.249
	0.5	5.034	20.955	0.25	0.2	4.191
Total (sum of products (1) * (2) for dropped sample)						54.559 : s
Size stability, % = (100 * s)/S = (100 *s)/100 = s = 54.6						
Size stability = 55 %						
Friability = (100 - s) = 45 %						

Charcoal Briquette						
Sieves, inches		Weight, g	Weight, % (1)	Average of sieve opening, in.		Product of (1) * (2)
Retained on	Passing			Inches	Normalizing factor (2)	
Sample 2 (50% husk; 50% shell)						
1	1.5	23.931	100	1.25	1	100 : S
dropped sample						
1	1.5	0.000	0.000	1.25	1	0.000
0.75	1	6.815	28.478	0.875	0.7	19.934
0.5	0.75	9.029	37.729	0.625	0.5	18.865
	0.5	7.808	32.627	0.25	0.2	6.525
Total (sum of products (1) * (2) for dropped sample)						45.324 : s
Size stability, % = (100 * s)/S = (100 *s)/100 = s = 45.3						
Size stability = 45 %						
Friability = (100 - s) = 55 %						

Charcoal Briquette						
Sieves, inches		Weight, g	Weight, % (1)	Average of sieve opening, in.		Product of (1) * (2)
Retained on	Passing			Inches	Normalizing factor (2)	
Sample 3 (50% husk; 50% shell)						
1	1.5	24.546	100	1.25	1	100 : S
dropped sample						
1	1.5	0.000	0.000	1.25	1	0.000
0.75	1	10.153	41.363	0.875	0.7	28.954
0.5	0.75	7.231	29.459	0.625	0.5	14.729
	0.5	7.008	28.550	0.25	0.2	5.710
Total (sum of products (1) * (2) for dropped sample)						49.394 : s
Size stability, % = (100 * s)/S = (100 *s)/100 = s = 49.4						
Size stability = 49 %						
Friability = (100 - s) = 51 %						

Charcoal Briquette						
Sieves, inches		Weight, g	Weight, % (1)	Average of sieve opening, in.		Product of (1) * (2)
Retained on	Passing			Inches	Normalizing factor (2)	
Sample 1 (25% husk; 75% shell)						
1	1.5	24.414	100	1.25	1	100 : S
dropped sample						
1	1.5	0.000	0.000	1.25	1	0.000
0.75	1	12.431	50.918	0.875	0.7	35.642
0.5	0.75	7.163	29.340	0.625	0.5	14.670
	0.5	4.693	19.223	0.25	0.2	3.845
Total (sum of products (1) * (2) for dropped sample)						54.157 : s
Size stability, % = (100 * s)/S = (100 *s)/100 = s = 54.2						
Size stability = 54 %						
Friability = (100 - s) = 46 %						

Charcoal Briquette						
Sieves, inches		Weight, g	Weight, % (1)	Average of sieve opening, in.		Product of (1) * (2)
Retained on	Passing			Inches	Normalizing factor (2)	
Sample 2 (25% husk; 75% shell)						
1	1.5	24.237	100	1.25	1	100 : S
dropped sample						
1	1.5	0.000	0.000	1.25	1	0.000
0.75	1	16.714	68.961	0.875	0.7	48.272
0.5	0.75	3.859	15.922	0.625	0.5	7.961
	0.5	3.656	15.084	0.25	0.2	3.017
Total (sum of products (1) * (2) for dropped sample)						59.250 : s
Size stability, % = (100 * s)/S = (100 *s)/100 = s = 59.3						
Size stability = 59 %						
Friability = (100 - s) = 41 %						

Charcoal Briquette						
Sieves, inches		Weight, g	Weight, % (1)	Average of sieve opening, in.		Product of (1) * (2)
Retained on	Passing			Inches	Normalizing factor (2)	
Sample 3 (25% husk; 75% shell)						
1	1.5	24.230	100	1.25	1	100 : S
dropped sample						
1	1.5	0.000	0.000	1.25	1	0.000
0.75	1	13.648	56.327	0.875	0.7	39.429
0.5	0.75	6.538	26.983	0.625	0.5	13.492
	0.5	3.845	15.869	0.25	0.2	3.174
Total (sum of products (1) * (2) for dropped sample)						56.094 : s
Size stability, % = (100 * s)/S = (100 *s)/100 = s = 56.1						
Size stability = 56 %						
Friability = (100 - s) = 44 %						

Charcoal Briquette						
Sieves, inches		Weight, g	Weight, % (1)	Average of sieve opening, in.		Product of (1) * (2)
Retained on	Passing			Inches	Normalizing factor (2)	
Sample 1 (100% shell)						
1	1.5	24.456	100	1.25	1	100 : S
dropped sample						
1	1.5	12.087	49.423	1.25	1	49.423
0.75	1	9.519	38.923	0.875	0.7	27.246
0.5	0.75	0.000	0.000	0.625	0.5	0.000
	0.5	2.815	11.510	0.25	0.2	2.302
Total (sum of products (1) * (2) for dropped sample)						78.972 : s
Size stability, % = (100 * s)/S = (100 *s)/100 = s = 79.0						
Size stability = 79 %						
Friability = (100 - s) = 21 %						

Charcoal Briquette						
Sieves, inches		Weight, g	Weight, % (1)	Average of sieve opening, in.		Product of (1) * (2)
Retained on	Passing			Inches	Normalizing factor (2)	
Sample 2 (100% shell)						
1	1.5	24.779	100	1.25	1	100 : S
dropped sample						
1	1.5	0.000	0.000	1.25	1	0.000
0.75	1	14.158	57.137	0.875	0.7	39.996
0.5	0.75	6.279	25.340	0.625	0.5	12.670
	0.5	4.330	17.474	0.25	0.2	3.495
Total (sum of products (1) * (2) for dropped sample)						56.161 : s
Size stability, % = (100 * s)/S = (100 *s)/100 = s = 56.2						
Size stability = 56 %						
Friability = (100 - s) = 44 %						

Charcoal Briquette						
Sieves, inches		Weight, g	Weight, % (1)	Average of sieve opening, in.		Product of (1) * (2)
Retained on	Passing			Inches	Normalizing factor (2)	
Sample 3 (100% shell)						
1	1.5	24.597	100	1.25	1	100 : S
dropped sample						
1	1.5	0.000	0.000	1.25	1	0.000
0.75	1	18.671	75.908	0.875	0.7	53.135
0.5	0.75	3.247	13.201	0.625	0.5	6.600
	0.5	2.642	10.741	0.25	0.2	2.148
Total (sum of products (1) * (2) for dropped sample)						61.884 : s
Size stability, % = (100 * s)/S = (100 *s)/100 = s = 61.9						
Size stability = 62 %						
Friability = (100 - s) = 38 %						

Annex 17: SEM test results

Coconut fibres from Mauritius:

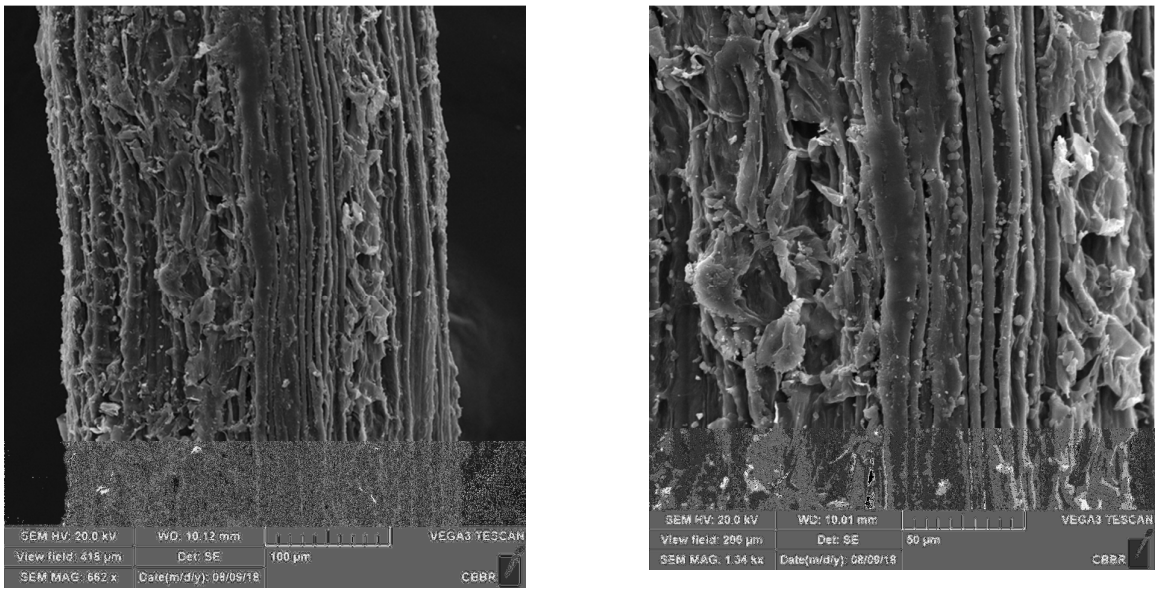


Figure A.17.1

Coconut fibres from Agalega:

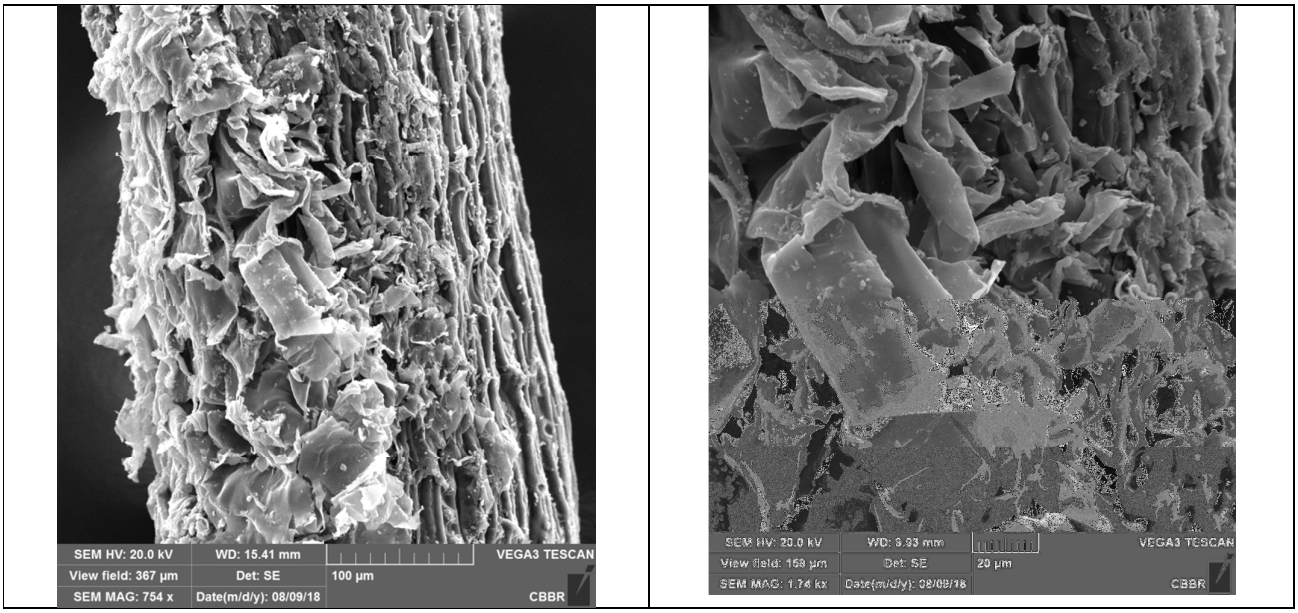


Figure A.17.2

Coconut fibres from Mauritius with pore sizes:

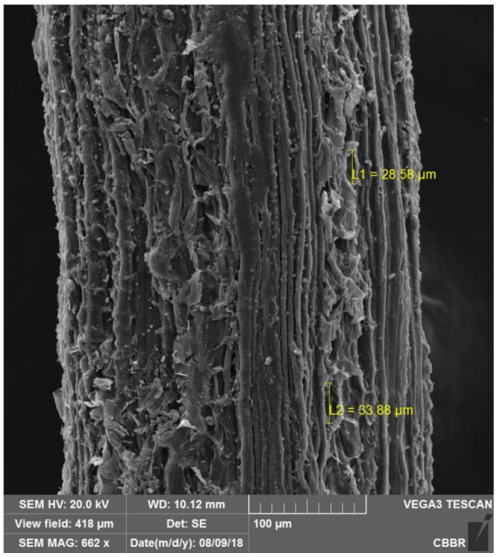


Figure A.17.3

Coconut fibres from Agalega with pore sizes:

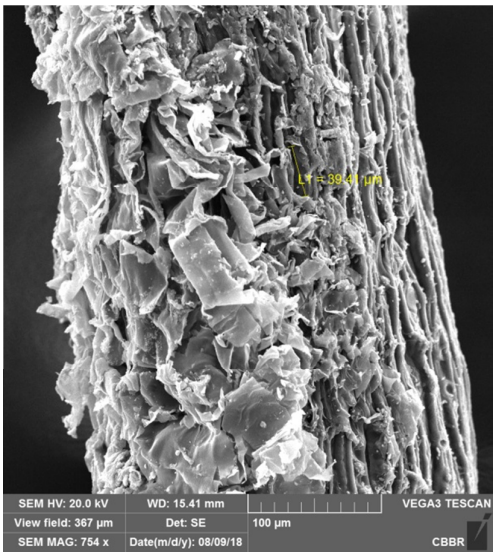


Figure A.17.4

Coconut fibres from composites, with sizes:

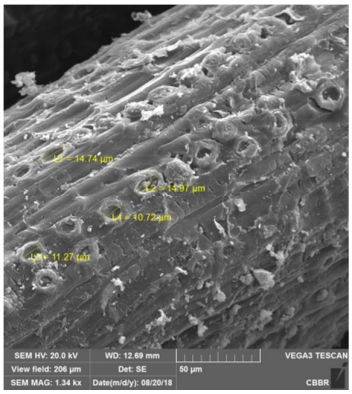
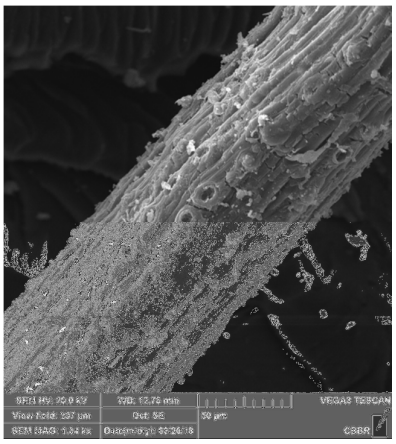
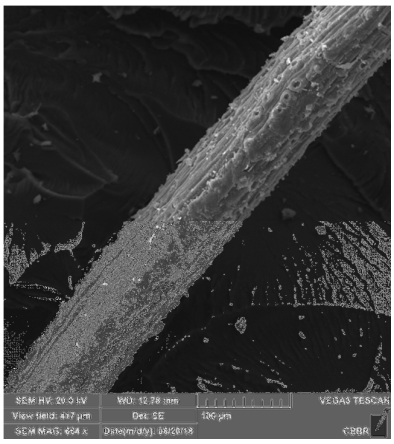


Figure A.17.5

More SEM micrographs for coconut fibres from Mauritius:





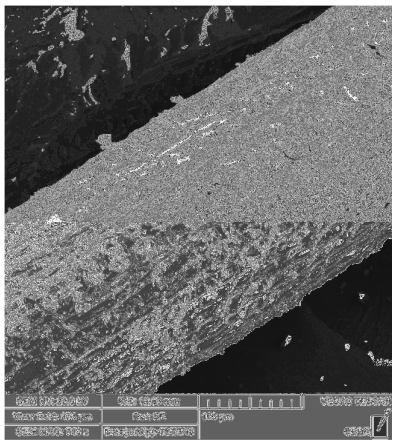
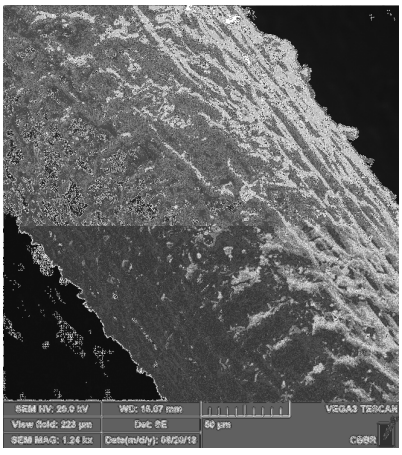
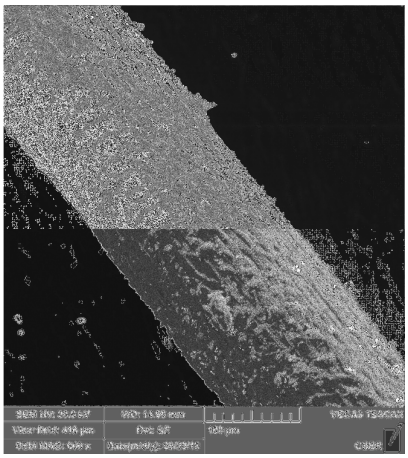


Figure A.17.6

More SEM micrographs for coconut fibres from Agalega:





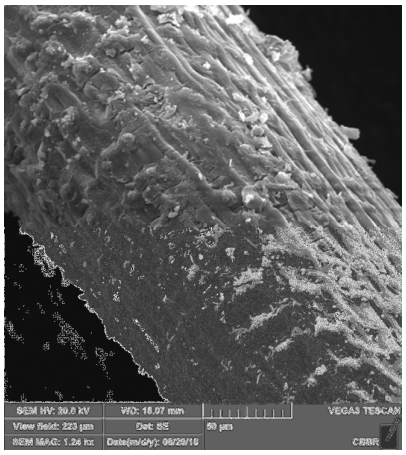


Figure A.17.6

SEM micrographs of specimens exposed under sheltered conditions after 92 days of exposure with:

(a) No coating (control)

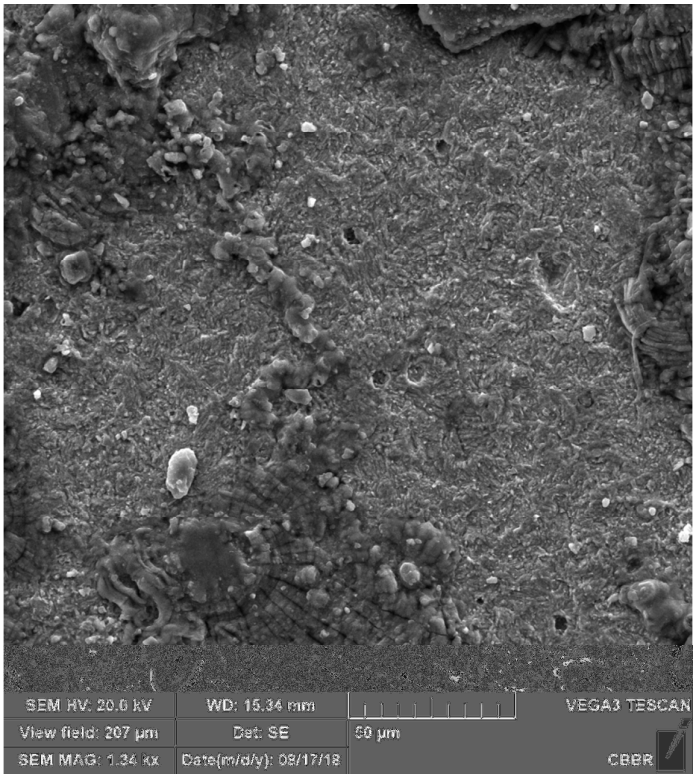


Fig. A.17.7

(b) Coating using 100% coconut oil

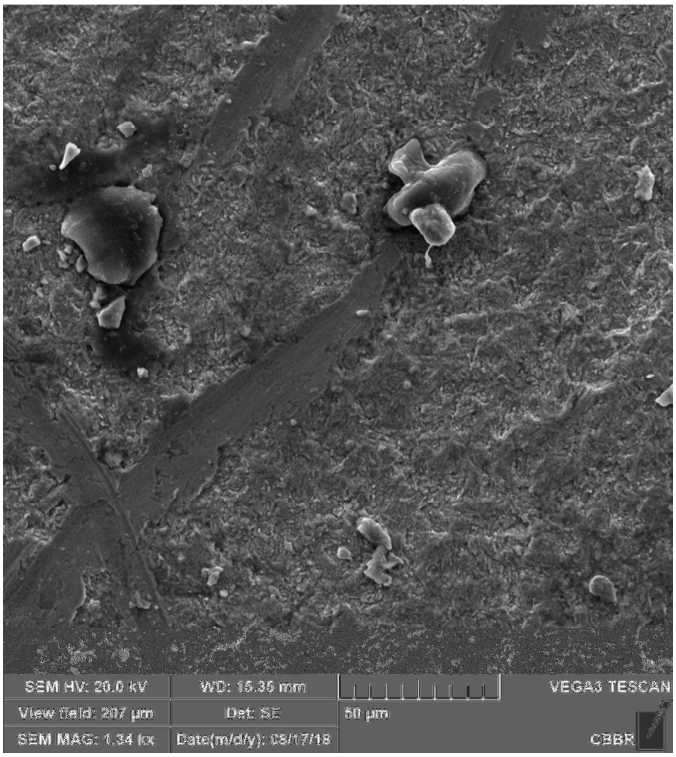


Fig. A.17.8

(c) Coating using 75% coconut oil and 25% honey

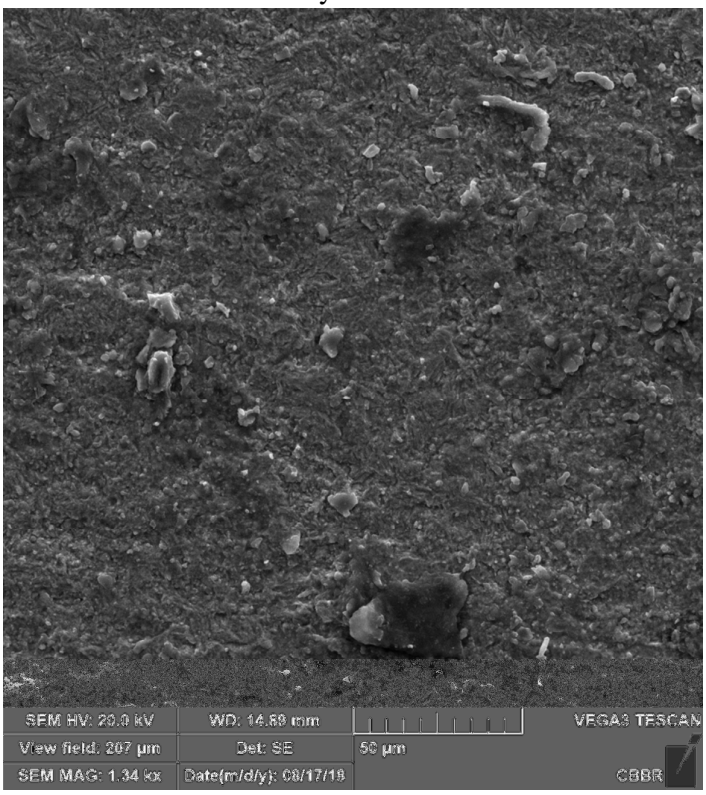


Fig. A.17.9

